

# EFFECT OF REPROCESSING ON POLYESTER/ MONTMORILLONITE NANOCOMPOSITES -PHD THESIS-

#### PREPARED BY

ENG: ZOUBEIDA TAHA TAHA

MECHANICAL ENGINEERING (BSC)

MATERIALS SCIENCE AND ENGINEERING (MSC)

## **Supervisors**

Dr. Andrea Ádámné Major, PhD
College professor

Dr. Ferenc Ronkay, Dsc Professor

# **DECLARATION**

I declare that I have developed this Ph.D. dissertation on my own, using the listed literature and documents and on the basis of my research results, my consultations and under the guidance of the supervisors.

•

Zoubeida Taha Taha Signature



## **ABSTRACT**

This research investigates the structural behaviour and properties of polyesters and their nanocomposites reinforced with montmorillonite (MMT). Both petroleum-based polyesters (polyethylene terephthalate (PET) and polybutylene terephthalate (PBT)) and bio-based polyesters (polylactic acid (PLA) and polybutylene succinate (PBS)) were studied. These four polyesters were compounded with 6 wt.% MMT to form nanocomposites. This thesis evaluates the influence of MMT addition on their crystallization behaviour, mechanical performance, thermal stability and degradation characteristics. Furthermore, special emphasis is placed on the impact of reprocessing on material degradation, including changes in intrinsic viscosity, crystallinity, shrinkage and dynamic mechanical properties of polyesters and their nanocomposites. A critical aspect of the increasing focus on polymer sustainability is taken into account.

The results demonstrate that while MMT significantly improves the performance of nanocomposites due to its nucleating and reinforcing capabilities, reprocessing results in polymer chain scission and reduced mechanical integrity. However, the presence of MMT helps maintain some structural organization during reprocessing, partially mitigating degradation effects. This thesis contributes to the understanding of the trade-off between performance and sustainability when recycling nanocomposites and provides insights into designing high-performance, recyclable materials for industrial applications.

#### **ACKNOWLEDGEMENTS**

I would like to express my deepest gratitude to my supervisors, *Dr. Andrea Ádámné Major* and *Professor Dr. Ferenc Ronkay*, for their valuable guidance, continuous support and encouragement throughout this research. Their expertise, insightful feedback and dedication have greatly contributed to the direction and quality of this work.

I especially extend my sincere thanks to *my colleagues*, especially *Emese Győry-Slezák* and *Dr. Béla Molnar*, at IMSYS Mérnöki Szolgáltató Kft. and John von Neumann University for their assistance, cooperation and support along the way.

A special thanks to *Mrs. Éva Ujlaky* for her kind help and encouragement, which were deeply appreciated.

I am grateful to *my wonderful friends* for their ongoing motivation and support throughout this journey.

I am profoundly grateful to *my amazing family* for their unwavering love, patience, and belief in me. Their constant support, even from afar, gave me the strength and focus to complete this journey.

This thesis would not have been possible without each of you. Thank you all.

# TABLE OF CONTENT

# **Table of Contents**

Li	st of	abbre	eviations and symbols	.viii
1.	Intr	oduct	ion	2
.2	Lite	rature	e review	4
	2.1.	Poly	vester materials	4
		.1.1	Petroleum-based polyesters	
	2.	.1.2.	Bio-based polyesters	
	2.2.	Effe	ct of MMT on the properties of polyester materials	6
	2.	.2.1.	Structure and crystallization of polyester/MMT nanocomposites	6
	.2	2.2.2	Mechanical properties of polyester/MMT nanocomposites	18
	2	.2.3.	Degradation and thermal properties of polyester/MMT nanocomposites.	30
	2.	.2.4.	Permeability and other properties of polyester/MMT nanocomposites	33
	2.3.	Prop	perties of recycled polyester/MMT nanocomposites	35
	2.4.	Crit	ical review of literature, aims of the thesis	39
3.	Mat	erials	and methods	42
	3.1.	Mat	erials	42
	3.2.	Met	hods	42
	3.	.2.1.	Sample preparation	42
	3.	.2.2.	Measurement methods	44
4.	Rest	alts a	nd discussions	48
	4.1.	Deg	radation of the polyesters during reprocessing	48
	4.2.	Shri	nkage characteristics of injection-moulded samples	49
	4.3.	Rhe	ological properties	53
	4.4.	Cry	stallization properties of polyesters and polyester/MMT	
		nan	ocomposites	57
	4.5.	Stru	cture of polyester/MMT nanocomposites	67
	4	.5.1.	Structure of nanocomposites analyzed by SEM	68
	4	.5.2.	Structure of nanocomposites by WAXD	70
	4.6.	Med	hanical properties of the nanocomposites	71
	4	.6.1.	Izod impact strength	71
	4	.6.2.	Flexural strength	74
	4.7.	Dvr	amic mechanical properties of the injection moulded specimens	77

5.	Summary8	32
	5.1. Utilization of results	34
	5.2. Theses - New scientific results	36
	5.3. Further work8	39
6.	My Publications9	0
7.	References9	12
8.	Appendix10	)4

# LIST OF ABBREVIATIONS AND SYMBOLS

## Abbreviations

ABS	Acrylonitrile-butadiene styrene
ALA	12-aminolauric acid
BHET	Bis (hydroxyethyl) terephthalate
CHDTPP	Chlorohexadecane triphenylphosphine
Cloisite 30B	Commercially modified clay
DA	Dodecylamine
DMA	Dynamic Mechanical Analysis
DSC	Differential Scanning Calorimetry
EDS	Energy Dispersive spectroscopy
EA	Di-(alkyl ester) dimethyl ammonium chloride
ETA	Ethoxylated tallow amine
GMA	Glycidyl methacrylate
HDPE	High-density polyethylene
HEA	1- [N, N-bis (2-hydroxyethyl) amino]-2-propanol
HTAB	Hexadecyl trimethyl ammonium bromide
IFR	Intumescent flame retardant
IM	Impact modifier
LCB	long chain branched
LEA	N-Lauryldiethanolamine
MMT	Montmorillonite
NaR-MMT	Sodium montmorillonite
ODA	Octadecylamine
Ol-MMT	modified clay with long-chain oleic acid
OMLS	Organically modified layered silicate
OMMT	Organically modified clay
PBS	Polybutylene succinate
PBT	Polybutylene terephthalate
PCL	Poly (ε-caprolactone)

PCN	Polymer clay nanocomposite							
PET	PET Polyethylene terephthalate							
PLA	Polylactic acid							
PP	Polypropylene							
PTT	Polytrimethylene terephthalate							
rPET Recycled polyethylene terephthalate								
SEM Scanning Electron Microscopy								
TEM Transmission Electron Microscopy								
TM	Tannin exfoliated montmorillonite							
ULDPE Ultra-low-density polyethylene								
WAXD Wide-angle X-ray scattering								
ZrP	Zirconium phosphonate							

# Symbols

β	[°]	Full width at half maximum
$\Delta H$	[J.g <sup>-1</sup> ]	Enthalpy change
CRF	[%]	Initial crystallinity percentage
D	[nm]	Crystalline size
d001	[nm]	Layer thickness
Е	[J]	Pendulum energy
E'	[MPa]	Storage modulus
E"	[MPa]	Loss modulus
FD	[mm]	Flow direction
IV	[dl/g]	Intrinsic viscosity
J(t)	[1/Pa]	Compliance
L, W	[mm]	Diameter (Length, width)
MFI	[g/10min]	Melt flow index
$M_w$	[gmol <sup>-1</sup> ]	Molecular weight
N	-	Number of MMT layers
P	[bar]	Pressure

RH       [%]       Relative humidity $T$ [°C]       temperature $T$ [sec]       Time $T$ [°C]       Crystallization temperature $TD$ [mm]       Transverse direction $T_g$ [°C]       Glass transition temperature $T_m$ [°C]       Melting temperature $T_m$ [°C]       Mould Temperature $V_g$ [kV]       Accelerating voltage $V_g$ [kV]       Accelerating voltage $V_g$ [w]       Weight $V_g$ [w]       Weight $V_g$ [w]       Crystallinity $V_g$ [w]       Wavelength $V_g$ [m]       Wavelength $V_g$ [m]       Wavelength $V_g$ [m]       Density $V_g$ [m]       Tensile strength $V_g$ [m]       Flexural strength $V_g$ [m]       Yield strength $V_g$ [m]       Visional strength $V_g$ [m]       Visional strength $V_g$ [m] <t< th=""><th>R</th><th>[°C/min]</th><th>Cooling rate</th></t<>	R	[°C/min]	Cooling rate
$T_c$ [°C]       Time $T_c$ [°C]       Crystallization temperature $TD$ [mm]       Transverse direction $T_g$ [°C]       Glass transition temperature $T_m$ [°C]       Melting temperature $T_m$ [°C]       Mould Temperature $V_a$ [kV]       Accelerating voltage $V_a$ [kV]       Accelerating voltage $V_a$ [w]       Volume Shrinkage $W_t$ [g]       Weight $X_c$ [%]       Crystallinity $\delta$ [%]       Elongation at break $\lambda$ [m]       Wavelength $v$ [mm/s]       Speed $\rho$ [g/cm³]       Density $\sigma$ [MPa]       Tensile strength $\sigma_y$ [MPa]       Flexural strength $\sigma_{xol}$ [k]/m²]       Izod impact strength $\sigma_{xol}$ [k]/m²]       Izod impact strength $\sigma_{xol}$ [k]/m²]       Crystalline fraction	RH	[%]	Relative humidity
$T_c$ [°C]       Crystallization temperature $TD$ [mm]       Transverse direction $T_g$ [°C]       Glass transition temperature $T_m$ [°C]       Melting temperature $T_{mould}$ [°C]       Mould Temperature $V_a$ [kV]       Accelerating voltage $V_a$ [kV]       Accelerating voltage $V_a$ [w]       Weight $V_a$ [w]       Weight $V_a$ [w]       Weight $V_a$ [w]       Crystallinity $V_a$ [w]       Crystallinity $V_a$ [w]       Elongation at break $V_a$ [w]       Wavelength $V_a$ [w]       Speed $V_a$ [w]       Density $V_a$ [mm/s]       Speed $V_a$ [m]       Tensile strength $V_a$ [m]       Flexural strength $V_a$ [w]       Izod impact strength $V_a$ [w]       Crystalline fraction	T	[°C]	temperature
TD[mm]Transverse direction $T_g$ [°C]Glass transition temperature $T_m$ [°C]Melting temperature $T_{mould}$ [°C]Mould Temperature $V_a$ [kV]Accelerating voltage $V_{shrinkage}$ [m³]Volume Shrinkage $Wt$ [g]Weight $X_c$ [%]Crystallinity $\delta$ [%]Elongation at break $\lambda$ [m]Wavelength $v$ [mm/s]Speed $\rho$ [g/cm³]Density $\sigma$ [MPa]Tensile strength $\sigma_f$ [MPa]Flexural strength $\sigma_v$ [MPa]Yield strength $\sigma_{zod}$ [kJ/m²]Izod impact strength $\chi_c$ [%]Crystalline fraction	T	[sec]	Time
$T_g$ [°C]       Glass transition temperature $T_m$ [°C]       Melting temperature $T_{mould}$ [°C]       Mould Temperature $V_a$ [kV]       Accelerating voltage $V_a$ [w]       Volume Shrinkage $W_t$ [g]       Weight $X_c$ [%]       Crystallinity $\delta$ [%]       Elongation at break $\lambda$ [m]       Wavelength $v$ [mm/s]       Speed $\rho$ [g/cm³]       Density $\sigma$ [MPa]       Tensile strength $\sigma_f$ [MPa]       Flexural strength $\sigma_{zod}$ [k]/m²]       Izod impact strength $\chi_c$ [%]       Crystalline fraction	$T_c$	[°C]	Crystallization temperature
$T_m$ [°C] Melting temperature $T_{mould}$ [°C] Mould Temperature $V_a$ [kV] Accelerating voltage $V_{shrinkage}$ [m³] Volume Shrinkage $Wt$ . [g] Weight $X_c$ [%] Crystallinity $\delta$ [%] Elongation at break $\lambda$ [m] Wavelength $\nu$ [mm/s] Speed $\rho$ [g/cm³] Density $\sigma$ [MPa] Tensile strength $\sigma_f$ [MPa] Flexural strength $\sigma_g$ [MPa] Yield strength $\sigma_g$ [MPa] Yield strength $\sigma_g$ [MPa] Izod impact strength $\sigma_g$ [%] Crystalline fraction	TD	[mm]	Transverse direction
$T_{mould}$ [°C]       Mould Temperature $V_a$ [kV]       Accelerating voltage $V_{shrinkage}$ [m³]       Volume Shrinkage $Wt$ .       [g]       Weight $X_c$ [%]       Crystallinity $\delta$ [%]       Elongation at break $\lambda$ [m]       Wavelength $v$ [mm/s]       Speed $\rho$ [g/cm³]       Density $\sigma$ [MPa]       Tensile strength $\sigma_f$ [MPa]       Flexural strength $\sigma_y$ [MPa]       Yield strength $\sigma_{zod}$ [kJ/m²]       Izod impact strength $\chi_c$ [%]       Crystalline fraction	$T_{\mathcal{S}}$	[°C]	Glass transition temperature
$V_a$ [kV]       Accelerating voltage $V_{shrinkage}$ [m³]       Volume Shrinkage $Wt$ .       [g]       Weight $X_c$ [%]       Crystallinity $\delta$ [%]       Elongation at break $\lambda$ [m]       Wavelength $\nu$ [mm/s]       Speed $\rho$ [g/cm³]       Density $\sigma$ [MPa]       Tensile strength $\sigma_f$ [MPa]       Flexural strength $\sigma_y$ [MPa]       Yield strength $\sigma_{zod}$ [kJ/m²]       Izod impact strength $\chi_c$ [%]       Crystalline fraction	$T_m$	[°C]	Melting temperature
$V$ shrinkage       [m³]       Volume Shrinkage $Wt$ .       [g]       Weight $X_c$ [%]       Crystallinity $\delta$ [%]       Elongation at break $\lambda$ [m]       Wavelength $\nu$ [mm/s]       Speed $\rho$ [g/cm³]       Density $\sigma$ [MPa]       Tensile strength $\sigma_f$ [MPa]       Flexural strength $\sigma_y$ [MPa]       Yield strength $\sigma_{zod}$ [kJ/m²]       Izod impact strength $\chi_c$ [%]       Crystalline fraction	Tmould	[°C]	Mould Temperature
$Wt.$ [g]Weight $X_c$ [%]Crystallinity $\delta$ [%]Elongation at break $\lambda$ [m]Wavelength $\nu$ [mm/s]Speed $\rho$ [g/cm³]Density $\sigma$ [MPa]Tensile strength $\sigma_f$ [MPa]Flexural strength $\sigma_y$ [MPa]Yield strength $\sigma_{zod}$ [kJ/m²]Izod impact strength $\chi_c$ [%]Crystalline fraction	$V_a$	[kV]	Accelerating voltage
$X_c$ [%]Crystallinity $\delta$ [%]Elongation at break $\lambda$ [m]Wavelength $\nu$ [mm/s]Speed $\rho$ [g/cm³]Density $\sigma$ [MPa]Tensile strength $\sigma_f$ [MPa]Flexural strength $\sigma_y$ [MPa]Yield strength $\sigma_{zod}$ [kJ/m²]Izod impact strength $\chi_c$ [%]Crystalline fraction	Vshrinkage	[m³]	Volume Shrinkage
$\delta$ [%] Elongation at break $\lambda$ [m] Wavelength $\nu$ [mm/s] Speed $\rho$ [g/cm³] Density $\sigma$ [MPa] Tensile strength $\sigma_f$ [MPa] Flexural strength $\sigma_y$ [MPa] Yield strength $\sigma_{zod}$ [kJ/m²] Izod impact strength $\chi_c$ [%] Crystalline fraction	Wt.	[g]	Weight
$\lambda$ [m] Wavelength $\nu$ [mm/s] Speed $\rho$ [g/cm³] Density $\sigma$ [MPa] Tensile strength $\sigma_f$ [MPa] Flexural strength $\sigma_y$ [MPa] Yield strength $\sigma_{zod}$ [kJ/m²] Izod impact strength $\chi_c$ [%] Crystalline fraction	$X_c$	[%]	Crystallinity
$ u$ [mm/s] Speed $ \rho$ [g/cm³] Density $ \sigma$ [MPa] Tensile strength $ \sigma_f$ [MPa] Flexural strength $ \sigma_y$ [MPa] Yield strength $ \sigma_{zod}$ [kJ/m²] Izod impact strength $ \chi_c$ [%] Crystalline fraction	δ	[%]	Elongation at break
$ ho$ [g/cm³] Density $\sigma$ [MPa] Tensile strength $\sigma_f$ [MPa] Flexural strength $\sigma_y$ [MPa] Yield strength $\sigma_{zod}$ [kJ/m²] Izod impact strength $\chi_c$ [%] Crystalline fraction	λ	[m]	Wavelength
$\sigma$ [MPa] Tensile strength $\sigma_f$ [MPa] Flexural strength $\sigma_y$ [MPa] Yield strength $\sigma_{zod}$ [kJ/m²] Izod impact strength $\chi_c$ [%] Crystalline fraction	ν	[mm/s]	Speed
$\sigma_f$ [MPa] Flexural strength $\sigma_y$ [MPa] Yield strength $\sigma_{zod}$ [kJ/m²] Izod impact strength $\chi_c$ [%] Crystalline fraction	ρ	[g/cm <sup>3</sup> ]	Density
$\sigma_y$ [MPa] Yield strength $\sigma_{zod}$ [kJ/m²] Izod impact strength $\chi_c$ [%] Crystalline fraction	σ	[MPa]	Tensile strength
$\sigma_{zod}$ [kJ/m <sup>2</sup> ] Izod impact strength $\chi_c$ [%] Crystalline fraction	$\sigma_f$	[MPa]	Flexural strength
$\chi_c$ [%] Crystalline fraction	бу	[MPa]	Yield strength
·	$\sigma_{zod}$	[kJ/m²]	Izod impact strength
n De de Constantina	$\chi_c$	[%]	Crystalline fraction
" [ra.s] Complex viscosity	η	[Pa.s]	Complex viscosity

#### 1. INTRODUCTION

A lot of modern industries and technologies require materials possessing a blend of special characteristics not commonly present in traditional materials like metal alloys and ceramics. Creating materials with distinct specifications that meet product requirements has been the interest of engineers for many years. For example, automakers are constantly looking for materials with structures that exhibit low density while maintaining strength, resistance to shocks and corrosion, rigidness, abrasion resistance and the integration of these properties cannot be easily combined. Frequently, materials that are strong, tend to have relatively high density, and any enhancement in hardness and strength typically leads to a decrease in the impact strength [1–4].

Composite materials have reached a significant position within the field of engineering materials due to their fitness for many industrial uses. They combine the features of two or more materials while relieving the disadvantages of each material. Furthermore, they provide the ability to control their characteristics, whether by altering the types and proportions of their component materials or by modifying their design and production techniques [2–6]. Polymer-based composites, one of the earliest advanced composite materials, have found extensive interest across various industrial applications, including ships, aircraft, radars and automobiles, due to their high strength, low cost and great stiffness-to-weight ratio when compared to metallic alloys [2, 3, 7, 8].

A nanocomposite is a solid material consisting of multiphases where at least one of these phases has dimensions of less than 100 nm in one, two, or three dimensions [9–13].

Polymeric materials used in most applications and daily products are polyesters due to their adaptability, low cost and high mechanical properties such as strength and moisture resistance. They are used as a main component in various industries such as clothing, textiles, home furniture, pillows, napkins, backpacks, air and water filters, packaging materials, computer and recording tapes, building and construction materials, electrical insulators, as well as in the medical field. In addition, biodegradable polyester materials find application in eco-friendly products, such as food containers and biodegradable bags [1–3, 7, 14].

Polyesters can be classified into two main types according to the raw materials used in the production. One of them is bio-polyester, which is produced from renewable resources like plants (as corn and sugarcane) and microorganisms, the most common for this type are polybutylene succinate (PBS) and polylactic acid (PLA) [15–19]. The other type is petroleum-

based polyesters, which are extracted from petrochemical raw materials. The most widely used are polybutylene terephthalate (PBT) and polyethylene terephthalate (PET) [20–23]. The choice depends on the characteristics required by the application, as both types have advantages and disadvantages. However, it is important to note that bio-based polyesters are more eco-friendly because they reduce dependence on fossil fuels [8]–[11].

Recently, the recycling of polyesters has great importance due to its ability to reduce the amount of waste, environmental effects and energy consumption and conserve resources [15, 16, 20]. Moreover, the recycling process affects the structure of the polymer, therefore, it can influence the mechanical properties of the polymer [20, 21].

In the present work, the effect of MMT on the morphology and mechanical properties of nanocomposites based on PET, PBT, PLA and PBS are discussed and the properties of these nanocomposites after mechanical recycling are compared.

#### 2. LITERATURE REVIEW

In this chapter, the properties of both petroleum-based and bio-based polyester composites are discussed extensively, especially those containing nanoclay.

## 2.1. Polyester materials

Polyester materials refer to a class of polymers composed of ester monomers. Polyester materials are created through a process called polycondensation [24–28]. They are also known as a material with multiple properties, including strength, flexibility, resistance to corrosion and moisture, ease of manufacturing, and electrical insulation. These properties can change depending on the type of polyester, the manufacturing process and any additional treatments applied to it. Polyester materials provide a balance between cost, performance, ease of care and recyclability, making them a popular choice in various industries and everyday consumer products. Their most familiar applications are in clothing, furniture, food packaging and plastic water and carbonated soft drinks bottles [1, 25–27, 29, 30]. Figure 1 shows the repeating units of the polyester types used.

They can be classified into two types, based on their origins: petroleum-based and bio-based polyesters. Aliphatic polyesters feature aliphatic hydrocarbon chains, which give them more flexibility and lower melting temperatures than aromatic polyesters, while aromatic polyesters typically have aromatic hydrocarbon rings in their repeating units [31–33].

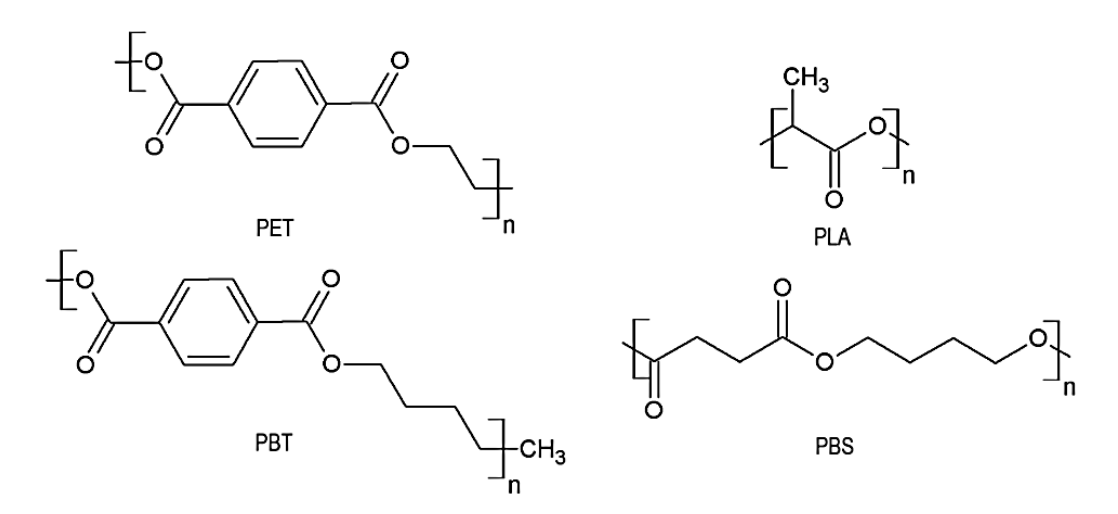


Fig. 1. Repeating units of the applied polyesters

#### 2.1.1. Petroleum-based polyesters

They are a type of synthetic polymers that are derived from petrochemical sources, primarily from petroleum. They are produced by polycondensation, which involves the combination of petrochemical compounds to create long chains of polyester molecules. These materials are hard and resistant to moisture and chemicals, making them suitable for a wide field of applications [16, 27, 34]. However, it is important to note that producing these materials from petroleum resources has environmental impacts, including the consumption of fossil fuels and greenhouse gas emissions. Efforts are being made to develop more sustainable alternatives to traditional polyester materials to reduce their environmental impact [16, 25, 34]. Common examples of this type include the following: polyethylene terephthalate (PET) which was first prepared in 1946 and was commercially introduced in 1953 as textile fiber, and soon thereafter as film [1, 35, 36]. It is considered a safe polymer for food contact and is regulated by health and safety agencies. One of its most important applications is bottles, which include those used in soft drinks, water and juices, food containers, electrical tapes and insulating materials, textile fibers and medical devices [37–40]. Another type is polybutylene terephthalate (PBT) which is also a semi-crystalline thermoplastic polymer with excellent mechanical and electrical properties, high heat resistance, high flexibility, low water absorption even in humid environments, high wear resistance and low creep. These attributes have made it a preferred choice in applications that require a combination of mechanical strength, heat resistance, electrical insulation and chemical resistance. Such as automotive components, electrical connectors, sockets, insulators, housing for electronic devices and equipment, gears, bearings, valve and pump components, kitchen appliances, various home electronics and medical devices [41–50].

#### 2.1.2. Bio-based polyesters

They are types of polymers derived from renewable biomass sources, such as plants or microorganisms, as opposed to traditional polyesters, which is typically made from petroleum-based chemicals. This type is characterized by good mechanical properties such as tensile strength and elongation at break, good barrier for both gases and water vapor, high chemical resistance, thermal resistance, ease of mouldability and biodegradability [16, 20, 30]. Also, bio-based polyester production aims to reduce dependence on fossil fuels and non-renewable resources, reduce environmental impact, greenhouse gas emissions, and enhance sustainability.

5

The properties of bio-based polyester can differ depending on the specific type of polyester and the raw materials used in its production [15, 21, 40, 51, 52], . One of the most important and most sought after material used is polylactic acid (PLA), which is a bio-based polyester derived from renewable resources such as cornstarch or sugarcane. It is produced by fermenting sugars to produce lactic acid, then polymerized to form PLA. It is a semi-crystalline polymer with low melting temperature and sensitivity to moisture. Due to its biodegradability and ease of use, PLA is commonly used in food packaging, disposable cups, plates, textiles, drug delivery systems, and 3D printing [14–16, 53–55].

Also, polybutylene succinate (PBS) is a bio-based polyester that belongs to the family of aliphatic polyesters. It is derived from succinic acid, which can be obtained from renewable resources. It has good mechanical strength, flexibility, and thermal stability. It is also widely used in various packaging applications, including films, bags and containers, textiles, and some medical applications [15, 16, 52, 56]. The properties and applications of these materials may vary, and their adoption is influenced by factors such as cost, performance, and market request. As technology continues to advance, the development of bio-based polymers is expected to play a crucial role in creating more sustainable alternatives to traditional plastics and polymers [15, 16, 30, 34, 51, 52, 57].

## 2.2. Effect of MMT on the properties of polyester materials

Combining polymers with nanofillers is a suitable way to develop new polymeric materials that collect the excellent properties of combined polymers. In recent years, many applications in industries have required the use of reinforced materials, so the development of nanocomposites has attracted much attention because they exhibit unexpected properties. In this way, the use of montmorillonite clay (MMT) as a reinforcing filler can lead to the production of nanocomposites that often show a significant improvement in their properties when compared to neat polymer or conventional composites due to their high strength, high aspect ratio and high modulus [58–63].

#### 2.2.1. Structure and crystallization of polyester/MMT nanocomposites

Factors such as nanoparticle loading, compatibility techniques, and dispersion method play crucial roles in determining the final properties of the nanocomposite material [60, 64]. Therefore, this section will present literature review that have demonstrated the effect of

6

montmorillonite addition on the structure and crystallization of the following polyesters, respectively: PET, PBT, PBS and PLA. Various types of tests were performed, such as rheological, morphological and crystallization, using a variety of analytical techniques like Differential Scanning Calorimetry (DSC), Scanning Electron Microscopy (SEM), Transmission Electron Microscopy (TEM), X-ray Diffraction (XRD) etc.

#### PET/MMT nanocomposites

Abbas Ghanbari et al. [65] added a multifunctional epoxide chain extender (Joncryl) at concentrations 0.5, 1, 2 wt.% to nanocomposites containing organoclays (one of them was Nanomer, which is Na+ montmorillonite modified with octadecyl trimethyl ammonium with a gallery spacing of 2.4 nm, the other type (C30B) was clay modified with methyl, tallow, bis-2-hydroxyethyl, and quaternary ammonium with a gallery spacing of 1.85 nm) produced using twin-screw extruder to study the properties of these nanocomposites. The results showed that the PET/C30B nanocomposite microstructure was very exfoliated, while the PET/ Nanomer contained large particles. The addition of the extender also improved the dispersion of Nanomer particles in the PET matrix at 0.5 wt.%. Also, the high stress forces of the reconnected PET chains as a result of the introduction of the extender led to increased clay delamination and distribution. The results showed that when chain extender was added at 0.5, 1, and 2 wt.% different levels of chain branching were achieved for PET macromolecules thus the formation of long chain branched (LCB) molecular structures, especially for samples containing 1 wt.% Joncryl. Also, higher shear sensitivity with improved viscoelastic properties was observed for the chain-extended samples.

Despite the excellent physical properties of polyethylene terephthalate (PET), it suffers from a low crystallization rate, a low temperature of thermal deformation and low modulus when it is in amorphous form. Therefore, Yimin Wang et al. [66] mixed it with montmorillonite (MMT) in the following ratios: 1, 3, 5 wt.% and studied the effect of this addition on the properties of the nanocomposite (PET/MMT). The results showed that adding MMT led to an increase in the crystallization rate because it acts as an effective nucleation agent, as shown in Figure 2.

7

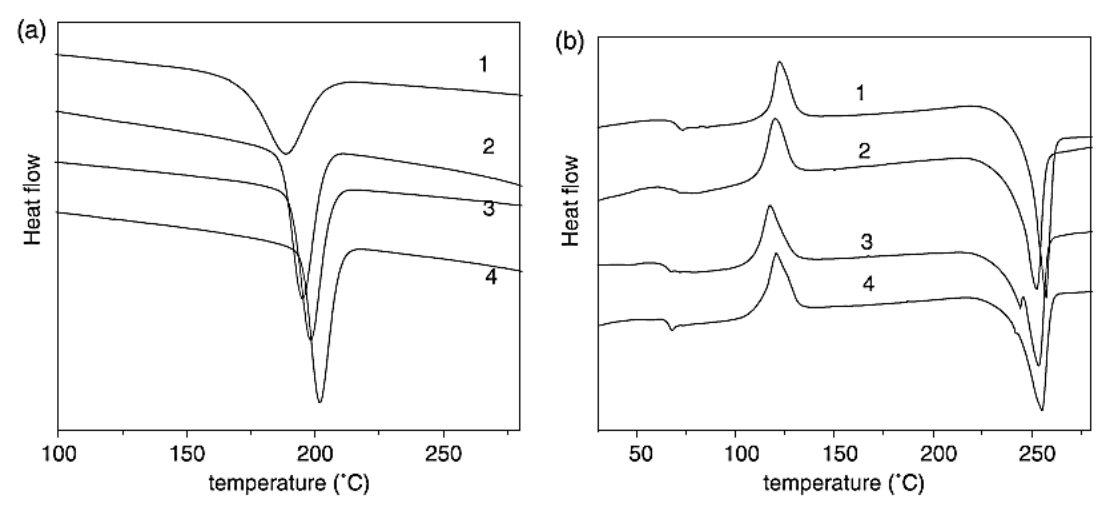


Fig. 2. DSC of PET/MMT (a) curves of cooling, (b) curves of heating, rate of heating and cooling are both 10 °C/min, ((1) pristine PET, (2) PET1M, (3) PET3M, (4) PET5M) [66]

To study the effect of adding MMT on the microstructure of PET, Weizhen Xiao et al. [67] added 2.5 wt.% of MMT to PET, then the final fibers were spun and pulled. The results showed the formation of crosslink points of the PET molecular network as a result of a strong interaction between MMT and the polymer PET, thus restricting the movement of the molecular segment of PET and making it a more continuous and complete molecular network, as Figure 3 showed. In the crystallization process, only small-sized crystals appeared in PET/MMT unlike pure PET, which had an especially large spherulite shape.

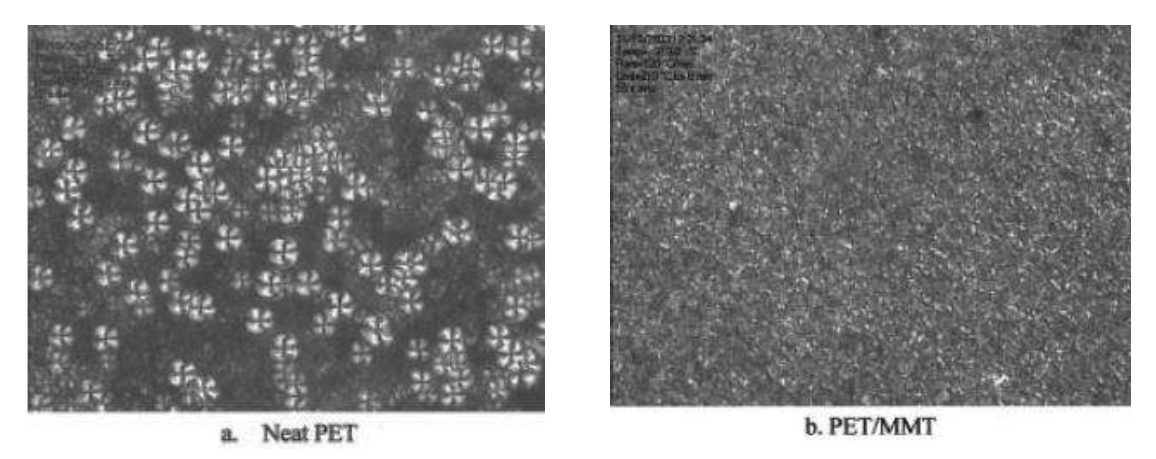


Fig. 3. Polarizing microscope images of crystallization [67]

Zhaojun Chen et al. [68] mixed a solution of bis(hydroxyethyl) terephthalate (BHET) with MMT at various concentrations, then mixed BHET-MMT with PET, and then compared PET/BHET-MMT (PETBM) with PET/sodium montmorillonite (NaR-MMT) hybrids

(PETNA), where these were preparations of nanocomposites without any organic modifier to study clay dispersion, intercalation and crystallization. The results showed that the addition of MMT led to an improvement in the glass transition temperature of clay composites modified with PET/BHET-MMT. They also indicated that the nanocomposite had the same transparency as PET without the addition, even at increased clay content. Moreover, there was an obvious difference in the clay dispersion in PETNA and PETBM even though the component was the same, as in PETNA it formed tightly packed layers while it was dispersed and disassembled at a size less than 30 nm in PETBM. It also showed the role of clay, as it could increase the crystallization rate when it was added in a small amount as a result of its effectiveness as a nucleation agent especially at higher crystallization temperatures.

Furthermore, Kazem Majdzadeh-Ardakani et al. [69] modified two types of clay (pristine (MMT) and commercially modified clay (Cloisite 30B) with long-chain oleic acid (ol), then mixed each of these nanoparticles (2 wt.%) with PET using a twin-screw extruder to study the properties of the nanocomposites. The results showed that the modified clay (ol-MMT) had a disordered structure of layered silicates, as this modification led to an increase in the gallery spacing of the silicate layers. In addition, they indicated that the dispersion of modified clay nanolayers in the PET matrix was improved and an exfoliated structure was obtained. The addition of modified clay also led to an improvement in crystallization behaviour.

To determine the effective activation energy, Arun K. Kalkar et al. [70] prepared nanocomposites of clay (1, 2, 3, 4, 5 wt.%) and PET using the two-stage melt polycondensation method. The results revealed that the effective activation energy is affected by the amount of clay in the composite, as it had higher values (>4 wt.%) but remained lower than it is in pure PET because clay is an effective heterogeneous nucleating filler, which is shown in Figure 4.

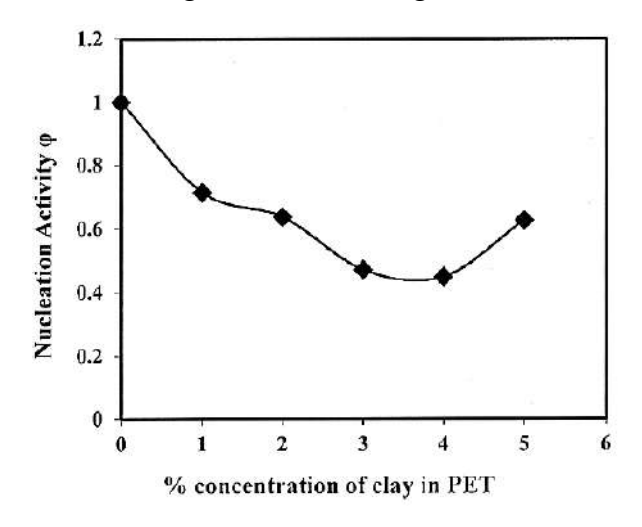
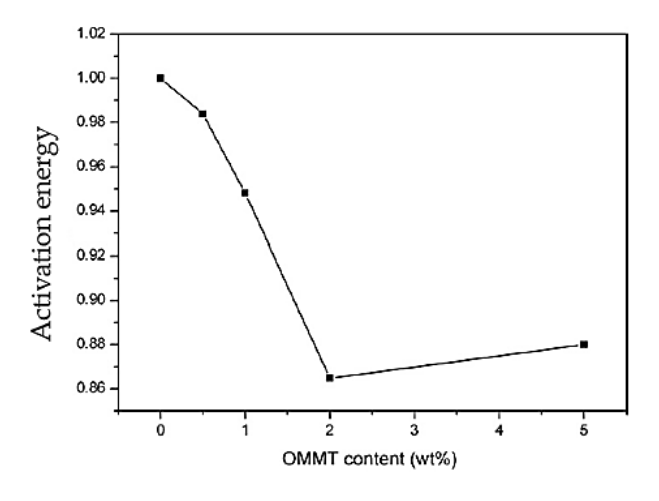


Fig. 4. Plot of nucleation activity  $\psi$  against % concentration of clay in PET [70]

It was also observed that the crystallization rate increased with decreasing temperatures. In addition, increasing the clay ratios led to an increase in crystallinity as a result of the gradually increasing effective nucleating density.

On the other hand, G. Antoniadis et al. [71] modified the clay with an organic modifier, chlorohexadecane triphenylphosphine (CHDTPP), then added it in the following ratios (0.5, 1, 2, 5 wt.%) to the PET matrix using melt polycondensation method to study its effect on activation energy and crystallization. The results showed that the addition of organically modified clay (OMMT) increased the melting temperatures by 0.7 °C to 3.8 °C. It also showed that modified clay works as a nucleating agent, as crystallization became faster with increasing clay ratio. As it increased, the nucleation activity enhanced because the crystallization peak temperature shifted to higher values, as shown in Figure 5. Therefore, the presence of OMMT led to a lower activation energy than pure PET. The OMMT particles in the PET matrix were homogeneously dispersed while in the exfoliated form they were dispersed as a result of the effectiveness of the modifier, where the large polymer macromolecules were able to penetrate between OMMT layers increasing the distance between them and leading to their separation.



*Fig. 5.* Nucleation activity of MMT in PET nanocomposites [71]

#### PBT/MMT nanocomposites

As for the effect of MMT on polybutylene terephthalate (PBT), Defeng Wu et al. [72] added MMT to PBT in different ratios (1, 2, 4, 6 and 8 wt.%) in order to study the rheological behaviour of the resulting nanocomposites. The results showed that the linear viscoelastic region of PBT/MMT nanocomposite is sensitive to the concentration of silicate and therefore decreases with increasing MMT concentration, as it became less than the viscoelastic region of

PBT. It also indicated that a percolation network was formed when MMT was added at a percentage of 3 wt.%, thus transferring the behaviour of the compound from a liquid to a solid state. Also, the addition of clay had an effect on the viscoelastic behaviour of PBT/MMT due to the interaction between the tactoids themselves and the interfacial adsorption of the polymer matrix and the tactoids. Moreover, the results indicated that the nature of the nanocomposites is like liquid crystals as a result of the strong interaction between the tactoids reorganizing the network.

Different concentrations of MMT (1, 3, 6, 9 wt.%) were also mixed with PBT to investigate the effect of MMT on crystallization by Defeng Wu et al. [73]. The results showed that the presence of MMT reduced the crystalline size of PBT, and also had a nucleating effect, as adding small amounts of it (1 wt.%) led to an increase in the crystallization rate at low temperatures, while a large concentration hindered the movement of the polymer chains. Moreover, small concentrations of MMT indicated the ease of coordination of crystal nuclei and the ease of incorporation of the surrounding polymer by additional nucleation sites as a result of the large distance between the dispersed platelets. In addition, the presence of MMT made crystallization slower at high crystallization temperatures due to impeding the formation of the crystal nucleus. Regarding the activation energy, the results indicated that adding MMT in small amounts led to a smaller activation energy than pure PBT, as shown in Figure 6.

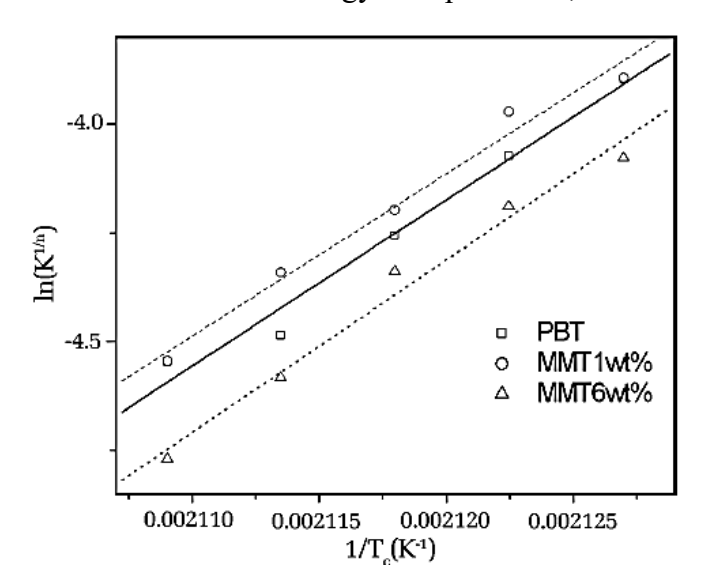


Fig. 6. Activation energy for isothermal crystallization [73]

Arun K. Kalkar et al. [74] prepared polymer clay nanocomposites (PCN), composed of different ratios of clay (from 1 to 8 wt. %) with PBT by melt intercalation with the aim of studying the effect of clay (MMT) on morphology and crystallization behaviour of PBT. The

results showed that at low loading rates (up to 3%), good dispersion of MMT occurred within the PBT matrix as a result of the satisfactory melt viscosity before crystallization during compounding, while agglomerations were found when loading increased, and this is shown in Figure 7. It also indicated that the surfaces of MMT nanoparticles acted as heterogeneous nucleation sites in nanocomposites (PBT/MMT).

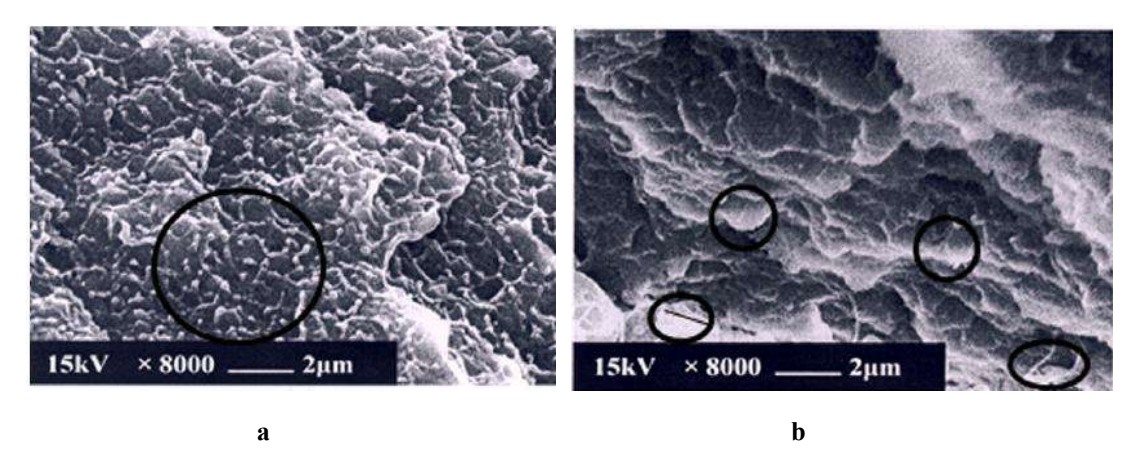


Fig. 7. SEM image of cryo-fractured surfaces of PBT/15A MMT clay nanocomposites (PCN): a) PCN3 (150–200 nm), b) PCN8 (800–1200 nm) [74]

In addition, nanocomposites containing 2, 4, 6 wt.% of MMT with PBT were prepared by B.H. Soudmand et al. [75] to determine the efficiency and properties of these nanocomposites in gear applications. The results showed that adding MMT had an effect on the crystallinity rate, as the crystallinity increased upon loading up to 4 wt.% of MMT, while it decreased upon adding MMT by 6 wt.%, which is shown in Table 1.

Table 1. Thermal analytical data obtained by non-isothermal heating and cooling DSC curves [75]

Compound	pound Heating Cooling			Cooling	g	
	T <sub>m</sub> (°C) ΔH <sub>m</sub> (J.g <sup>-1</sup> )		X <sub>c</sub> (%)	T <sub>c</sub> onset (°C)	T <sub>c</sub> (°C)	
PBT	225	50.15	35	204	193	
РВТ/ММТ2	224	57.75	40	203	194	
РВТ/ММТ4	224	57.94	42	203	194	
РВТ/ММТ6	223	52.35	38	199	192	

Defeng Wu et al. [76] also mixed the following ratios (1, 3, 6, and 9 wt.%) of MMT with PBT. They found that adding MMT led to a decrease in the crystallization temperatures of PBT at different cooling rates. The study also found that adding MMT in small ratios, up to 3 wt.%, led to accelerating the crystallization process because it acted as an effective heterogeneous nucleating agent, while adding a higher ratio reduced the crystallization rate, as a result of the formation of a hindrance due to the presence of MMT, which led to delaying crystallization. Moreover, the addition at low rates resulted in the formation of a partly exfoliated structure, while high rates formed an intercalated structure, as shown in Figure 8.

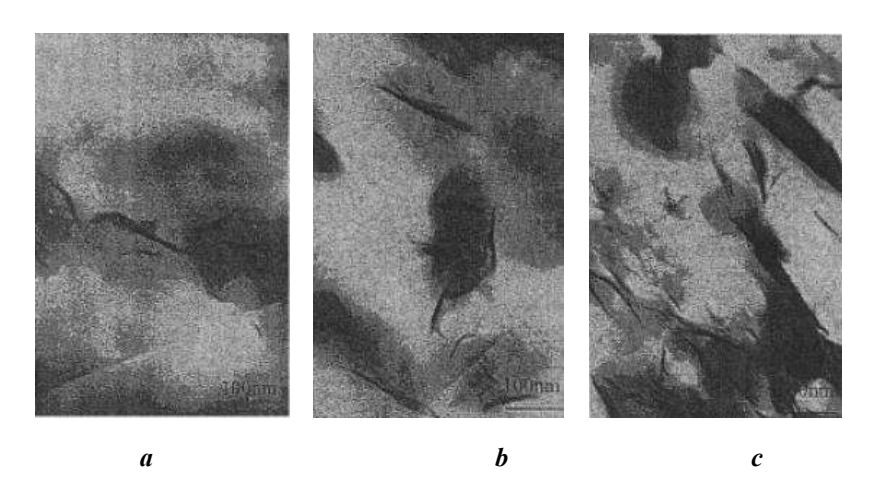


Fig. 8. TEM images of PBT/MMT samples: a) PBT/MMT 1wt%, b) PBT/MMT 6wt% at a magnification of 100,000 X, and c) PBT/MMT 9wt% at a magnification of 50,000X [76]

In addition, some researchers modified the clay and studied its effect on the properties of PBT, including Sung Yeon Hwang et al. [77] who modified the clay surface with urethane before adding it in different ratios (0.5 - 2 wt.%) to PBT by in situ polymerization method. The results showed that the presence of urethane groups facilitated the penetration of the polymer chains into MMT layers as a result of increasing the gallery spacing of silicate layers. It was also found that the modified clay acted as a strong heterogeneous nucleation agent that accelerated the crystallization rate.

Furthermore, Ranjana Sharma et al. [78] were interested in studying the rheological behaviour of nanocomposites by composing impact-modified poly butylene terephthalate/polytrimethylene terephthalate (PBT/PTT) blends with different ratios of organoclay (2, 3 and 5 wt.%) where ultra-low density polyethylene grafted glycidyl methacrylate (ULDPE-g-GMA) was used as an impact modifier. The results indicated that because of the strong interfacial interaction between the polymer matrix and the silicate layers, the complex viscosity ( $\eta^*$ )

enhanced at low frequencies with an increase in the ratios of clay in the nanocomposite, while it decreased when frequencies increased, as shown in Figure 9. The study revealed that the clay layers are uniformly distributed in the polymer matrix.

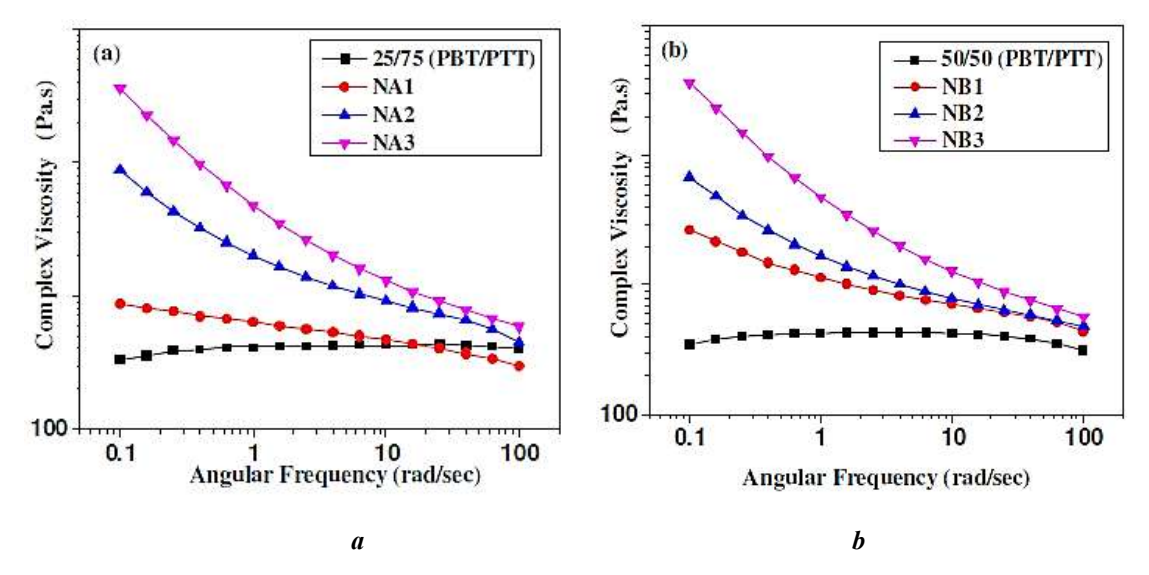


Fig. 9. Complex viscosity of impact modified a) 25/75 PBT/PTT nanocomposites, b) 50/50 PBT/PTT nanocomposites having 2, 3 and 5 wt.% organoclay [78]

#### PBS/MMT nanocomposites

The effect of clay on the structure of poly(butylene succinate) (PBS) was investigated by S. Taktak et al. [79], who mixed PBS with various amounts of MMT (1, 2, 3, 5 wt.%). The results showed that at a low concentration of MMT (up to 2 wt.%), the structure of the composites was intercalated and the dispersion was good, while above this threshold, MMT agglomerates were observed in the PBS matrix.

Y.J. Phua et al. [80] also found that when they mixed different concentrations of MMT (2, 4, 6, 8, 10 wt.%) with PBS using an internal mixer at different relative humidities (RH) (30, 60, 100 %), as the clay content increased, moisture absorption increased due to the formation of hydrogen bonds between the hydrophilic MMT and PBS. Moreover, it was observed that when exposed to moisture, the tensile fractured surface changed from smooth to rough due to the increase in ductility of the PBS/MMT matrix as a result of increased plasticization of PBS, as shown in Figure 10. The addition of clay at different relative humidities led to a decrease in crystallinity due to the MMT obstructing the movement and ability of the chains to fold. The increase in clay content and relative humidity also caused elevated agglomeration of MMT and increased surface roughness, thus leading to early failure of the nanocomposites.

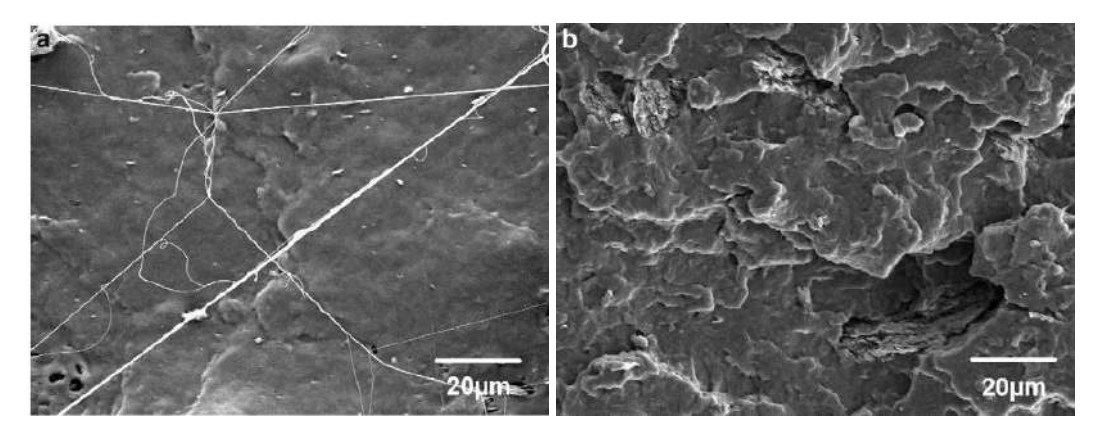


Fig. 10. SEM micrographs of the tensile-fractured surfaces of PBS /2 wt.% MMT a) before and b) after moisture absorption at 100% RH [80]

Yoshihiro Someya et al. [81] mixed PBS with various types of unmodified and modified MMT (dodecylamine (DA), octadecylamine (ODA), N-lauryldiethanolamine (LEA), 12-aminolauric acid (ALA) and 1-[N,N-bis(2-hydroxyethyl)amino]-2-propanol (HEA)) in different ratios (1, 3, 5, 10 wt.%) by melt intercalation. The results showed that the incorporation of clay led to improved crystallization of all nanocomposites as a result of the clay acting as an effective nucleating agent. They indicated that the intercalation and dispersion differed according to the type of MMT, where LEA-M had the highest intercalation and the dispersion was good, while MMT and HEA-M had a stacked intercalation structure.

Also, Suprakas Sinha Ray et al. [82] modified the clay surface with octadecyl trimethyl ammonium cation and then added it in different concentrations (2, 3.6, 5.4 wt.%) to PBS using a twin-screw extruder to study its effect on the structure of the resulting nanocomposites (PBS/MMT). The results revealed that the incorporation of modified MMT resulted in a well-ordered intercalated structure, and this ordering escalated with increasing MMT content. Moreover, it was observed that the crystallization rate increased due to the presence of strong interactions between the MMT surface and the PBS matrix because the clay particles served as nuclei for crystallization. They also found that as the clay content increased, the behaviour of the nanocomposite changed to solid, due to the good dispersion of MMT.

Suprakas Sinha Ray et al. [83] also confirmed the importance of MMT modified with octadecylammonium on the structure of PBS when they prepared the nanocomposite with different ratios of MMT (1.7, 2.8 wt%). MMT was observed in the form of several stacked silicate layers with random orientation in PBS.

## PLA/MMT nanocomposites

Yingwei Di et al. [84] used organic clay (Cloisite 30B) at different concentrations (2, 5, 10 wt.%) to prepare PLA/30B nanocomposites using an internal mixer to study its effect. The results showed that the incorporation of clay 30B created an exfoliated structure in the nanocomposites. The presence of 30B clay increased the crystallization rate at low clay contents (up to 5 wt.%) because it acted as a strong nucleating agent, while high ratios of it led to decreased crystallinity by impeding the movement of the PLA chains, thus acting as inhibitors of crystallization. The results showed that the incorporation of 30B clay resulted in smaller PLA cells and increased density due to the improved melt viscosity and elastic properties of nanocomposites, as shown in Figure 11.

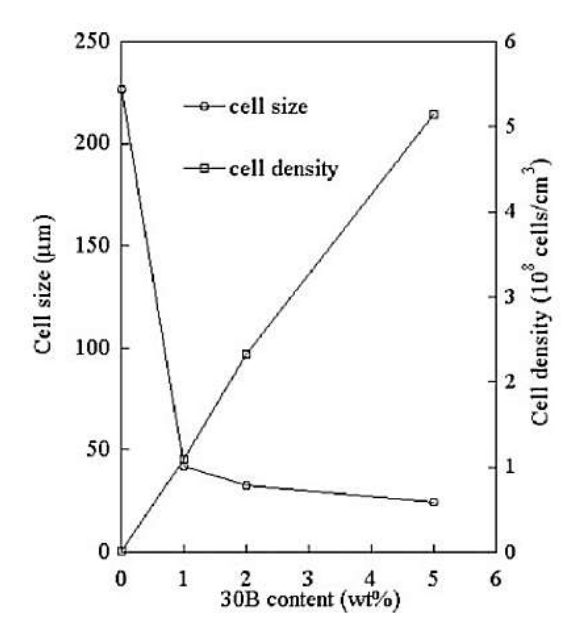
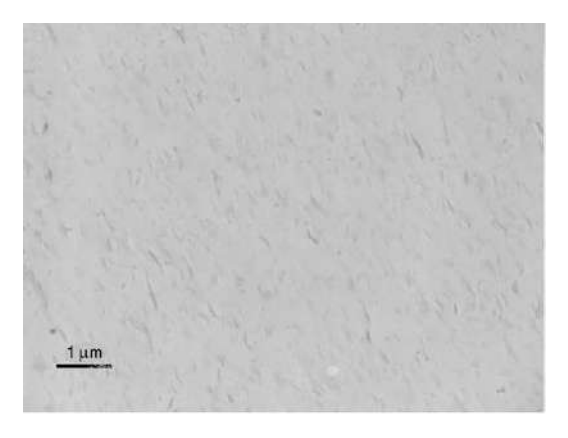


Fig. 11. The cell size and cell density of PLA nanocomposite foams with different weight fractions of 30B [84]

Besides, K. Fukushima et al. [85] added 5 wt.% of several types of nanofillers (organically modified montmorillonite (CLO), organically modified zirconium phosphonate (ZrP), and unmodified sepiolite (SEP)) to PLA. The results showed that CLO was uniformly distributed. This is due to the decrease in the thickness of the interlayer, as shown in Figure 12. It also led to the preservation of the optical transparency of PLA because of the satisfactory dispersion of these particles as their size was smaller than the visible wavelength.



*Fig.* 12. *SEM micrograph of PLA* + 5% *CLO* [85]

The effect of incorporating 1wt.% of MMT on the dispersion and properties of poly(ε-caprolactone) (PCL)/ poly(lactic acid) (PLA) blends was studied by Bo Zhu et al. [86]. They found that MMT is distributed at the PCL/PLA (70/30) interface. The blends' interface also changed from a smooth to a rough surface as a result of the increased interaction between the two phases of PCL and PLA. Furthermore, good dispersion of the PLA matrix within the PCL was observed in the presence of MMT.

In addition, researchers modified the clay and studied its effect on PLA. Suprakas Sinha Ray et al. [87] modified montmorillonite using dimethyldioctadecylammonium cation and then mixed organically modified layered silicate (OMLS) at different concentrations (4, 5, and 7 wt.%) with PLA using a twin-screw extruder. The results indicated that a small amount of OMLS acted as a nucleating agent for crystallization, leading to the formation of numerous small-sized crystals, thus enhancing the crystallization rate of PLA/OMLS nanocomposites.

Also, J. L. Feijoo et al. [88] added 4 wt.% of modified montmorillonite to two types of MMTs (dimethyl-hydrogenated tallow ammonium and dimethyl-benzyl-dihydrogenated tallow ammonium used in DELLITE 72T and DELLIT E 43B, respectively) to PLA. The results indicated that both types led to an increase in the interlayer distance in the silicate layers and an intercalated and stacked structure. It also showed that DELLIT E 43B had a better dispersion in the PLA matrix compared to DELLIT E 72T, as a result of the strong interaction with PLA and thus obtaining higher thermal stability.

After that, the montmorillonite was modified with biocompatible/biodegradable chitosan (m-MMT), and it was added at different concentrations (1.5, 3, 6 wt.%) to PLA and the properties of the resulting nanocomposites were studied by Tzong-Ming Wu et al. [89]. It was observed that increasing the m-MMT content to more than 3 wt.% reduced the crystallization of PLA/m-MMT nanocomposites.

#### 2.2.2. Mechanical properties of polyester/MMT nanocomposites

Since the addition of MMT led to a change in the structure of all types of polyesters, a change has also occurred in the mechanical properties of the resulting nanocomposites. The researchers studied its effect on PET, PBT, PBS and PLA. C.I.W. Calcagno et al. [90] mixed polypropylene/polyethylene terephthalate (PP/PET) with MMT and maleic anhydride grafted polypropylene (PP-MA) using a twin-screw extruder. The results showed that the addition of MMT and the compatibilizer together caused an improvement in tensile strength, elongation at break, storage modulus and loss modulus, especially at temperatures higher than T<sub>g</sub> of PP, due to the enhancement of adhesion between the polymers and the transfer of stress between these phases.

Yimin Wang et al. [66] also found that the addition of MMT achieved improvement in tensile strength (from 54 to 67.7 MPa), impact strength (from 26 to 26.9 J/m), elongation at break and flexural strength when added in a small amount (1 wt.%) due to the good dispersion of MMT in the PET matrix. However, increasing the amount of MMT to more than 1 wt.% resulted in a decrease in these properties compared to those of the pure PET.

Moreover, they found that the addition of modified MMT in low quantities led to an improvement in the tensile strength and storage modulus, as shown in Table 2, where the results indicated that the properties increase up to 3 wt.% of MMT and then decrease as a result of the presence of agglomerates of modified MMT within the PET matrix [68].

*Table 2. Mechanical properties of nanocomposites* [68]

Sample	Storage modulus (GPa)	Tensile strength (MPa)		
NPET	1.68	35.6 ± 1.0		
PETNA2	1.61	35.9 ± 3		
PETBM1	1.73	38 ± 1.6		
PETBM2	1.98	42 ± 1.7		
РЕТВМЗ	2.27	30 ± 2.1		

Likewise, according to Kazem Majdzadeh-Ardakani et al. [69], at 2 wt.% of MMT there was a remarkable improvement in mechanical properties such as strength (which increased by 8 %

for PET/ol-MMT and 16% for PET/ol-30B) and Young's modulus (by 7% for PET/ol-MMT and 25% for PET/ol-30B) due to the enhancing effect of clay particles as shown in Figure 13.

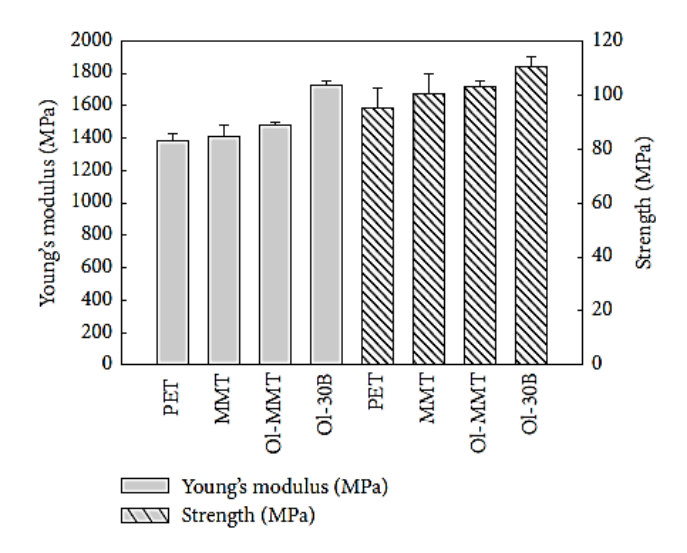


Fig. 13. Strength of the sidewall of stretch-blown PET and nanocomposite bottles [69]

As for PBT, the effect of the size and ratio of MMT and screw speed on the mechanical properties of injection-moulded PBT clay nanocomposites was studied after adding organically modified MMT in the following ratios (0.5, 1, 2, 3, 4 wt.%) and size (8, 35 µm) to PBT by a twin-screw extruder at different speeds (80 and 100 rpm). The results showed that adding MMT led to an increase in tensile strength and wear resistance. The larger particle size also contributed to the increased tensile strength, as shown in Figure 14. Besides, the results indicated that increasing the screw speed led to improved mechanical properties. In addition, the best mechanical properties were achieved by adding 1 wt.% MMT regardless of the organoclay size and screw speed due to the good dispersion of MMT in the PBT matrix [91].

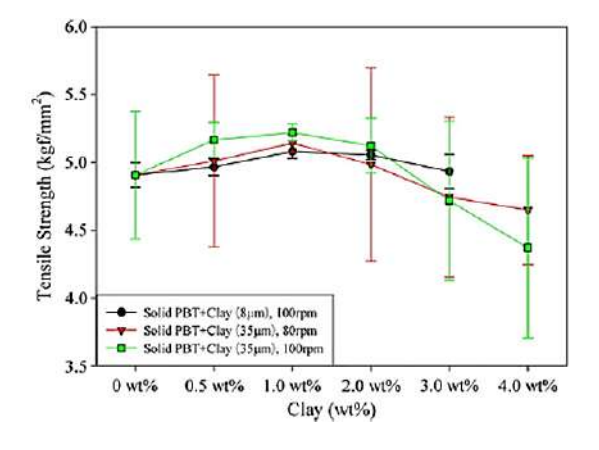


Fig. 14. Tensile strength comparison of solid PCN at differing clay loadings, clay sizes, and screw speeds
[91]

Ranjana et al. [92] also noticed a significant improvement in tensile strength, tensile modulus, and stress at break when adding 3 wt.% of OMMT and use of a 2 wt.% impact modifier (IM) which is Ultra-low-density polyethylenegrafted glycidyl methacrylate, as shown in Table 3. The increases were 41.3, 24.6 and 34.8 %, as a result of the high aspect ratio and the large surface area of clay platelets. In contrast, both the elongation at break and Izod impact strength decreased when adding OMMT, because it formed sites for crack propagation which makes the material brittle.

*Table 3. Mechanical properties of impact modified PBT/PTT blends-based nanocomposites* [92]

Sample name	Sample code PBT/PTT/IM/OMMT	Tensile modulus (MPa)	Tensile strength (MPa)	Stress at break (MPa)	Elongation at break (%)	Izod impact strength (J/m)
NA1	23/73/2/2	1776	43.6	30.1	4.2	57.5
NA2	22.5/72.5/2/3	1887	40.2	42.2	3.3	56.1
NA3	21.5/71.5/2/5	1877	36.7	37.7	2.0	54.6
NB1	48/48/2/2	1762	40.5	40.5	2.2	58.2
NB2	47.5/47.5/2/3	1883	44.7	44.7	3.6	56.7
NB3	46.5/46.5/2/5	1881	39.1	39.8	2.1	55.4
NC1	73/23/2/2	1752	40.3	38.2	7.5	57.9
NC2	72.5/22.5/2/3	1880	41.4	40.7	5.1	57.1
NC3	71.5/21.5/2/5	1875	38.8	38.7	3.0	55.9

The results of B.H. Soudmand et al. [93] showed that the Izod impact strength and elongation at break decreased with increasing MMT ratio due to the aggregation of nanoclay particles, which act as sites of strong stress concentration and thus help the diffusion of cracks with low energy dissipation. However, both the tensile strength and Young's modulus increased due to the formation of a strong interphase at the polymer-filler interface, it was noted that the increase was slight when MMT was added in large ratios (6 wt.%) [77, 93].

Moreover, the increase reached 95% at 3 wt.% of MMT, and after that, it began to decrease, as shown in Figure 15 [74].

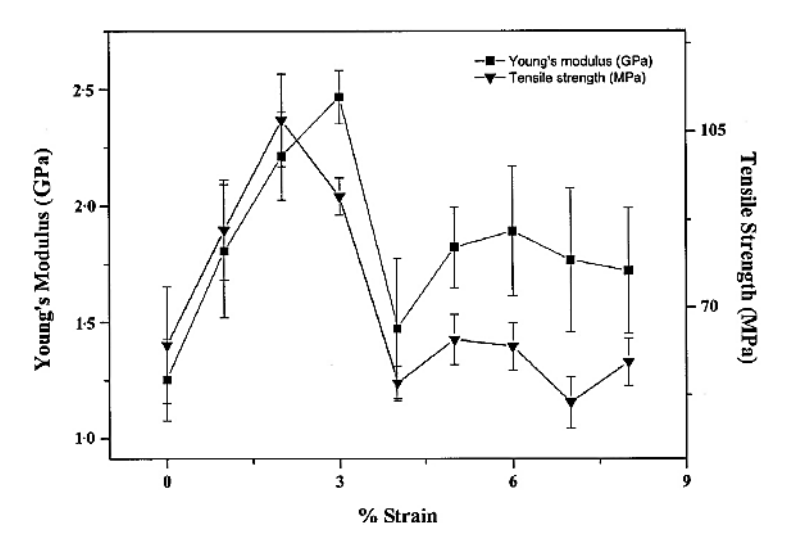


Fig. 15. Tensile modulus and tensile strength at break point of PBT/MMT [74]

Regarding the loss and storage moduli, the results showed that the incorporation of organic clay led to an increase in both the loss modulus (G") and the storage modulus (G'), especially at low frequencies. It was also observed that the values of these moduli enhanced with increasing clay content [78]. Furthermore, Soudmand et al. [75] found that high temperatures led to an increase in the storage modulus (E') when the ratio of MMT increased due to good adhesion between PBT and MMT. Also, the addition of MMT resulted in a decrease in the damping factor ( $\tan \delta$ ) and thus a decrease in power dissipation compared to pure PBT was observed as shown in Figure 16.

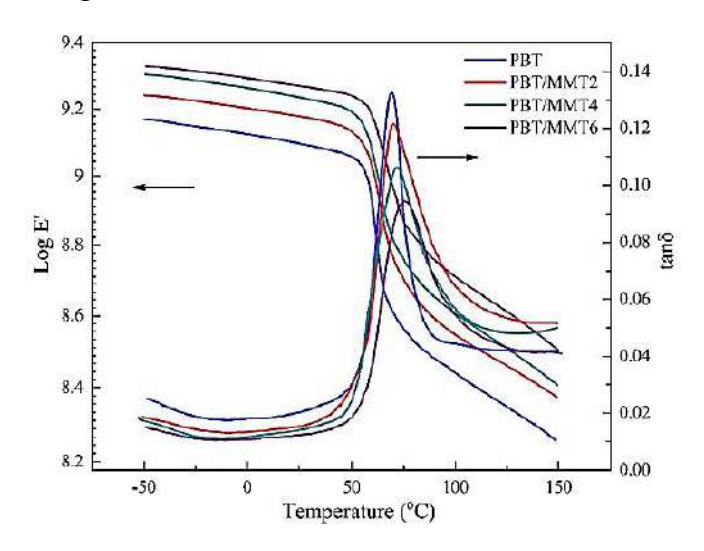


Fig. 16. Storage modulus and damping factor for PBT/MMT and pure PBT [75]

On the other hand, Defeng Wu et al. [72] demonstrated the independence of G' and G" from temperature, as shown in Figure 17.

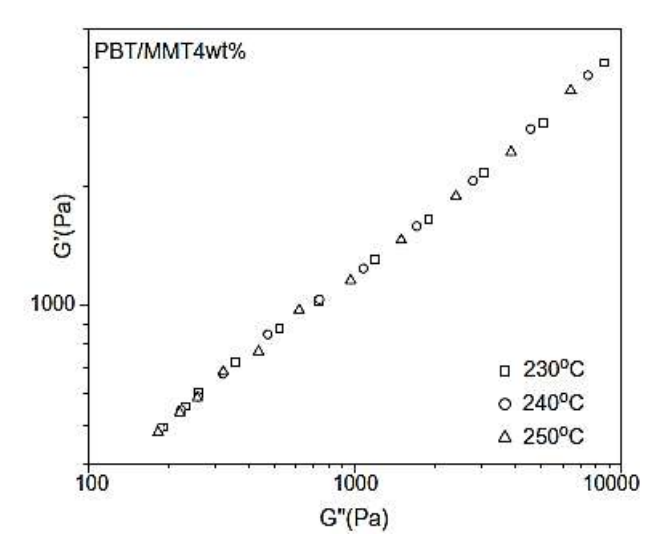


Fig. 17. G' and G'' for PBT/MMT 4 wt.% [72]

Regarding the effect of nano clay on the mechanical properties of polybutylene succinate (PBS), montmorillonite (MMT), commercial ODA-modified organoclay (DM) and organoclay modified by hexadecyltrimethylammonium bromide (HTAB) were added to PBS (PBS-g-MA) by Y.J. Phua et al. [94]. The results showed that the type of clay plays a role in the properties of PBS, as mixing organic clay modified by HTAB has an effect on the properties due to its improvement in the dispersion of clay within the PBS matrix, so the mechanical properties, such as tensile strength, flexural strength and impact strength in the PBS/HM compound, were improved due to the active role of PBS-g-MA as a compatibilizer, as shown in Table 4.

*Table 4. Mechanical properties of PBS and the nanocomposites* [94]

	Compound						
Properties	PBS	PBS/2DM	PBS/MMT	PBS/HM10	PBS/HM15	PBS/MA	PBS/HM10/MA
Tensile strength (MPa)	32.6 ± 2.7	33.6 ± 1.2	25.4 ± 2.0	34.0 ± 0.4	32.1 ± 2.0	29.0 ± 2.2	39.4 ± 0.5
Tensile modulus (MPa)	589 ± 6.8	631 ± 9.1	616 ± 25	661 ± 8.4	665 ± 21	599 ± 14	684 ± 23
Elongation at break (%)	10.9 ± 2.6	12.9 ± 2.4	5.4 ± 0.4	16.7 ± 1.2	13.3 ± 0.8	6.7 ± 1.4	14.0 ± 1.3
Flexural strength (MPa)	33.3 ± 1.9	36.1 ± 0.9	28.0 ± 0.9	37.5 ± 1.2	36.0 ± 0.6	32.1 ±1.3	40.3 ± 0.6
Flexural modulus (MPa)	570 ± 14	619 ± 11	659 ± 16	683 ± 23	671 ± 18	598 ± 21	694 ± 8.1
Impact of Notched (kJ/m²)	8.8 ± 1.4	9.4 ± 1.8	8.3 ± 2	13.8 ± 1.4	12.9 ±1.1	6.2 ± 0.5	15.7 ± 1.3
Impact of unnotched (kJ/m²)	104 ± 2.3	108 ± 8.1	99.1 ± 4.3	116 ± 11	112 ± 3.5	84.9 ± 1.8	121 ± 2.5

Yoshihiro Someya et al. [81] also showed that adding all types of MMT led to an improvement in both tensile and flexural modulus and flexural strength, while tensile strength and elongation at break decreased, which is shown in Table (5), where the ratio of MMT was 3 wt.%.

 Table 5. Mechanical Properties of PBS and PBS/Clay Composites with an Inorganic Content of 3 wt.% [81]

	Tensile properties			Flexural	
Clay	Strength (MPa)	Modulus (GPa)	Elongation at break (%)	Strength (MPa)	Modulus (GPa)
None	33.7	0.707	7.60	44.3	0.754
MMT	33.3	0.811	7.87	49.9	0.913
DA-M	31.3	1.013	6.32	49.6	1.096
ODA-M	30.8	1.002	6.34	48.4	1.025
LEA-M	29.7	1.044	6.30	48.6	1.036
HEA-M	33.5	0.836	6.99	44.6	0.774
ALA-M	32.2	0.857	6.37	45.1	0.807

Increasing the content of MMT also led to an enhancement in the tensile modulus by about 69% at 5.4 wt.%, while the tensile strength decreased with further increasing MMT, as shown in Figure 18 [82].

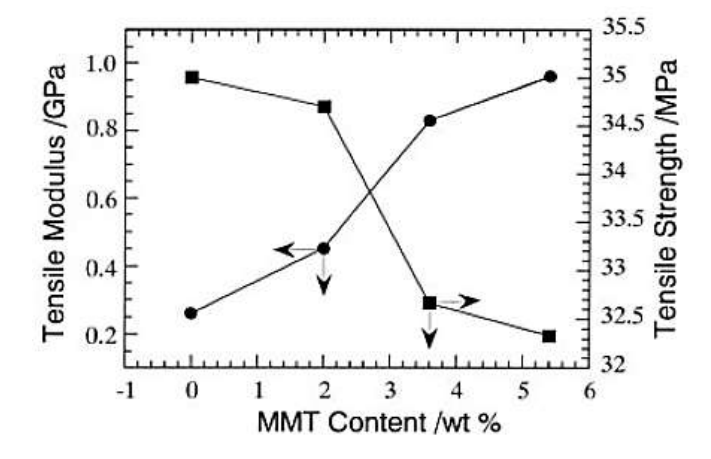


Fig. 18. Tensile properties of neat PBS and various PBSCNs [82]

Also, the addition of clay modified with octadecyl ammonium led to an improvement in the tensile strength and tensile modulus of the resulting nanocomposites [83]. In addition, the incorporation of 5 wt.% tannin exfoliated montmorillonite nanoparticles (TM), developed the flexural modulus and flexural strength as shown in Figure 19 [95].

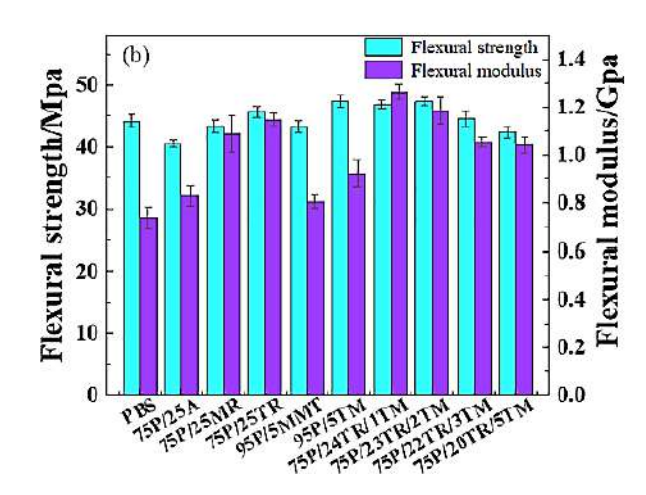


Fig. 19. Flexural strength and modulus of pure and flame retarded PBS composites [95]

Furthermore, the plasticizers present in OMMT had a positive effect due to their good dispersion when added 1.5 wt.% of OMMT to PBS/20 IFR(intumescent flame retardant), as they led to an increase in the tensile modulus, as Figure 20 shows in the tensile and strain curves [96].

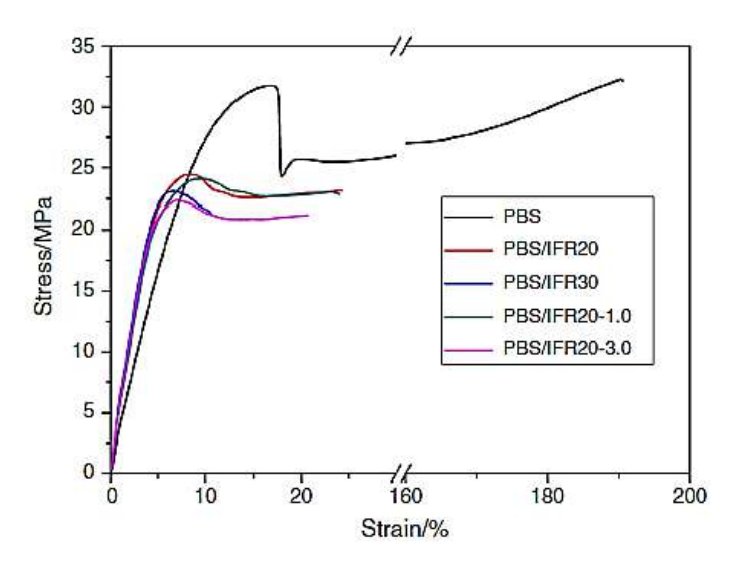


Fig. 20. Tensile stress–strain curves of PBS and its flame-retarded composites [96]

On the other hand, Attila Bata et al. [97] found that the addition of OMMT resulted in a reduction of Izod impact strength by approximately 35% at room temperature, and yield strength and yield strain by 30%. It was also observed that this decrease in properties intensifies at higher clay contents, about (5-10 wt.%), as shown in Table 6, as a result of restricting the movement of the polymer chains due to the interaction between PBS and OMMT, which prevents crystallization. At the same time, Young's modulus and storage modulus enhance with increasing OMMT content.

 Table 6. Mechanical properties of PBS-MMT nanocomposites [97]

OMMT content	Notched Izod impact strength at 23 °C	Notched Izod impact strength at -20 °C	Young's modulus	Yield strength	Strain at yield
w/w%	kJ/m²	kJ/m²	MPa	МРа	%
o	8.1 ± 0.5	4.3 ± 0.9	715 ± 12	40.1 ± 0.2	16.7 ± 0.5
2.5	5.0 ± 0.5	3.5 ± 0.3	880 ± 14	39.1 ± 0.2	14.2 ± 0.4
5	4.9 ± 0.3	3.4 ± 0.1	984 ± 10	38.0 ± 0.4	12.7 ± 0.4
7.5	4.4 ± 0.4	3.4 ± 0.1	1129 ± 14	36.0 ± 0.2	11.8 ± 0.2
10	4.2 ± 0.2	2.6 ± 0.5	1265 ± 15	35.6 ± 0.1	10.7 ± 0.1

It was important to examine the effect of adding MMT on PLA. Therefore, Siti Hajar Othman et al. [98] added two types of clays (MMT and halloysite) in different ratios (1, 3, 5, 7, 9 wt.%) to PLA using the casting method. The results detected that adding both types of nanoclays at low amounts (up to 3 wt.%) led to an improvement in tensile strength, Young's modulus and elongation at break, where the increase was about 16%, 77%, 133% for PLA/MMT and 14 %, 50% and 79% for PLA/halloysite respectively. Increasing the nanoclay content in the nanocomposites (from 5 to 9 wt.%) led to a decrease in these properties due to the weak interaction between the PLA matrix and the nanoclay and thus the appearance of clay agglomerates inside the PLA matrix. Figure 21 shows the tensile strength of the nanocomposites.

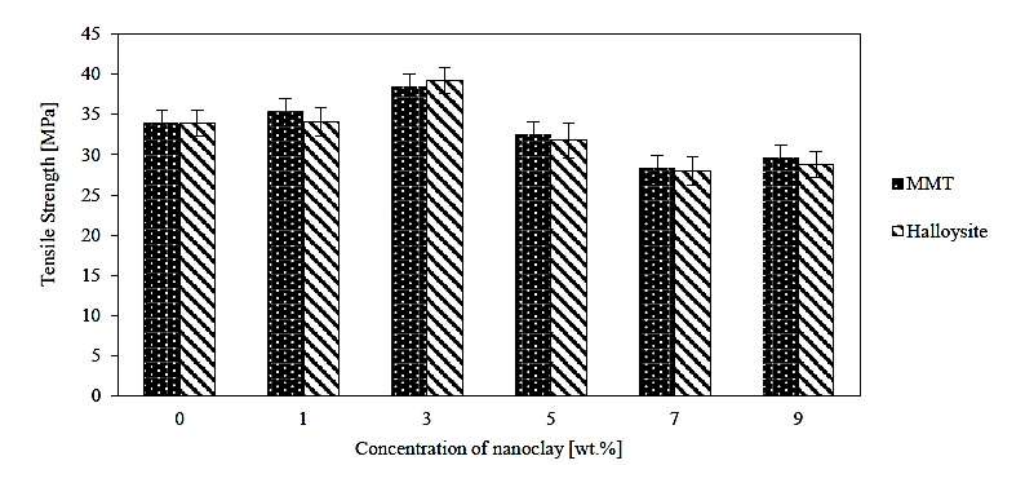


Fig. 21. Effects of types and concentrations of nanoclays on tensile strength [98]

Wu Xuanjun et al. [99] combined (3, 5, 8 wt.%) OMMT with PLA using solvent casting. It was found that the incorporation of clay in small ratios (up to 5 wt.%) led to an increase in the elongation at break of about (100%) due to the plasticization occurring on the surface of the silicate interlayers. In contrast, MMT led to a decrease in the modulus of elasticity and tensile strength, due to the heterogeneous distribution and weak adhesion between PLA and MMT, which is shown in Table 7 [99].

Samples	Elastic modulus (MPa)	Tensile strength (MPa)	Elongation at break (%)	
PLA	1600	36.67	3.68	
PLAMMT3	59	8.34*	265.62	
PLAMMT5	101	8.74*	352.65	
PLAMMT8	179	5.04*	35.07	

*Table 7. Mechanical properties of PLA and various PLA/MMT nanocomposites* [99]

Luqman I. Alrawi et al. [100] added (2, 4, 6, and 8 wt.%) MMT to PLA using solvent casting. The results indicated that the incorporation of MMT at low ratios (up to 4 wt.%) resulted in an increase in tensile strength as a result of the good dispersion of MMT particles within the PLA matrix due to the good interaction between them resulting from the enlarged contact surface area. The modulus of elasticity also increased as a result of the increased crystallization rate because MMT acted as a nucleating agent in the nanocomposites. The addition of MMT led to a decrease in the elongation at break due to cross-linking and degradation of the polymer chains, as shown in Figure 22.

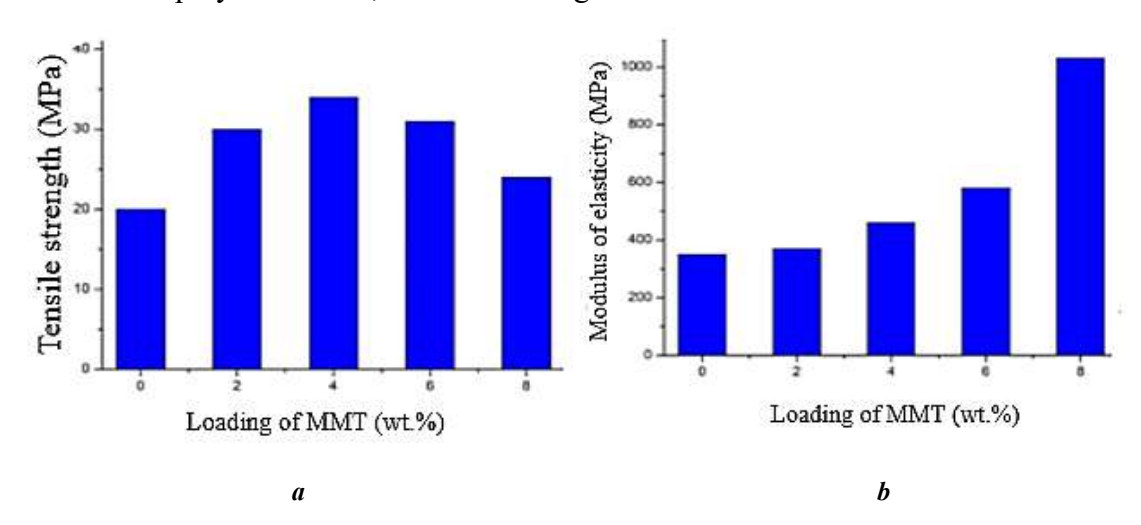


Fig. 22. Mechanical properties of PLA/MMT nanocomposites with different loadings of MMT: a) tensile strength and b) modulus of elasticity [100]

<sup>\*</sup> The true value of tensile strength

Furthermore, there was an improvement in both the storage modulus (G') and loss modulus (G") when adding 5 wt.% of CLO because it formed an interconnected structure within the PLA matrix as a result of the strong interactions between PLA and CLO, and thus an improvement in the melt viscosity was found [85]. An increase in storage and loss modulus was observed when Cloisite 30B was added at low ratios (up to 5 wt.%) [84].

Moreover, the addition of MMT affected the properties of the PLA/30 % of treated aloe vera fiber (TAF) mixture, as the results revealed that adding MMT in a small ratio (1 wt.%) led to an improvement in the impact, tensile, and flexural strength by about 10.43, 5.72 and 6.08 %, respectively, whereas the excess addition of MMT (2, 3 wt.%) led to a decrease in mechanical properties. The addition of MMT also improved the tensile and flexural modulus due to the improvement of the interfacial bonding between PLA and TAF in the presence of MMT. Furthermore, it was noted that the presence of MMT at a low ratio improved abrasion resistance [101].

Incorporation of 1wt.% of MMT into the PCL/PLA blend also enhanced tensile strength and elongation at break, but Young's modulus decreased because the clay acted as a coupling agent that helped to improve mixing between the two polymers, as shown in Figure 23 [86].

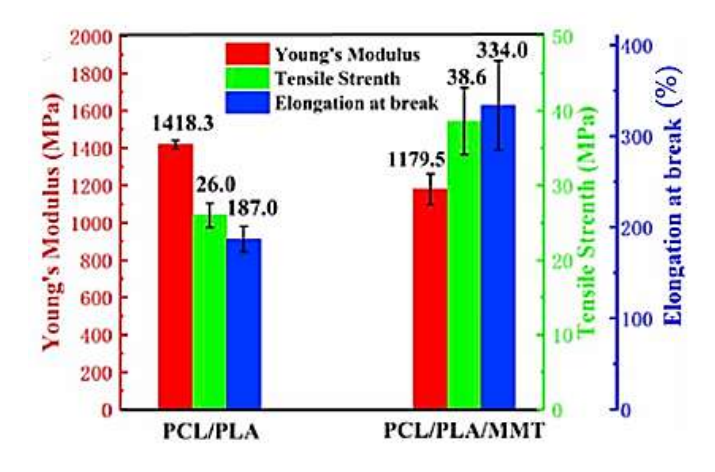


Fig. 23. The mechanical properties of PCL/PLA nanocomposites [86]

Likewise, clay modification played a role in changing the properties of the nanocomposite, as Jefferson Lopes Alves et al. [102] modified the montmorillonite chemically by adding several surfactants (di-(hydrogenated tallow) dimethyl ammonium chloride (HTA), trihexyl tetradecyl phosphonium chloride (TDP), di-(alkyl ester) dimethyl ammonium chloride (EA) and ethoxylated tallow amine (ETA)). The modified clay was added in different ratios (2, 6, 8 wt.%) to the PLA. The results showed that adding modified clay affected the final properties of the product, as mixing all types of OMMT led to an improvement in flexural modulus

compared to PLA without clay and this improvement increased with increasing OMMT content, while the flexural strength decreased with this increase because the clay served as a rigid filler capable of absorbing the external mechanical load. The same applies to the storage modulus because the modified clay tends to restrict the movement of the chains. They indicated that the addition of two types of clays, namely (EA, ETA) improved the ductility and increased the impact resistance of the nanocomposites due to the good dispersion of these fillers within the PLA matrix, while the remaining types led to a decrease as a result of their aggregation, so they were local stress concentrations, leading to the appearance and spread of cracks, as shown in Figure 24.

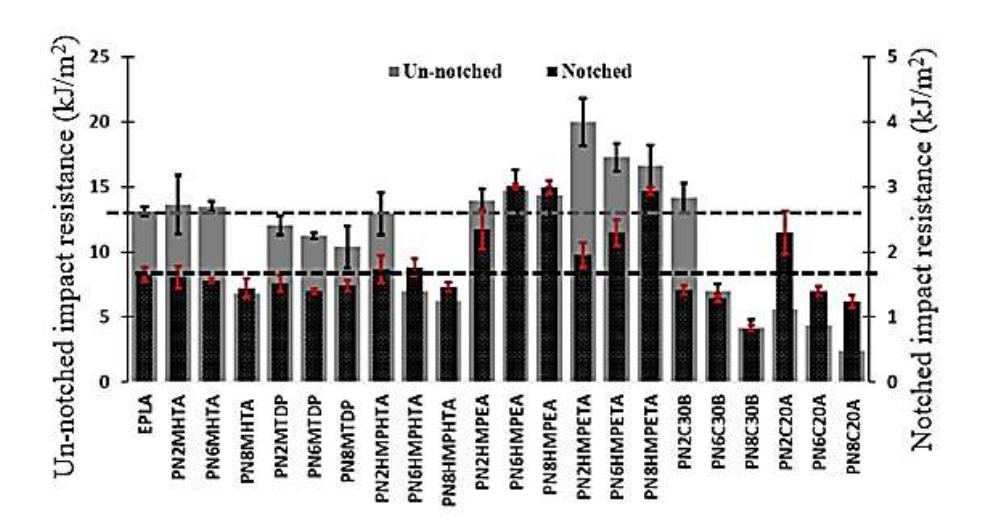


Fig. 24. Evaluation of the impact resistance with organic-modified montmorillonites (OMT) type and content [102]

Also, the presence of MMT modified with dimethyl dioctadecyl ammonium cation (OMLS) in the PLA matrix at high temperature (above T<sub>g</sub>) improved both the loss (G'') and storage modulus (G'). In addition, incorporating OMLS at small ratios (up to 5 wt.%) increased the strength and flexural modulus and distortion at break [87].

After modifying montmorillonite with biocompatible/biodegradable chitosan (m-MMT) and adding it at different concentrations (1.5, 3, 6 wt.%) to PLA, there was an improvement in the storage modulus of the manufactured nanocomposite, which increased with increasing m-MMT content because of the chemical similarity between PLA and m-MMT and the presence of inorganic silicate layers, the increase in storage modulus reached 70% at 3 wt.% and 107%. at 6 wt.% [89].

In addition, it was found that irradiation of the composites with an electron beam to crosslink PLA with organoclay (MMT) in the presence of triallyl cyanurate (TAC) improved the

tensile strength, while the elongation at break decreased, especially at high irradiation doses, as shown in Table 8. A suitable balance was also observed between tensile strength and elongation at break at low irradiation doses (30 kGy) [103].

Samples	Tensile strength (MPa)	Tensile modulus (GPa)	Elongation at break (%)	
PLA	60.7 ± 1.1	2.60 ± 0.07	9.2 ± 0.3	
PLA-MMT	59.5 ± 0.5	1.51 ± 0.03	80.8 ± 7.0	
PLA-MMT-TAC 0kGy	56.1 ± 1.4	2.09 ± 0.02	66.6 ± 8.0	
PLA-MMT-TAC 30kGy	63.6 ± 0.5	2.08 ± 0.02	47.8 ± 5.6	
PLA-MMT-TAC 50kGy	62.3 ± 0.5	2.11 ± 0.13	32.9 ± 3.3	
PLA-MMT-TAC 70kGv	62.4 ± 1.2	2.15 ± 0.05	16.1 ± 5.1	

Table 8. Mechanical properties of PLA/MMT/TAC (0, 30, 50, and 70 kGy) nanocomposites [103]

#### 2.2.3. Degradation and thermal properties of polyester/MMT nanocomposites

Despite the excellent physical properties of polyesters, they suffer from a low thermal stability when they are in amorphous form. The addition of MMT affected the thermal properties, as it was found that adding 1% of MMT achieved thermal stability of PET, as the onset temperature of thermal degradation and the temperature of thermal deformation of PET increased by 12 °C and 35 °C, respectively [66]. Adding 2.5 wt.% of MMT and increasing the drawing temperature led to an improvement in thermal stability and a decrease in the degree of orientation of PET fibers compared to pure PET fibers as shown in Figure 25 [67].

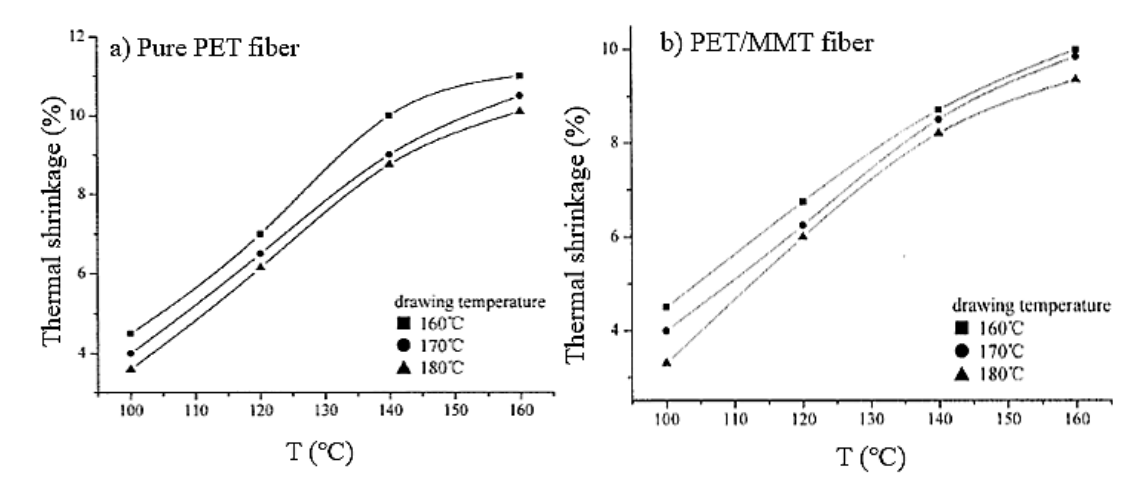


Fig. 25. Thermal shrinkage of fibers at various environmental temperatures [67]

Furthermore, the addition of clay modified with long-chain oleic acid achieved high thermal stability, so the resulting nanocomposites were able to withstand the processing temperature of PET. The results displayed that the presence of fatty acids (ol) led to increased degradation of ol-30B after modification [69]. On the other hand, the good nano-dispersion between MMT and PET led to decreased degradation of the nanocomposite due to the enlargement of the contact area and strong interaction between the type of filler and PET which would conduct the stress along the clay surface [68].

Also, adding MMT (up to 3 wt.%) to PBT increased the thermal stability of PBT/MMT compared to pure PBT [91]. Likewise, the results indicated that the addition of MMT increased the gears' resistance to heat, which led to an increase in the life of the gears by 107% when a load of 6 Nm of constant torques was applied [75].

Since PBS is highly combustible, Yuhai Wang et al. [96] added OMMT in different ratios (0.5, 1, 1.5 and 3 wt.%) and 20% IFR to it using twin-screw extrusion in order to study the thermal properties of the resulting PBS/IFR/OMMT nanocomposites. The results showed that the addition of OMMT improved flame-retardancy due to the enhanced interfacial interactions occurring between OMMT and PBS matrix. Adding 1.5 wt.% of OMMT improved the flame-retardant property of PBS/20 IFR by about 40.1 % due to the synergistic effect between OMMT and IFR, while increasing the ratio of OMMT reduced this effect. Also, adding it in this ratio provided a physical barrier that prevents the transfer of heat and mass to the material due to its catalytic effect on the formation of carbonaceous char.

Suprakas Sinha Ray et al. [104] added two types of organically modified layered silicates (OMLS) (montmorillonite (MMT) modified with octadecyl ammonium chloride and saponite (SAP) modified with quaternary hexadecyl tri nbutylphosphonium bromide) to PBS in different ratios (1.5, 2.5, 3.3, 4 and 5.5 wt.%) to determine the effect of its type on the properties of PBS. The results showed that both the concentration and type of surface modification affect the nanocomposite properties. Also, the addition of both types in a ratio of 3.3 wt.% improved the biodegradability of the compound compared to pure PBS, as the presence of clay facilitated the appearance of cracks that increased the surface area and thus increased attack by microorganisms, as shown in Figure 26, where PBS, PBSCN4, and PBSCN6 samples were examined after 35 days.

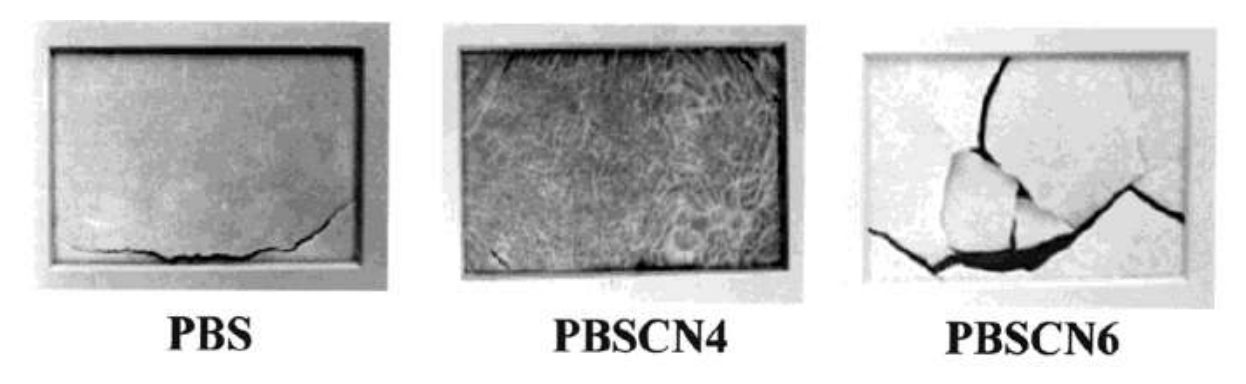


Fig. 26. Images of PBS, PBSCN4, and PBSCN6 sheets recovered from compost after 35 days [104]

In addition, the flame-retardant efficiency and smoke suppression were improved by modifying the surface and interface of tannin when preparing a nanocomposite consisting of PBS and ammonium polyphosphate particles (TFR). The results showed that the addition of 5 wt.% of TM led to flame retardation and a decrease in total smoke production compared to pure PBS by 30.8 % and 77.4 %, respectively [95].

The same effect of MMT can be seen when added to PLA as the results showed that DELLIT E 43B had a higher dispersion in the PLA matrix compared to DELLIT E 72T, as a result of the stronger interaction with PLA and thus obtaining higher thermal stability [88]. Also, increasing m-MMT content in the PLA matrix led to a decrease in molecular weight (M<sub>w</sub>) and an increase in the ability to decompose the polymer chains during the degradation process, as shown in Figure 27 [89].

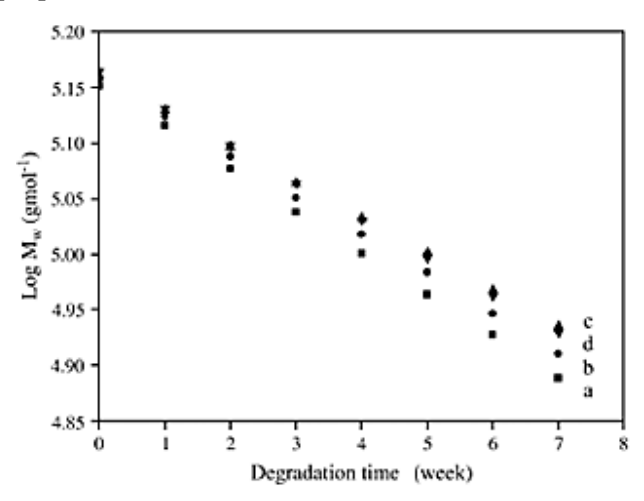


Fig. 27. Time dependence of weight average molecular weight (log Mw) of a) neat PLA matrix, b) 1.5 wt.% PLA/m-MMT, c) 3 wt.% PLA/m-MMT and d) 6 wt.% PLA/m-MMT degraded in PBS solution at 37.5 °C [89].

On the other hand, the thermal stability of PLA/TAC compounds increased in the presence of MMT, while decomposition was delayed due to the formation of cross-linked

structures that significantly reduced the mobility of the polymer chains when treated with an electron beam [103].

This also appeared when MMT was added to PLA/30 % TAF, as its addition led to an increase in thermal stability as a result of restricting the movement of the chains and impeding the decomposition process, as shown in Figure 28 [101].

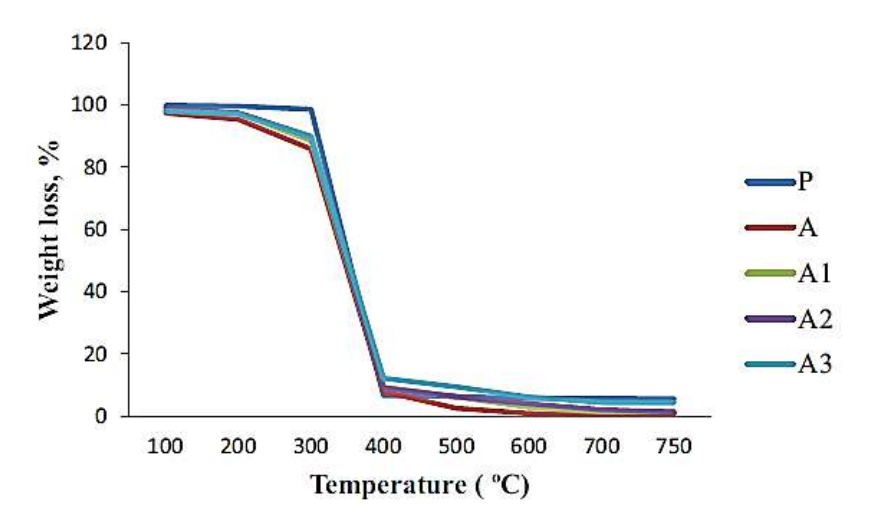


Fig. 28. TGA curve of PLA (P), PLA-30TAF (A), PLA-30TAF-1MMT (A1), PLA30TAF-2MMT (A2) and PLA-30TAF-3MMT (A3) [101]

#### 2.2.4. *Permeability and other properties of polyester/MMT nanocomposites*

Kazem Majdzadeh-Ardakani et al. [69] confirmed that adding 2 wt.% of two types of clays (ol -MMT and ol-30B) to PET led to a significant development in the barrier properties (increased by 53% for PET/ol-MMT and 74% for PET/ol-30B) as a result of good adhesion of the clay to the PET matrix [69].

One study showed that the presence of MMT delays the transmission of gas molecules in the PLA matrix due to the formation of a tortuous path (maze) that hinders its diffusion and thus improves the gas barrier properties, as shown in Figure 29 [87].

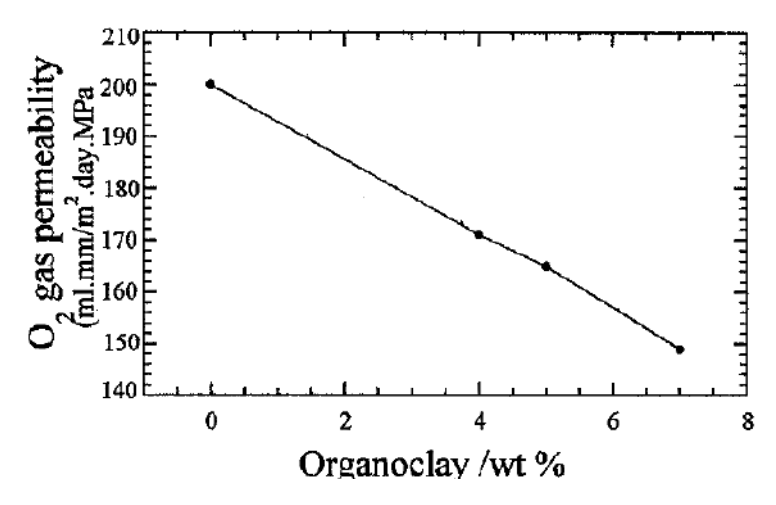


Fig. 29. Oxygen gas permeability of pure PLA and various PLACN [87]

The researchers indicated that the incorporation of 5 wt.% of CLO resulted in a decrease in oxygen permeability of about 30% [85]. The same results can be seen by adding MMT and halloysite in a small ratio, as it led to a decrease in the oxygen transmission rate by 33% when adding MMT and 16% when adding halloysite, while the opposite occurred when increasing the concentration of nanoclay. Furthermore, it was observed that the transparency of nanocomposites decreases when incorporating nanoclay, as the decrease reached 10% compared to pure PLA, and it also increases with the addition of more clay, as shown in Figure 30 [98].

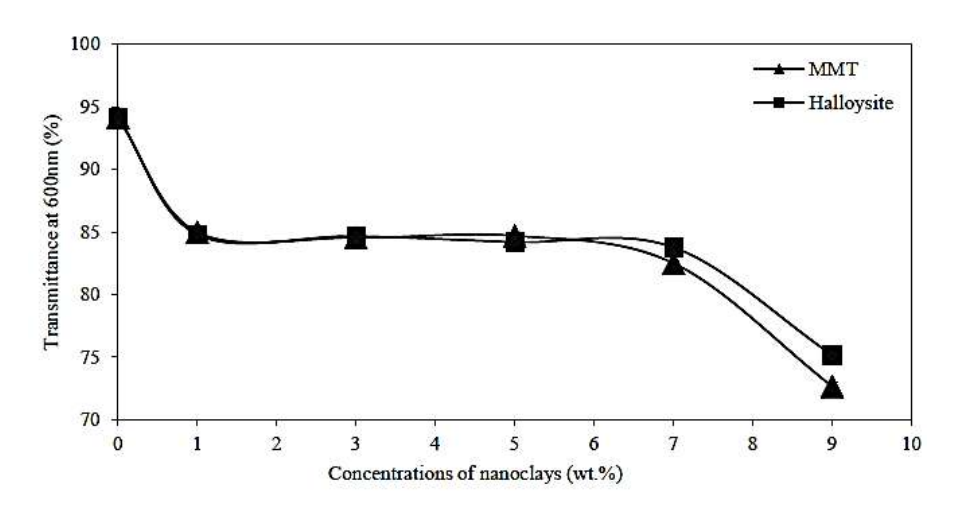


Fig. 30. Light transmittance (%) of PLA/MMT and PLA/Halloysite films [98]

In addition, it was found that an increase in the MMT ratio in PLA/30% TAF had an excellent effect on water resistance due to the formation of a clay barrier that restricted water flow in all paths and thus reduced water absorption [101].

Other studies revealed that increasing the amount of MMT in the PBS matrix led to an increase in the ability of material to store electrical charges in a stable way because the clay particles trap the charge carriers and thus inhibit their mobility, as shown in Figure 31 [79].

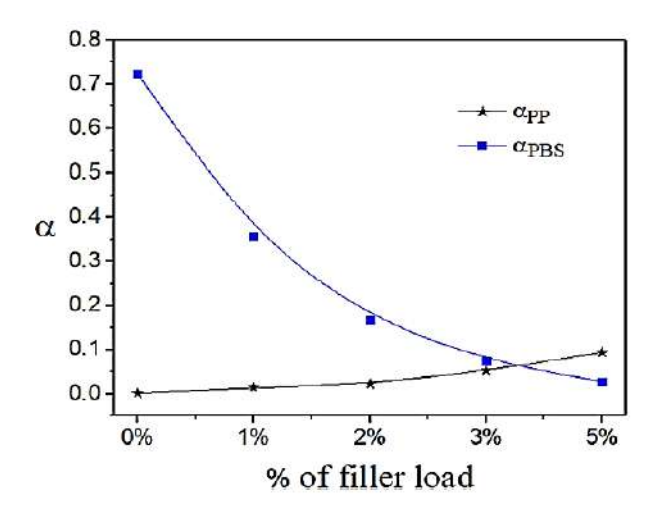


Fig. 31. Fraction a of the released charge as a function of fillers loads for PBS [79]

Polyester/MMT nanocomposites show enhanced electrical properties compared to pure polyester due to the incorporation of MMT nanoparticles. These properties can be tailored by controlling several parameters such as the type and concentration of MMT nanoparticles, the processing conditions and the compatibility between the polymer matrix and the nanoparticles [105–116].

# 2.3. Properties of recycled polyester/MMT nanocomposites

Polyester recycling offers many environmental benefits, including reducing the demand for fossil fuel-derived raw materials, conserving energy, and diverting waste from landfills. Additionally, recycling helps to mitigate pollution and greenhouse gas emissions associated with the production and disposal of virgin polyesters [20, 21, 117, 118]. Physical recycling is more commonly used for petroleum-based polyesters [119–122], while composting is used at the end of the life cycle for bio-based polyesters. However, bio-polyesters can also be recycled via physical recycling, conserving the energy invested in producing the material [117, 123, 124]. Since nanocomposites are more widely used in various fields of life, recycling different types of MMT-reinforced polyester nanocomposites has received great attention in recent years because it helps to reduce the amount of waste, energy consumption, environmental impact, and conserve resources [15, 16, 20, 125–127]. The recycling process can also affect the structure of the polymer, including its crystallinity, and thus influence the mechanical properties

of polymers [20, 21, 110, 128, 129]. So, Rizuan Mohd Rosnan et al. [130] studied the effect of MMT on the mechanical, thermal and morphological properties of recycled polyethylene terephthalate (rPET) and high-density polyethylene (HDPE) nanocomposites. They added MMT in a ratio of 1, 3, 5 wt.% to 70:30, 90:10 of rPET/HDPE using a single-screw extruder, then they used an injection moulding machine to prepare the test samples. The results revealed that the addition of MMT impacted the mechanical properties of rPET/HDPE as the tensile strength and impact strength of the nanocomposites increased when adding MMT up to 3 wt.% (24.9 MPa for 90:10, 34.8 MPa for 70:30 of rPET/HDPE) then decreased for the blends due to clay agglomeration, as shown in Figure 32.

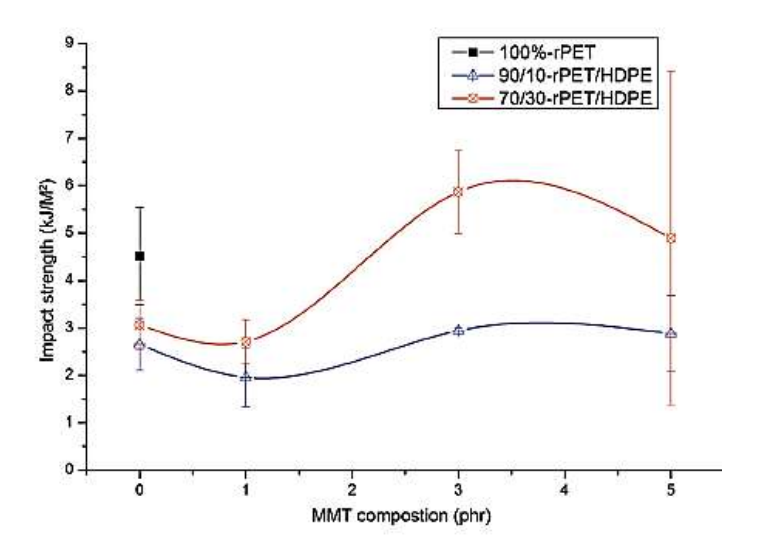


Fig. 32. Effect of MMT concentrations on impact strength at different rPET/HDPE ratios [130]

The presence of MMT led to a decrease in the tensile modulus and shear viscosity. Also, the results showed that due to the presence of MMT, there was an improvement in adhesion between the two phases by preventing coalescence and a decrease in interfacial tension, as the particles were dispersed, uniform, and smaller dimensions, as shown in Figure 33. Moreover, the incorporation of MMT improved the thermal stability of the nanocomposites as a result of the clay having good thermal stability.

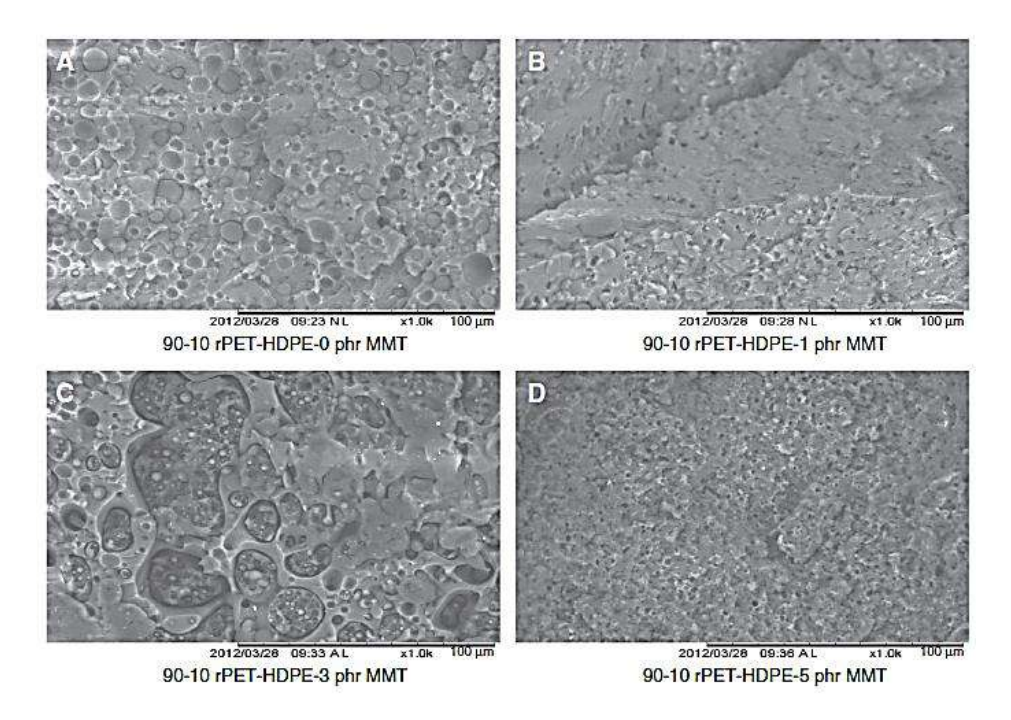


Fig. 33. Morphology of the fracture surface of 90:10 rPET/HDPE with A) 0 phr, B) 1 phr, C) 3 phr, and D) 5 phr [130]

A. L. F. de M. Giraldi et al. [131] also prepared a composite material from rPET with MMT modified with organophilic quaternary ammonium (2.5, 5 wt.%) using twin-screw extrusion at two different speeds (150 and 250 rpm) to study the effect of these speeds and MMT content on the thermal properties of the resulting nanocomposites. The results revealed that the presence of MMT led to an increase in the crystallization temperature and relative crystallinity of the material. Melting enthalpy for the first (ΔH<sub>m1</sub>) and second heating (ΔH<sub>m2</sub>) values increased with rising clay content at both speeds as they increased from 42 to 48 [J/g], and from 36 to 41 [J/g], respectively. This is because MMT had a nucleating effect without affecting the size and perfection of the crystals. Furthermore, there was a small decrease in glass transition temperatures from 78.5 °C to 74.1 °C when mixing the clay at 250 rpm and 150 rpm due to molecular mobility that led to the growth of existing crystals during the heating crystallization. It was noted that the rotation speed of the screw had an effect on the dispersion of the clay, as exfoliated clay platelets appeared at the low speed (150 rpm) as a result of the diffusion of rPET chains into the clay galleries, while at the higher rotation speed (250 rpm) some aggregates and platelets did not appear exfoliated.

The same can be seen when Mohd Zahidfullah Abd Razak et al. [132] prepared test samples composed of acrylonitrile-butadiene styrene (ABS) and rPET in a ratio of 70:30 and 30:70 with MMT (1, 3, 5 wt.%). The incorporation of MMT led to an increase in both tensile

and flexural strength, at the best results were achieved at 1 wt.% of MMT, and above that, a decrease was observed in the abovementioned properties. Increasing the ratio of MMT up to 3 wt.% resulted an increase in the tensile and flexural modulus for both blends (70:30, 30:70). It was noted that this addition led to a decrease in the impact strength as a result of the freezing of the macromolecular chains by the MMT particles, which led to an inability to adapt to deformation.

Furthermore, MMT affected the melt flow rate, as increasing the clay content led to a decrease for 30:70 ABS/rPET, while it increased for the 70:30 ABS/rPET because increasing the ratio of exfoliated nanoclay led to a decrease in the viscosity of the polymeric nanocomposite, as shown in Figure 34.

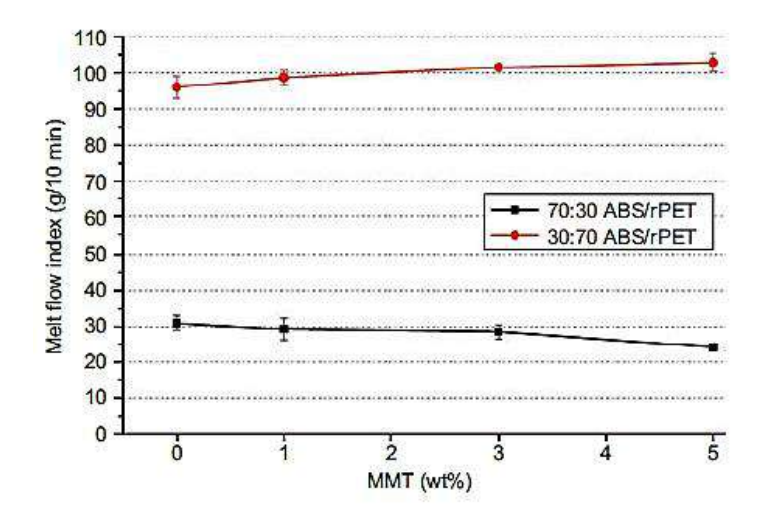


Fig. 34. Effect of MMT concentrations in different ABS/rPET ratios on the melt flow rate [132]

The addition of clay to the 30:70 ABS/rPET compound achieved good distribution and dispersion due to the proper adhesion of the MMT in the polymer matrix, however agglomeration and phase separation occurred in the 70:30 ABS/rPET compound.

To find out the effect of OMMT on virgin and recycled PLA, Lakhdar Sidi Salah et al. [133] mechanically recycled PLA and then added 2, 4 wt.% of OMMT to it. The results showed that adding clay improves the thermal stability of both virgin PLA and recycled PLA as a result of the good dispersion of the clay, thus forming a barrier to the liberation of thermal decomposition products. It also showed an improvement in the microhardness of both types of nanocomposites due to restricting the movement of molecular chains, as shown in Figure 35. It was observed that increasing the thickness of the samples and increasing OMMT content in PLA matrix led to enhanced in energy absorption, as it was higher in the samples containing

rPLA (20.3%) than rPLA (14.5 %) due to the shortening of the polymer chains resulting from reprocessing.

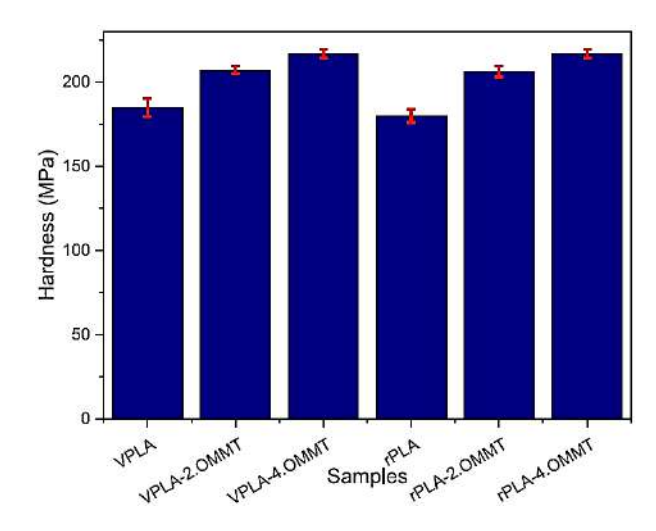


Fig. 35. Microhardness of PLA-based materials [133]

## 2.4. Critical review of literature, aims of the thesis

From the overview of the literature, it is evident that polyesters, whether petroleum-based (PET and PBT) or bio-based (PLA and PBS), have significant potential for various industrial applications due to their mechanical properties, chemical resistance, recyclability and thermal resistance. Bio-based polyester alternatives are gaining importance due to their sustainability and low environmental footprint. These different polyesters have shown distinct behaviours in terms of crystallization, degradation, and mechanical properties.

Also, the incorporation of MMT nanoparticles in amounts as small as 5% has been demonstrated to significantly change the morphology and crystallization behaviour of polyester matrices. However, these effects are highly dependent on the type of polyester, cooling rates and processing conditions. Studies indicate that MMT acts as an effective nucleating agent, improving the crystallization rate and thermal stability of nanocomposites. For example, PET/MMT nanocomposites exhibit enhanced crystallization rates due to the influence of MMT particles, leading to improved thermal properties. Similarly, PBT/MMT nanocomposites exhibit improved thermal and mechanical properties due to the fine distribution of MMT particles.

One key observation from the reviewed literature is that mechanical performance benefits from MMT reinforcement, but the effects vary depending on the type of polyester and the degree of MMT dispersion within the matrix. MMT addition generally enhances tensile strength

and stiffness while sometimes reducing impact strength due to particle agglomeration. For example, PLA/MMT nanocomposites show improved tensile strength but suffer from reduced flexibility, highlighting the contradictory effects of MMT.

Although significant progress has been made in understanding the role of nanofillers in polyester composites, there remain critical gaps, such as enhancing interfacial adhesion between the polymer matrix and MMT, improving nanoclay dispersion, and reducing agglomeration during addition, which can negatively impact material properties. Additionally, inconsistencies in properties across different polyester types indicate a need for specifically designed protocols to achieve maximum performance.

The literature also confirms the environmental and economic significance of recycling polyester materials, as it reduces waste, minimizes carbon footprint, and saves resources. However, recycling often changes the polymer chain structure, resulting in changes in the mechanical and thermal properties of polyesters, including impact strength and modulus of elasticity, which may impact their reusability in high-performance applications.

Recycling polyester/MMT nanocomposites introduces an additional complexity, as the recycling process affects both the polymer matrix and the dispersion of MMT particles. The recycling can lead to chain scission in the polymer matrix, reducing molecular weight and changing crystallinity. However, MMT can mitigate some of these effects by acting as a physical barrier to molecular mobility. Despite the critical role that recycling plays in the design of sustainable materials, the literature has not widely addressed this field, especially the recycling of PBT, PBS and their nanocomposites.

Based on these observations, the primary objective of this thesis is to provide a comprehensive investigation into the effects of recycling and MMT nanoclay enhancement on the morphological, crystalline, and mechanical properties of bio- and petroleum-based polyesters, specifically PET, PBS, PBT, and PLA. The primary aims include:

- Analyze how repeated recycling affects the structural integrity and mechanical performance of polyester matrices.
- Evaluate the role of MMT in modifying the crystallization behaviour and mechanical properties during recycling under different cooling rates and processing conditions.
- ➤ Study the structural and morphological changes in polyester/MMT composites using advanced characterization techniques such as SEM and WAXD and determine how reprocessing changes MMT dispersion.

➤ Compare the performance of bio-based polyesters (PLA and PBS) with their petroleum-based counterparts (PET and PBT) under identical recycling conditions.

- > Evaluate the sustainability and industrial viability of recycled polyester nanocomposites for long-term applications.
- > Provide insights into optimizing processing parameters to minimize material degradation and maximize recyclability.
- > Develop more sustainable composite material recycling strategies for industrial applications.

#### 3. MATERIALS AND METHODS

In this section the applied materials and processing methods will be introduced.

#### 3.1. Materials

Table 9 shows the type, origin and melt flow rate (MFR) values of the two petroleum-based polyesters and the two bio-based polyesters tested.

Table 9. Tested polyesters

Name	Origin	Type (Producer)	MFR test parameters	MFR value*	
PET	Petroleum-based	Neopet 80 (Neogroup)	260 °C / 1.2 kg	21 g / 10 min	
РВТ	Petroleum-based	Pocan B1305 (Lanxess)	250 °C / 2.16 kg	47 cm <sup>3</sup> / 10 min	
PLA	Bio-based	Ingeo 3100 HP (Natureworks)	210 °C / 2.16 kg	24 g / 10 min	
PBS	Bio-based	BioPBS FZ91PM (PTT MCC Biochem)	190 °C / 2.16 kg	6 g / 10 min	

<sup>\*:</sup> based on technical data provided by manufacturers.

Nanomer I.30P-type (Nanocor, USA) montmorillonite (MMT) nanoclay treated with 28-32 wt.% octadecyl-ammonium was used with the abovementioned types of polyesters. The polymers were processed and examined with 6 wt.% MMT and without any nanoclay reinforcement. Most studies [77, 89, 93, 102, 134, 135] have revealed that MMT loading level in the range of 4-6 wt.% is usually used to improve mechanical properties.

#### 3.2. Methods

#### 3.2.1. Sample preparation

All materials were carefully dried before the processing steps. The drying times/temperatures used were: for PET 160 °C/4 h; for PBS 80 °C/5 h; for PBT 120 °C/4h and for PLA 90 °C/5 hours. The MMT additive was also dried at 100 °C/4 h before processing.

To prepare samples the materials were first processed with a Labtech 26-44 twin-screw extruder (Labtech Engineering, Thailand) with a screw diameter of 26 mm and an L/D ratio of 48 was used, with melt temperatures ranging between 250-270 °C for PET, 240-250 °C for PBT, 150-170 °C for PBS and 180-190 °C for PLA and a screw speed of 55 rpm in all cases.

The extrusion step was repeated again to simulate reprocessing (1X extr and 2X extr specimens).

After that, injection moulding was used to make morphological and mechanical test specimens (60×60×2 mm³). A 50 MEtII electric injection moulding machine (Mitsubishi, Japan) was used with the following parameters: mould temperature: 60 °C; injection speed: 60 - 65 mm/s, holding pressure 50 bar for 10 sec. The zone temperatures were between 260-280 °C for PET, 250-260 °C for PBT, 160-170 °C for PBS and 190-200 °C for PLA as shown in Figure 36.



Fig. 36. Injection moulded test specimens: a) PET; b) PBS; c) PBT; d) PLA

#### 3.2.2. Measurement methods

## 3.2.2.1. Intrinsic viscosity (IV)

Intrinsic viscosity values were measured at 30 °C in a 60/40 weight mixture of phenol/tetrachloroethane solvent with a concentration of 0.5 g/dl to determine the effect of recycling on the molecular weight of the polymers and their degradation, using an RPV-1 automatic solution viscometer (PSL Rheotek, USA) according to ASTM D4603 standard.

## 3.2.2.2. Melt flow Index (MFI)

The mass flow rate (MFR) was measured using an LMFI-2LENNCN-type melt flow index meter (Dynisco, Germany). Prior to the measurements, the polymers were dried in an Une 200-type drying oven (Memmert, Germany) for 4 hours at the following temperatures: 80 °C for PBS, 120 °C for PBT, 160 °C for PET, and 90 °C for PLA. The MFR measurements were carried out under the following conditions: PBS at 190 °C with a 2.16 kg load, PBT at 250 °C with a 2.16 kg load, PET at 260 °C with a 1.20 kg load, and PLA at 210 °C with a 2.16 kg load.

# 3.2.2.3. Differential Scanning Calorimetry (DSC)

To measure temperature related physical changes, a DSC 131 EVO device (Setaram, France) was used. The measurements were carried out in a nitrogen atmosphere with a flow rate of 50 ml/min, and the weight of the examined samples ranged between 10-15 mg. To determine the melting and crystallization temperatures, one heating and one cooling ramp were applied both with a rate of 10 °C/min and 1 °C/min, the temperature range was between 20-320 °C for all materials. The initial crystallinity percentage (CRF) of PET, PBT, PBS, and PLA [%] was calculated according to equation 1, where  $\Delta H_m$  is the melting enthalpy of the sample [J/g],  $\Delta H_{cc}$  is the enthalpy of cold crystallization [J/g] and  $\emptyset_{MMT}$  is the mass ratio of MMT. The term  $\Delta H_m^0$  is a reference value corresponding to the melting enthalpy of a 100% crystalline polymer, which is 140 J/g for PET [136]; 195 J/g PBS [137]; 145 J/g for PBT [138] and 93 J/g for PLA [139].

$$CRF \ [\%] = \frac{\Delta H_m - \Delta H_{CC}}{\Delta H_m^0 (1 - \emptyset_{MMT})} \ .100 \ \%$$
 (1)

Crystallization characteristics were also investigated using a non-isothermal DSC program where the samples were heated from room temperature to +30 °C above their melting

temperature (T<sub>m</sub>) at a rate of 20 °C/min. Their thermal history was erased by holding them at that temperature for 4 minutes. After that, the temperature was cooled to 0 °C at various cooling rates (2.5, 5, 10, 20, and 40 °C/min) then heated with a rate of 20 °C/min.

#### 3.2.2.4. Izod impact test

To measure the Izod impact strength of the polymer composites, a V-shaped notch was made in the specimens and they were tested by a 5113.10.01 type (Zwick, Germany) impact tester. The samples were examined at room temperature according to the ISO 179-1 standard with a pendulum energy of 2.75 J. The tests were replicated 10 times for each composition. The specimens were 50 x 8 x 2 mm<sup>3</sup>.

#### 3.2.2.5. 3-point-bending test

To determine the value of flexural strength and modulus, a three-point bending test according to ISO 178 standard was performed using a universal mechanical tester L3369 (Instron, USA). The span was 32 mm, the crosshead speeds were 1 mm/min for modulus determination, and 10 mm/min for other calculations, respectively.

# *3.2.2.6.* Shrinkage

In-plane shrinkage was calculated after one day for all injected test samples in both directions (transverse and flow) by measuring the specimen dimensions with a CD-15APX-type (Mitutoyo, Japan) digital caliper. The weight of the samples was also measured by an AS 60/220.R analytical balance (Radwag, Poland) to determine the density. The volume shrinkage was calculated from the equation 2. The thickness change was measured by an MDC-25PX-type (Mitutoyo, Japan) digital micrometer.

$$Volume\ shrinkage = \frac{V_m - V_{sp}}{V_m} = \frac{l_t^m * l_f^m * t^m - l_t^{sp} * l_f^{sp} * t^{sp}}{l_t^m * l_f^m * t^m} \tag{2}$$

where  $\Delta l_t^{sp} = l_t^m - l_t^{sp}$  is the change of the specimen length in the transverse direction,  $\Delta l_f^{sp} = l_f^m - l_f^{sp}$  is the change of the specimen length in the flow direction and  $\Delta t^{sp} = t^m - t^{sp}$  is the change of the specimen thickness.  $l_t^m$ ,  $l_f^m$  and  $t^m$  are the mould length in the transverse direction, in the flow direction and the mould thickness, respectively. While  $l_t^{sp}$ ,  $l_f^{sp}$  and  $t^{sp}$  are the length of the specimen in the transverse direction, in the flow direction and the thickness, respectively.

#### 3.2.2.7. Scanning Electron Microscopy (SEM)

The morphological properties of the composites were characterized from the fractured surface of the injection moulded specimens after Izod impact test by SEM. Samples were prepared and then 6 nm gold coating was applied to them. An EVO MA 10 instrument (Zeiss, Germany) at an accelerating voltage of 15 kV was used on the samples. Energy dispersive spectroscopy (EDS) (AMETEK, OCTANE PRO) was used in conjunction with SEM to provide information about the elemental composition of a sample.

## 3.2.2.8. Wide-angle X-ray scattering (WAXD)

Basal spacing measurements of MMT platelets in the injection moulded specimens were performed using a MiniFlex II (Rigaku, Japan) device with a Cu Kα target at room temperature within the 2° to 90° range. 30 kV was used to run the X-ray generator at a scan speed of 2°/min. From the (001) peak, the interlayer spacing (d<sub>hkl</sub>) was determined using Bragg's Law.

$$n\lambda = 2d \sin \theta$$
 (3)

where:  $\lambda$  is the wavelength of the incident X-ray beam, which has a value of 1.54 Å, n is an integer known as the order of the reflection, d is the distance between the crystal planes and  $\theta$  is the angle between the incident X-ray beam and the crystal plane. The Scherrer equation (equation 4) was also used to determine the crystal size (D).

$$D = \frac{K\lambda}{\beta \cos \Theta} \tag{4}$$

where  $\beta$  is the full width at half-maximum of the peak and k is a constant (usually 0.9).

## 3.2.2.9. Dynamic Mechanical Analysis (DMA)

A Q800-type dynamic mechanical analyzer (DMA) with a three-point bending head (TA Instruments, Inc., New Castle, DE, USA) was used to determine the glass transition temperature ( $T_g$ ) of the nanocomposites. The specimens were 50 x 10 x 4 mm<sup>3</sup>. PET, PBS, PBT and PLA nanocomposites were tested at temperatures ranging from 30-80 °C, -60-100 °C, 30-150 °C and 30-70 °C, respectively. For each specimen, the heating rate was 2 °C/min. The measurements had an amplitude of 15  $\mu$ m and a frequency of 1 Hz.

#### 3.2.2.10. Rheological tests

An ARES G2-type oscillation rheometer (TA Instruments, Inc., New Castle, DE, USA) with a 25 mm diameter sheet-sheet measurement head and a 1 mm gap size setting was used to

perform the rheometric tests. At 5 % deformation, the polyesters and nanocomposites were tested in the frequency range of 0.05- 300 rad/s. Two parallel measurements were done in each case, and their average was calculated. A complex viscosity value as a function of frequency was displayed after the values were fitted using the Carreau-Yasuda model.

### 4. RESULTS AND DISCUSSIONS

The results obtained are discussed in detail in the following chapter.

## 4.1. Degradation of the polyesters during reprocessing

The intrinsic viscosity of each type of polyester used was measured before and after the extrusion steps to monitor material degradation during multiple reprocessing. Measurements were only performed on the matrices of polyesters without adding MMT so that MMT would not affect the flow times during the measurement. It was also assumed that the nanocomposites containing MMT and without MMT were subjected to similar stresses during processing as a result of being treated with the same parameters. The measured results can be seen in Table 10.

Name	IV of original materials [dl/g]	IV of 1X extr samples [dl/g]	IV of 2X extr samples [dl/g]	
PET	$0.79 \pm 0.01$	$0.69 \pm 0.01$	$0.67 \pm 0.01$	
PBS	$1.49 \pm 0.01$	$1.48\pm0.01$	$1.46\pm0.01$	
PBT	$0.84 \pm 0.01$	$0.83\pm0.02$	$0.82\pm0.01$	
PLA	$1.24\pm0.02$	$1.20\pm0.01$	$1.17\pm0.02$	

**Table 10.** Effect of reprocessing on IV of PET, PBS, PBT and PLA

The intrinsic viscosity results showed that reprocessing had a different effect on the intrinsic viscosity of the different types of polyesters. It can be seen that reprocessing had no noticeable effect on the IV of PBS and PBT as the decrease after the second extrusion was only about 2 %. While PET had a significant decrease in IV, about 13 % after the first extrusion and 16 % after the second extrusion. For PLA, the decrease was 3 % after the first extrusion and 5% after the second, meaning that PET showed the highest degradation due to its high melting point and processing temperature, which makes it more prone to chain scission during processing [140, 141].

Furthermore, ammonium-modified MMT is known to decompose at high temperatures, generating acidic sites that enhance polymer degradation [142]. Therefore, although direct IV measurements were not performed on nanocomposites, the observed degradation trends for polyesters suggest that MMT may amplify this effect when present, especially in PET/MMT nanocomposites. In addition, melt flow index (MFI) measurements were performed and the

results, shown in the Appendix (Figure 65), were evaluated to further understand the degradation behaviour upon both MMT addition and recycling.

## 4.2. Shrinkage characteristics of injection-moulded samples

The results showed that the addition of MMT and recycling had an effect on shrinkage in both directions (transverse direction (TD) and flow direction (FD)) compared to the neat polyester. Figure 37 shows the measured mould shrinkage parameters of injection moulded plate specimens. It was found that PBS and PBT had higher shrinkage than PET and PLA.

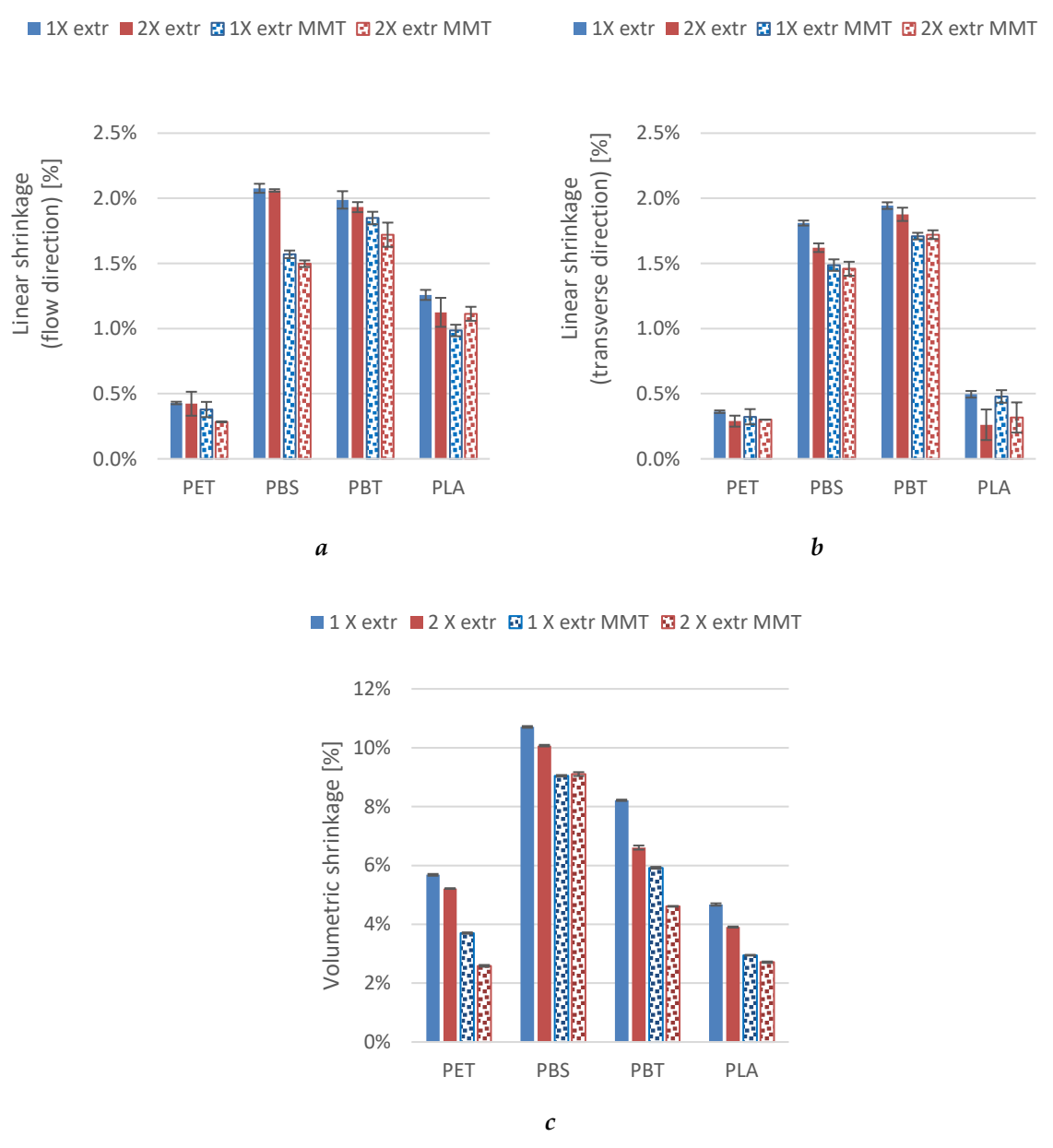


Fig. 37. Shrinkage of the injection-moulded polyesters and polyester/MMT-nanocomposites after 1X and 2X reprocessing (a) flow direction (FD); b) transverse direction (TD); c) volumetric shrinkage

A reduction of shrinkage occurred when MMT was incorporated into the polyester matrix in all cases: after the first treatment, the linear shrinkage decreased by 0.01-0.5% and the volumetric one decreased by 1.7-2.3%. The same result can be seen after 2x extrusion, where the linear shrinkage decreased by 0.01-0.6%, and the volumetric by 1.0-2.6% for the different materials, as shown in Figure 38.

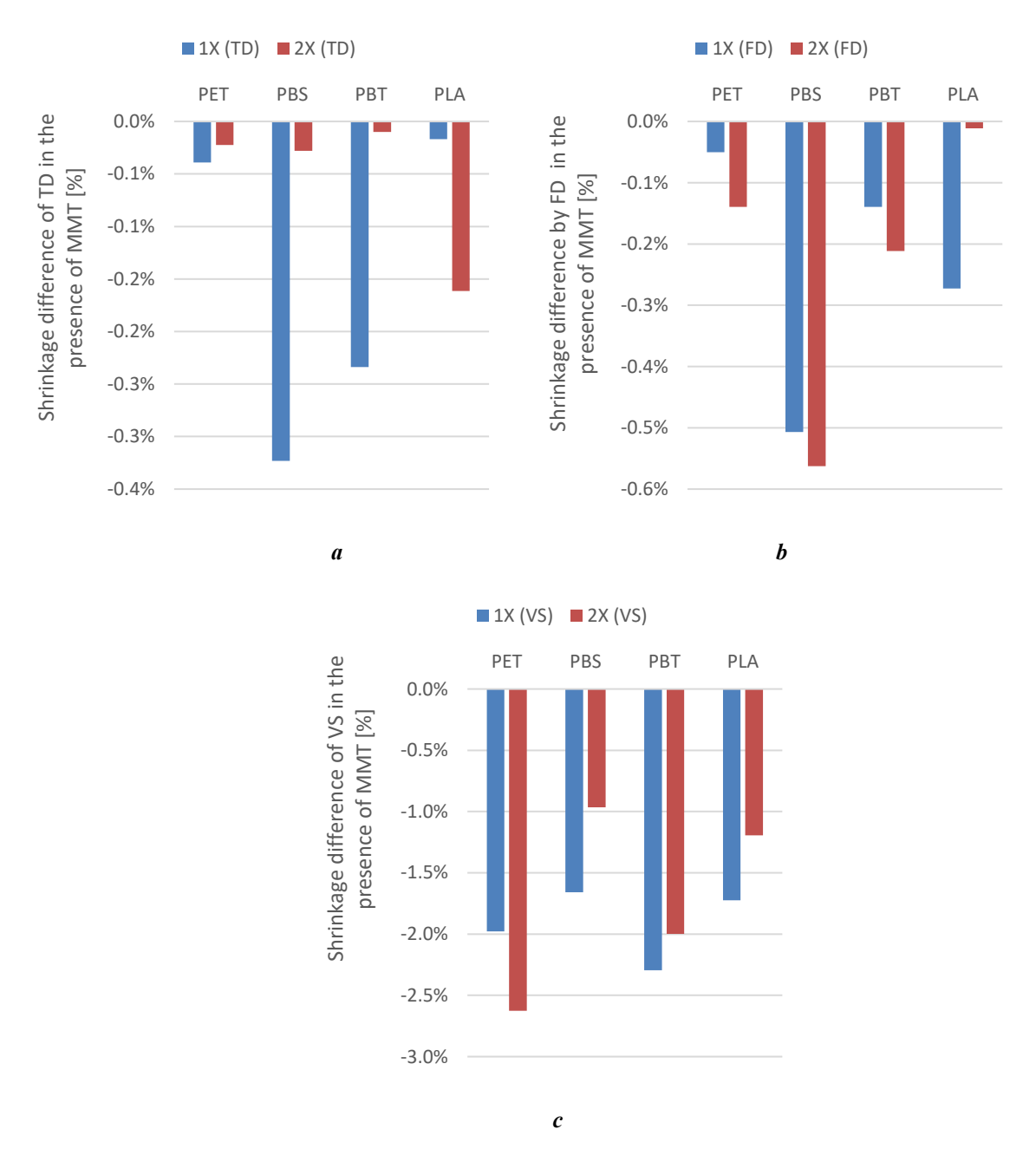


Fig. 38. Effect of the presence of MMT on the reprocessing of different polyesters a) transverse direction;
b) flow direction; c) volumetric shrinkage

Figure 39 shows that if the materials are recycled without MMT, the shrinkage in the transverse and the flow directions decreases by 0.1-0.2% and the volumetric shrinkage by 0.5-1.6%. While the decrease in shrinkage between the first and second processing was smaller for

the MMT-reinforced polyester nanocomposites, as it was between 0.01-0.1% in the case of linear shrinkage and 0.2-1.6% for volumetric shrinkage. Except for PLA, in which case the shrinkage decreased by 0.16% in the transverse direction, while the shrinkage increased in the flow direction by 0.13%.

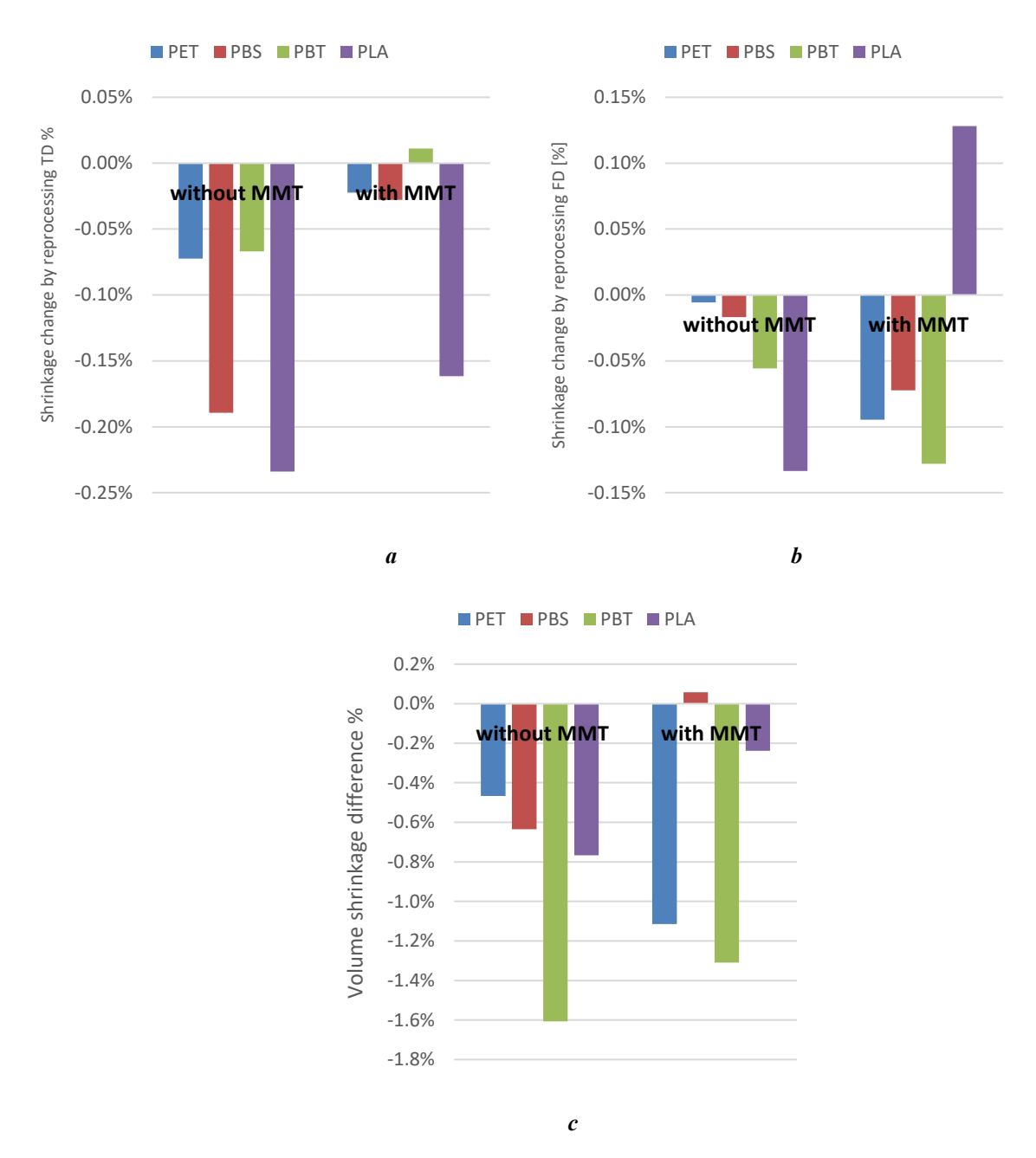
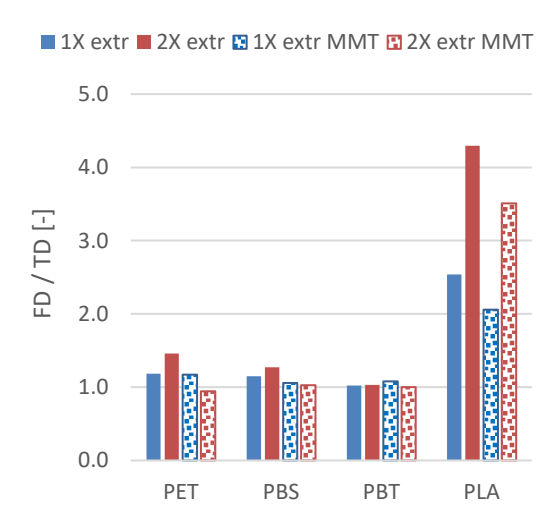


Fig. 39. Effect of reprocessing on the shrinkage difference a) TD; b) FD; c) volumetric shrinkage change.

The difference in shrinkage in the in-plane directions is characterized by the FD/TD ratio that indicates anisotropy. This ratio ranges from 0.9 to 1.5 for PET, PBS, and PBT, but for PLA it increases after the first processing to 2.1-2.5 and further to 3.5-4.3 after the second processing, as shown in Figure 40. For PLA, the relatively small wall thickness (2 mm) and the significantly

lower mould temperature used (60 °C) rather than the temperature recommended by the manufacturer (80-130 °C) could lead to a strong orientation of the molecular chains in the flow direction, which leads to greater relaxation of the chains thus higher shrinkage [143].



**Fig. 40.** FD/TD ratio of the shrinkage of the injection-moulded polyesters and polyester/MMT-nanocomposites after 1x and 2x reprocessing

The volume and mass of the samples were measured 24 hours post-production. It was found that reprocessing had a noticeable effect on the mass. A negative relationship was found between mass and volumetric shrinkage for all types of polyesters tested as in Figure 41. This can be attributed to the structural changes that occur during post-shrinking time, as the polyester chains rearrange and get closer to one another, reducing the space available for shrinkage thus the result is a low shrinkage.

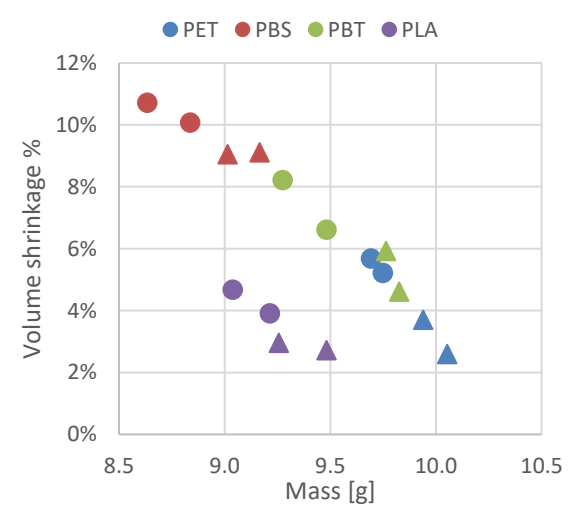


*Fig. 41.* Volume shrinkage as a function of mass in the case of different polyesters (•: without MMT, ▲: with MMT; the colours indicate the type of material)

# 4.3. Rheological properties

Figure 42 shows the effect of reprocessing and MMT addition on the complex viscosity of injection moulded samples. A rotational rheometer was used at the frequency range of 0.5-500 rad/s. The results showed that the viscosity values ranged from 300-3000 Pa for each sample. It was also revealed that all samples had shear thinning behaviour over the studied range. For PET, the complex viscosity of the sample after the first processing (1X extr) was the highest in the entire range. Similarly, reprocessed PET without MMT (2X extr) had a similar behaviour but with a slightly lower viscosity. When MMT was added, the complex viscosity decreased by 10-20% compared to materials without nanoclay. The significant decrease in viscosity can be attributed to the degradation of the polymer chain, which reduces the molecular weight of PET by 13-15% and the effect of MMT cannot compensate for this loss [144, 145]. PBS showed a similar behaviour, but on a much lower scale where the unreinforced samples had a higher viscosity than the PBS/MMT nanocomposites. Also, recycling of PBS and PBS/MMT increased the viscosity, but the viscosity values of all samples remained close to each other. Regarding PLA and PBT, the opposite happened as the viscosity increased with the addition of MMT more than it decreased due to degradation, especially at low frequencies. The viscosity values were almost similar for each sample of these materials at the upper end of high frequencies. Recycling also decreased the viscosity of the unreinforced polyester materials. However, their nanocomposites (PBT/MMT and PLA/MMT) behaved differently as recycling provided better dispersion of MMT, which enhanced its reinforcing effect, thus the viscosity increased with decreasing frequencies [146, 147]. Their curves did not converge to a constant value at these frequencies. The viscosity, when MMT was combined with both PLA and PBT, was higher than that of the samples without MMT addition at low frequencies.

The shape of the curves of the unreinforced samples of PET, PBT, and PLA was like a conventional rheology curve (shear thinning), while the samples reinforced with MMT showed an almost linear decrease over the examined frequency range. In the case of PBS, all the curves of the reinforced and unreinforced samples resembled the conventional rheological curve. In addition, the results showed that the plateau phase was not obvious near the minimum of the frequency range for all materials, but the shape of the curves was close to it. Because of the interparticle interaction of MMT, non-Newtonian behaviour was also observed at lower frequencies.

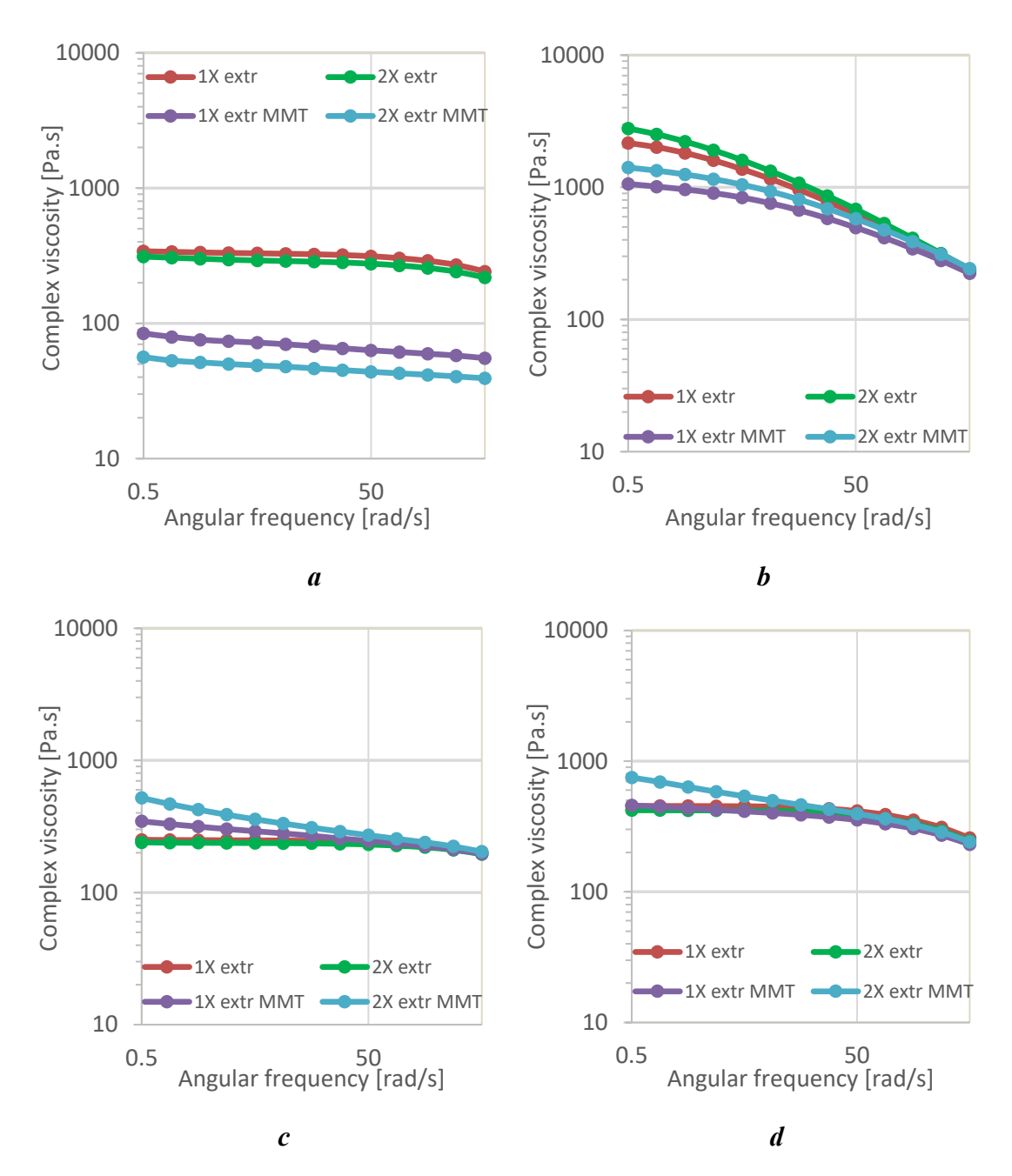


Fig. 42. Effect of recycling and adding MMT on the complex viscosity of various types of polyesters and polyester/MMT nanocomposites (a) PET, b) PBS, c) PBT and d) PLA)

The storage modulus (G') was also measured as a function of angular frequency for the polyesters and their nanocomposites (Figure 43), and it was found that the storage modulus has opposite trends of the viscosity curves. The storage modulus values for all materials without MMT were almost identical, while there was a difference in the values when MMT was applied. This difference was minor for the PET and PBS nanocomposites, while the contrast was significant for the PBT and PLA materials. The inclusion of MMT in these latter polyesters (PBT and PLA) led to a higher storage modulus due to the enhancing effect of the nanoparticles

resulting from the network formed by MMT within the polyester matrix. Also, the recycling of these nanocomposites improved the storage modulus, as the higher values were for the recycled samples due to the improved dispersion of MMT in the matrix. Higher storage modulus was obtained when recycled in the presence of MMT in all samples except PET. This indicates that MMT not only enhances the polymer matrix but also mitigates the negative effects of thermal degradation during repeated extrusion. The storage modulus values of the reinforced materials of PBT and PLA were greater than the unreinforced materials, while the opposite was observed for PET and PBS.

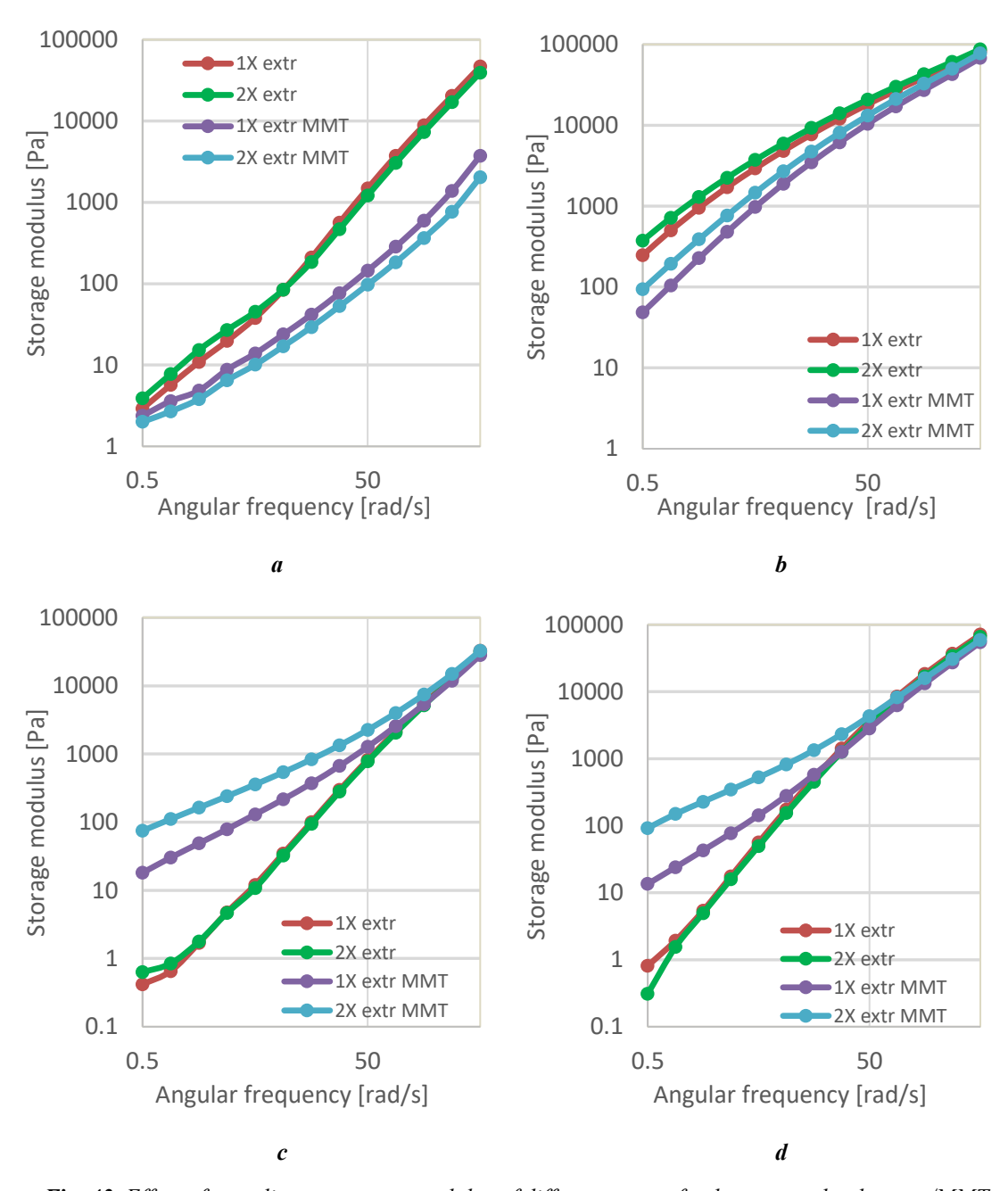


Fig. 43. Effect of recycling on storage modulus of different types of polyesters and polyesters/MMT nanocomposites (a) PET, b) PBS, c) PBT, d) PLA)

Figure 44 shows the creep compliance investigation of polyesters used with and without MMT addition before and after recycling. It was observed that the difference between the creep compliance of pure polyesters before and after recycling was very small for both PBS, PBT and PLA. That is, the molecular weight has no significant effect on the compliance, thus there is no significant change in molecular weight. But if there is a significant change, it has a notable effect on the viscosity of the material in the melt state over time. It was also found that the incorporation of MMT with PBS, PBT and PLA enhanced their creep resistance because the MMT molecules limited the movement of the chains, so the compliance of the MMT-filled materials was lower than the pure materials. The combined effect of reprocessing and MMT addition resulted in the lowest compliance values, indicating better MMT dispersion and more elastic behaviour.

On the other hand, PET had a different behaviour from the other polymers. In contrast to what was measured for PBS, PBT and PLA, pure PET showed lower compliance than its nanocomposites. Recycling reinforced samples also resulted in higher compliance. This is consistent with the results obtained for viscosity, where PET behaved inversely to the other three materials (PBS, PBT and PLA) on the viscosity curve. The zero-viscosity value can be inferred from the linear section of the creep curves.

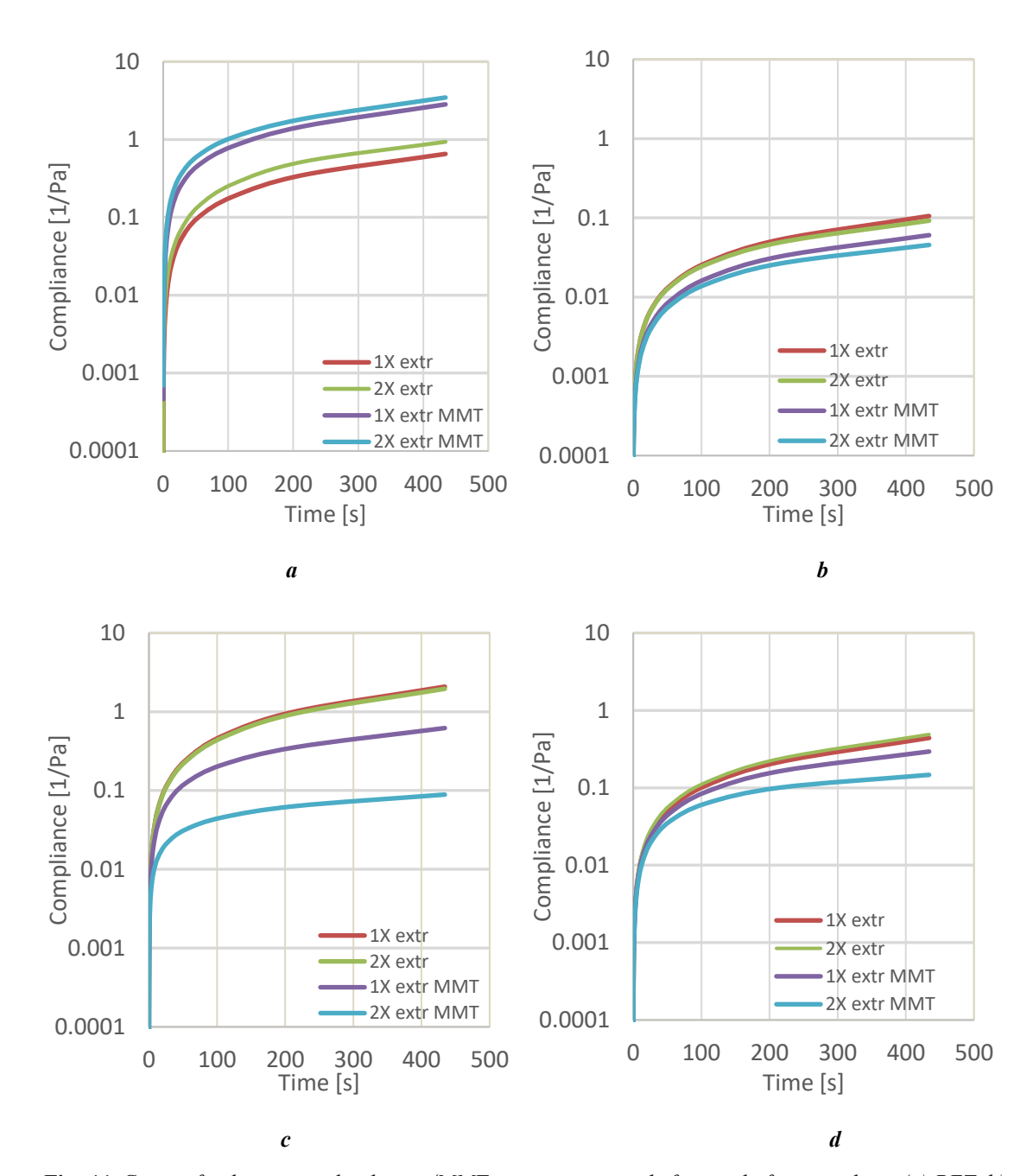


Fig. 44. Creep of polyesters and polyester/MMT nanocomposites before and after recycling: (a) PET, b)

PBS, c) PBT, d) PLA)

# 4.4. Crystallization properties of polyesters and polyester/MMT nanocomposites

Figure 45 presents the differential scanning calorimetry (DSC) heating curves of the used polyesters and their nanocomposites. These curves provide insights into the thermal behaviour of the polymers, specifically their melting behaviour and crystalline structure. The curves indicate the melting temperatures (T<sub>m</sub>) of the polymers, which serve as critical indicators of their thermal stability and crystallinity. Both reprocessing and the addition of MMT

reinforcement were observed to have a minor effect on the Tm. The changes in  $T_m$  can be attributed to structural modifications or interactions between the polymer matrix and MMT particles during thermal cycles.

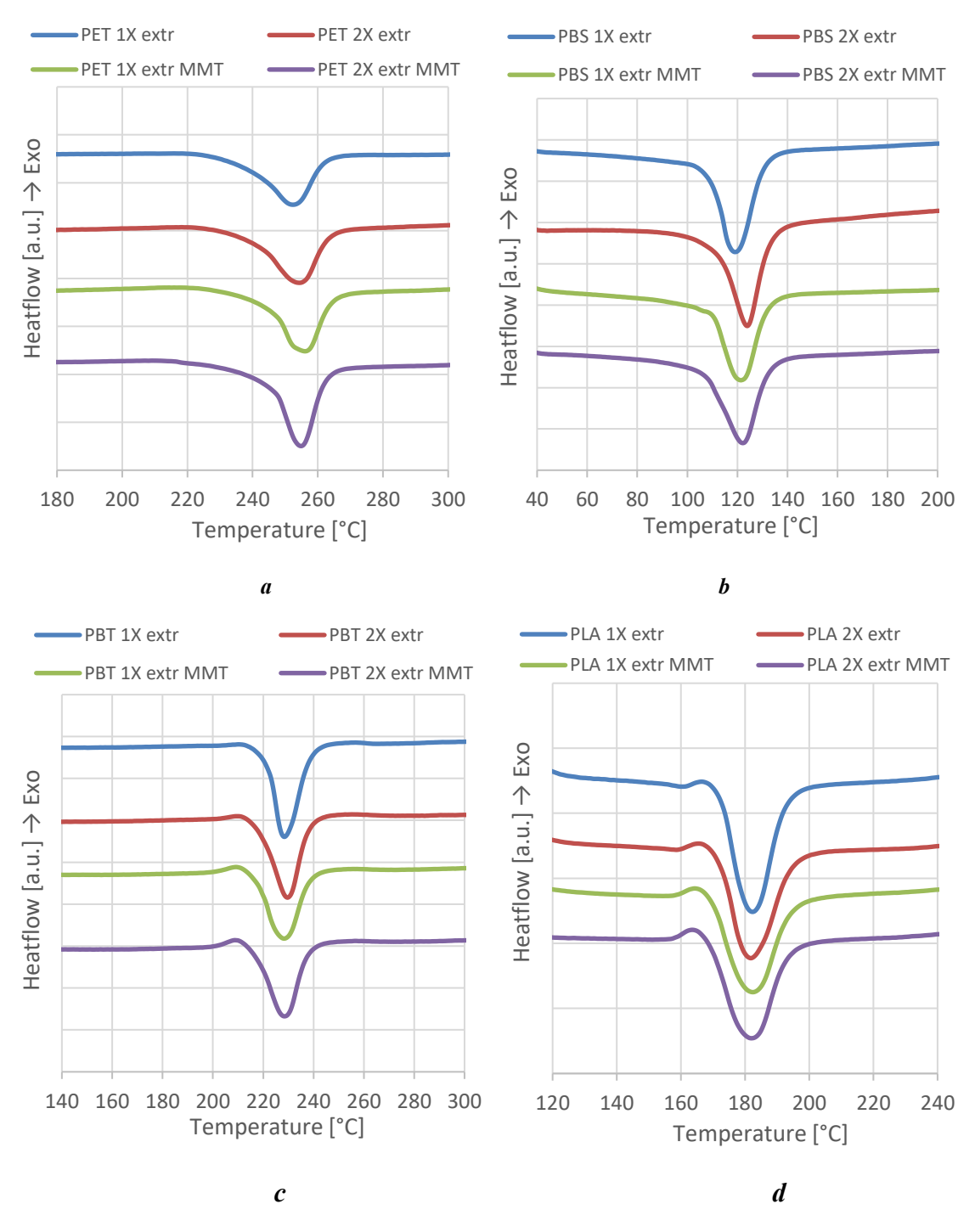


Fig. 45. DSC heating curves of the samples (a) PLA; b) PET; c) PBT; d) PBS)

Figure 46 displays the cooling curves of the samples. These curves highlight the crystallization behaviour of the polymers during the cooling (the onset and peak temperatures). Differences in cooling behaviour provided information about the structural changes or improvements in crystalline phases due to additives and thermal cycling.

Overall, Figures 45 and 46 illustrate how the structural properties of polyesters are affected by external factors such as reprocessing and reinforcement.

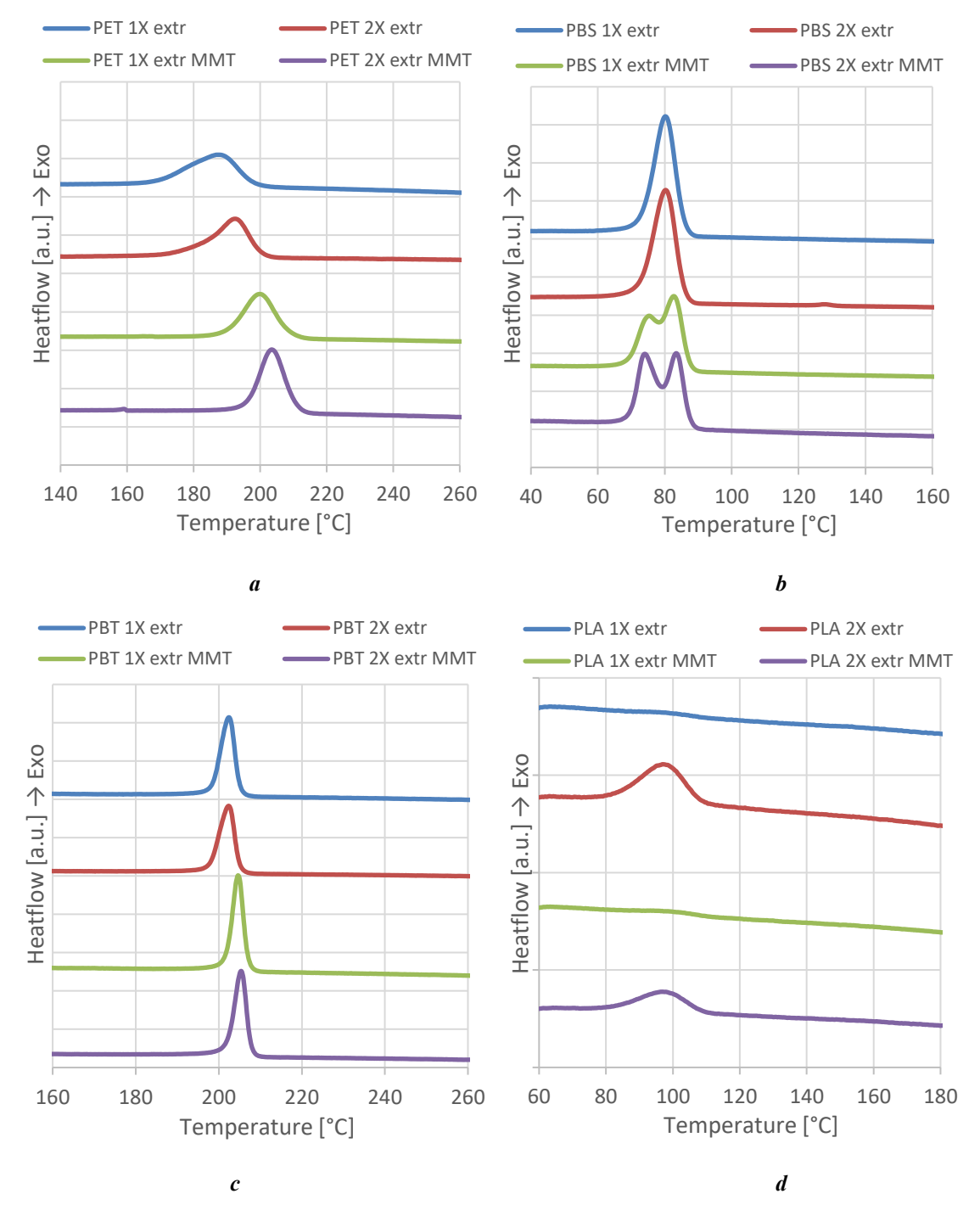


Fig. 46. DSC cooling curves of the samples (a) PET; b) PBS; c) PBT; d) PLA)

DSC measurements were used to determine the melting, crystallization temperatures and the initial crystallinity of the injection moulded samples as shown in Table 11. Where multiple crystallization peaks occurred, the temperature of the first peak was used.

**Table 11.** Average melting temperatures  $(T_m)$  from heating and average crystallization temperatures  $(T_c)$  from cooling DSC curves.

	1X extr		2X extr		1X extr MMT		2X extr MMT	
	T <sub>m</sub> [°C]	T <sub>c</sub> [°C]						
PET	253.8	187.9	254.0	192.6	255.9	200.0	254.7	203.5
PBS	120.7	80.2	120.8	80.3	121.1	81.1	122.2	82.7
PBT	229.2	199.5	230.6	199.4	228.9	201.3	228.2	201.9
PLA	182.7	97.8	182.2	97.4	182.3	99.6	181.6	97.9

Regarding the melting temperature ( $T_m$ ), the results showed that reprocessing and adding MMT to the different types of polyesters do not significantly affect them. It can also be observed that reprocessing hardly affects the crystallization temperature ( $T_c$ ) during the cooling of the melt for PBT, PBS and PLA. However, the crystallization temperature increased by 5 °C for PET due to the higher degree of order of the molecular chains. As a result of the role of MMT as a nucleation agent, its addition led to an increase in the crystallization temperature by 1-2 °C for PBT, PBS and PLA and by 11-12 °C for PET.

The glass transition temperature ( $T_g$ ) of the different polyesters was determined by using DMA, which was 69-72 °C for PET, -26 °C for PBS, 51-54 °C for PBT and 53-55 °C for PLA. In the case of semi-crystalline polymers, crystallization occurs between  $T_m$  and  $T_g$ . In the lower temperature region, the nucleation rate is higher, while in the upper region, the crystal growth rate is higher [148]. Figure 47 shows the position of the average  $T_m$ ,  $T_c$  and  $T_g$  transition temperatures related to the mould temperature ( $T_{mould}$ ) of 60 °C.

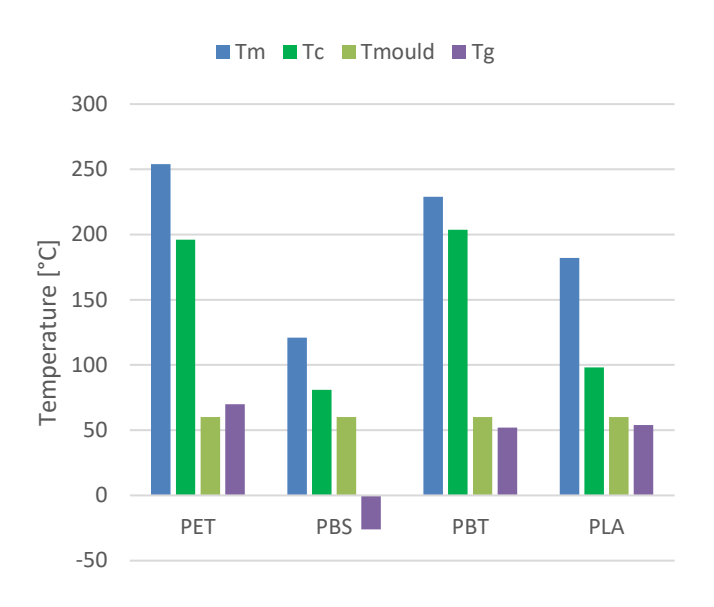


Fig. 47.  $T_m$ ,  $T_c$ ,  $T_g$  transition temperatures and  $T_{mould}$  for different polyesters

The crystallization of the polyesters reinforced with nanoclay and not reinforced at all, was studied based on the results of non-isothermal crystallization. The results indicated that both undercooling and crystallization were linearly related to the natural logarithm of the cooling rate. It showed, as presented in Figure 48, that the effect of reprocessing and adding MMT on the crystallization of polyesters differed according to the type of polyester. The incorporation of MMT had no effect on the crystallization of PET, but its addition had an effect on recycling, as its addition led to an increase in the crystallization rate compared to PET without MMT, which decreased in the recycling. It was also found that the crystallization of PBT decreased during reprocessing with or without MMT, although the presence of MMT enhanced the crystallinity compared to pure PBT. It can be noted that the difference in crystallinity between the samples was not big at high cooling rates in the case of PET and PBT, either pure or their nanocomposites. Regarding PLA, reprocessing resulted in increased crystallinity for both pure PLA and those containing MMT. Reinforcement with MMT for PLA exhibited a significant effect at low cooling rates. Reprocessing and the addition of MMT did not significantly influence the crystallinity of PBS, as the crystallinity was quite close in all four cases. In summary, it can be concluded that MMT increased the crystallinity values while reprocessing decreased them.

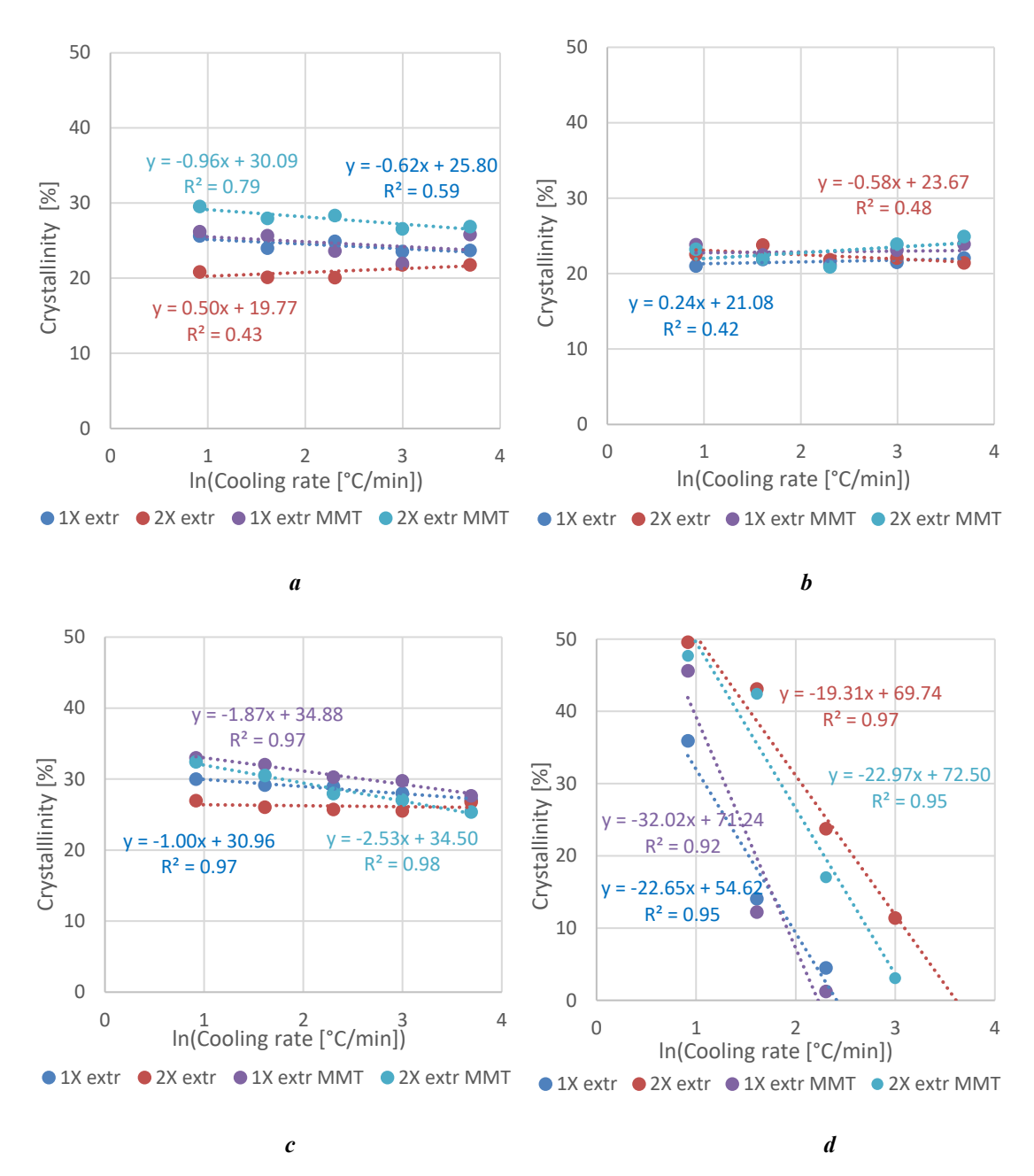


Fig. 48. Effect of cooling rate on crystallinity (a) PET, b) PBS, c) PBT, d) PLA)

The undercooling temperature of different polyesters and polyester nanocomposites was calculated to understand the crystallization behaviour by the difference between the equilibrium melting temperature ( $T_{m,0}$ ) and the peak crystallization temperature ( $T_{c,p}$ ) during the cooling scan ( $\Delta T_c$ ) [149] as shown in Figure 49. Strong, positive correlations were found in most of the samples. The addition of MMT and reprocessing slightly changed the trends for samples produced from the same polymer except for PET. The data indicated that PET was more affected by cooling rate changes. Both MMT incorporation and reprocessing in the case of PET reduced the undercooling temperature which enhanced crystallization. It is known that the less

likely the polymer is to crystallize, the higher the supercooling, due to the rigidity resulting from the groups it contains or the length of the molecular chains [31].

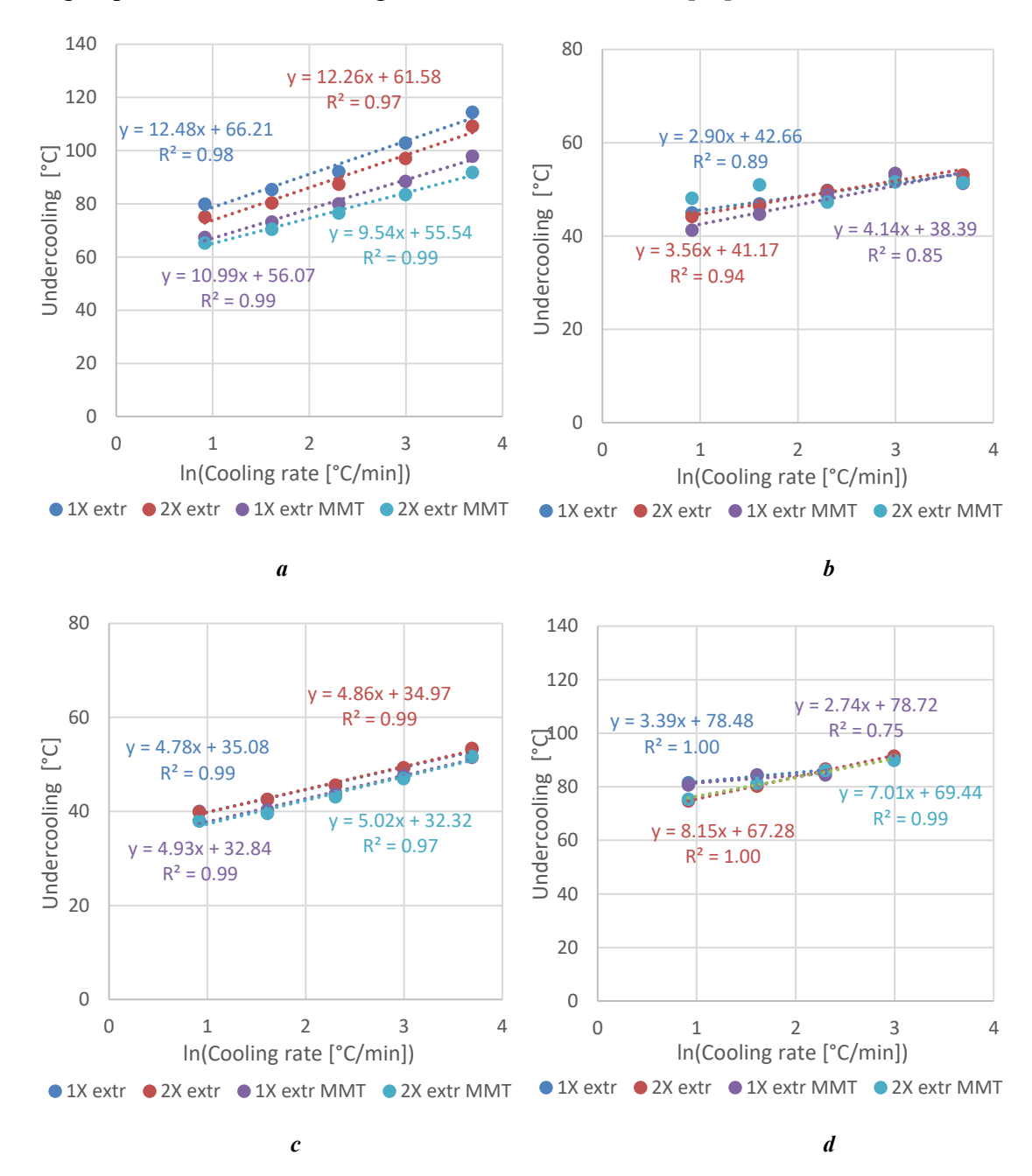


Fig. 49. Effect of cooling rate on undercooling of a) PET, b) PBS, c) PBT, d) PLA

For polyesters and polyester/MMT composites, Figure 50 shows the undercooling at a cooling rate of 1 °C/min (50/a) and 10 °C/min (50/b). Comparing the results at 10 °C/min and 1 °C/min, the undercooling was smaller for all materials at the lower cooling rate. This is because the polymer molecules have enough time to form crystals at higher temperatures when the cooling rates are lower. However, at higher cooling rates, less time is spent at a given

temperature, and thus crystallization can only begin at lower temperatures [150]. Both reprocessing and the addition of MMT reduced the undercooling of PET and PBT at 1 °C/min, but MMT had a more pronounced effect. For PLA, which is known to crystallize slowly due to the rigid segments in its chains [151], the results showed the highest undercooling. It was also observed that after adding MMT, the undercooling increased slightly, but the recycling for both cases (with and without MMT) greatly reduced the results. In the case of PBS, MMT incorporation reduced undercooling, but recycling in the presence of MMT hindered crystallization.

According to the analysis of the results collected at 10 °C/min of cooling rate (Figure 50/b), PET showed the highest undercooling of about 93 °C. PET also showed the largest difference between the samples, with reprocessing and MMT addition contributing to a decrease in undercooling. Notably, MMT had a more pronounced effect on the reduction of undercooling than reprocessing. In the case of PLA, undercooling was about 80 °C, indicating its great resistance to crystallization during accelerated cooling. Both reprocessing and MMT incorporation caused slight inhibition of crystallization in contrast to the results at slower cooling rates (1 °C/min). For PBS and PBT, slight changes in undercooling were shown with reprocessing or the presence of MMT, highlighting their greater stability in crystallization behaviour under the tested conditions.

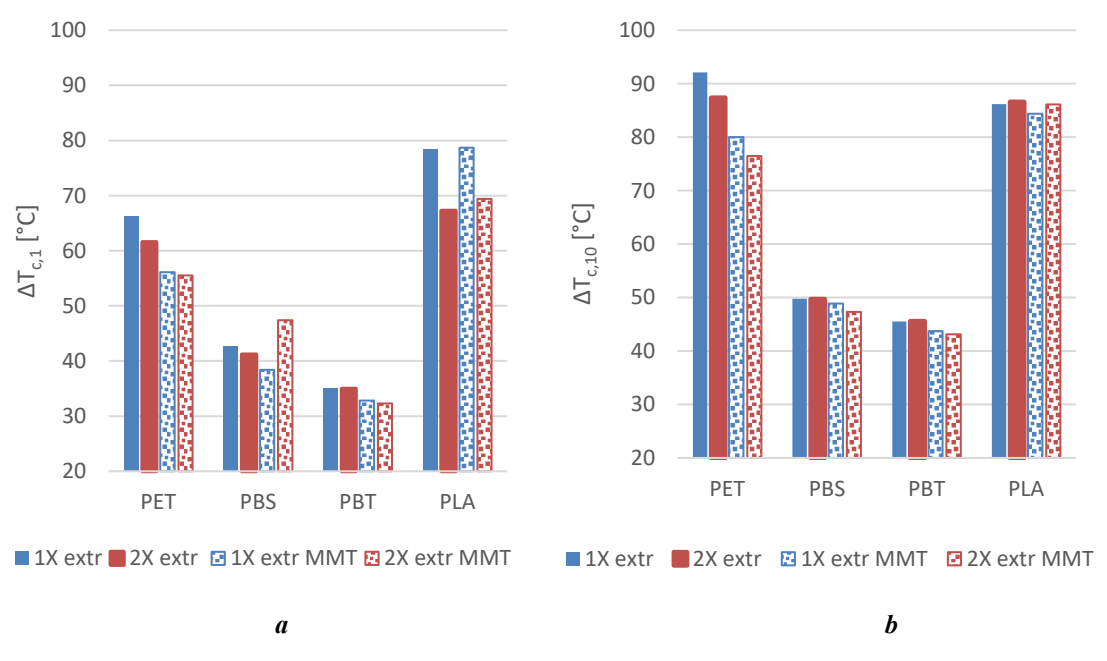


Fig. 50. Undercooling after the processing steps a) at 1°C/min and b) at 10°C/min cooling rates

The crystallinity at cooling rates of 1 °C/min and 10 °C/min is shown in Figure 51. The incorporation of MMT with PET at 1 °C/min slightly improved the crystallinity. Furthermore, the recycling of its nanocomposites (2X extr MMT) resulted in a significant improvement in crystallinity due to the action of MMT as a nucleating agent, while the recycling of unreinforced PET caused a hindrance in crystallinity. The results revealed that PLA had the highest crystallinity values, especially for the recycled samples. Recycling with or without MMT significantly increased the crystallinity but in the presence of MMT it had a greater effect because of its nucleating effect. For PBS, both reprocessing and MMT incorporation slightly enhanced the crystallinity. However, PBS/MMT recycling resulted in the lowest crystallinity among PBS samples with MMT. In the case of PBT, recycling reduced crystallinity but the presence of MMT promoted crystallinity in both cases (1X extr MMT and 2X extr MMT).

Comparing the results of Figure (51/a) and (51/b), it is clear that the cooling rate had a significant effect on the crystallization of PLA, as it increased undercooling as shown in Figure (50/b) and the crystalline fraction decreased significantly at a cooling rate of 10 °C/min, reflecting its resistance to crystallization under accelerated cooling. The used PLA contains only 0.3% D-lactic acid units and is designed to crystallize during processing in most conventional injection moulding equipment [152]. The results showed that when a uniform mould temperature of 60 °C was used for all materials (despite the recommendation of the manufacturer which is a high mould temperature of 80 to 130 °C), this hindered the crystallization of PLA due to the higher cooling rates except for the recycled sample and without MMT, where reprocessing enhanced the values. This can be explained by the fact that at high cooling rates, chain mobility and chain length have a greater effect on the crystallization process, compared to low cooling rates, and therefore rigid PLA chains are less prone to crystallization. The incorporation of MMT reduced the crystallization of PLA at high cooling rates, as it stopped acting as a nucleating agent. In the case of PET, reprocessing decreased the crystallinity of pure PET. The exact opposite was observed during the reprocessing of MMTcontaining samples, where crystallization was enhanced due to the effective nucleating role of MMT at high cooling rates. Although the inclusion of MMT decreased the crystallinity compared to pure PET, PBT and PBS showed higher crystallization rates due to their higher molecular mobility [153–155], and lower undercooling about 47-49 °C for PBS and 43-45 °C for PBT, and higher crystalline fraction (40-45 % for PBS and 26-28 % for PBT). The incorporation of MMT enhanced the crystallization of PBT, while recycled PBT decreased crystallinity, in contrast to lower cooling rates. It was found that reprocessing in PBS and

PBS/MMT did not significantly affect the crystallization of PBS, but the addition of MMT hindered the crystallization slightly because it interfered in the ordering of the molecular chains [104].

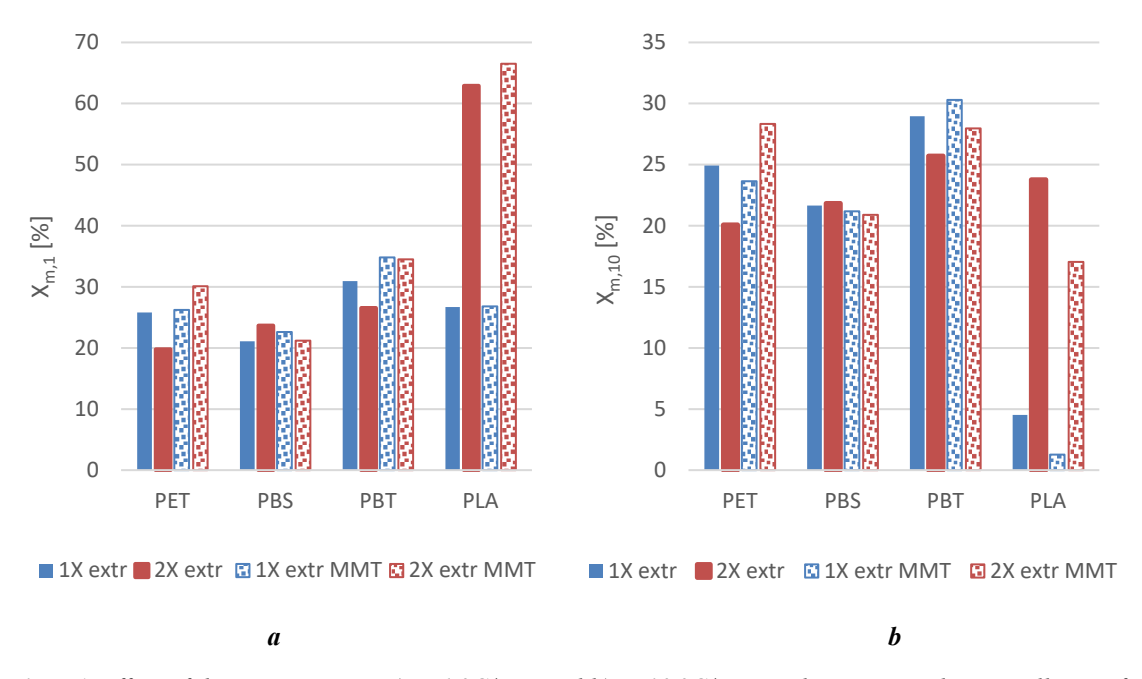


Fig. 51. Effect of the processing at a) at 1 °C/min and b) at 10 °C/min cooling rate on the crystallinity of polyester samples and their nanocomposites

Overall, cooling rates strongly affected crystallization, with higher rates reducing crystallization for all materials, particularly PLA and PET, while the effects of reprocessing and MMT varied depending on the type of polymer and conditions.

Figure 52 shows the mass and volume shrinkage of different polyesters as a function of crystallinity. It is clear that the mass is not only determined by the crystalline fraction but is influenced by the MMT content and process parameters. The actual effective time of holding pressure depends on the time it takes for the gate to freeze for a given material, although the holding pressure was set at 50 bar and 10 s for all polyesters used. This prevents further flow of material into the tool cavity.

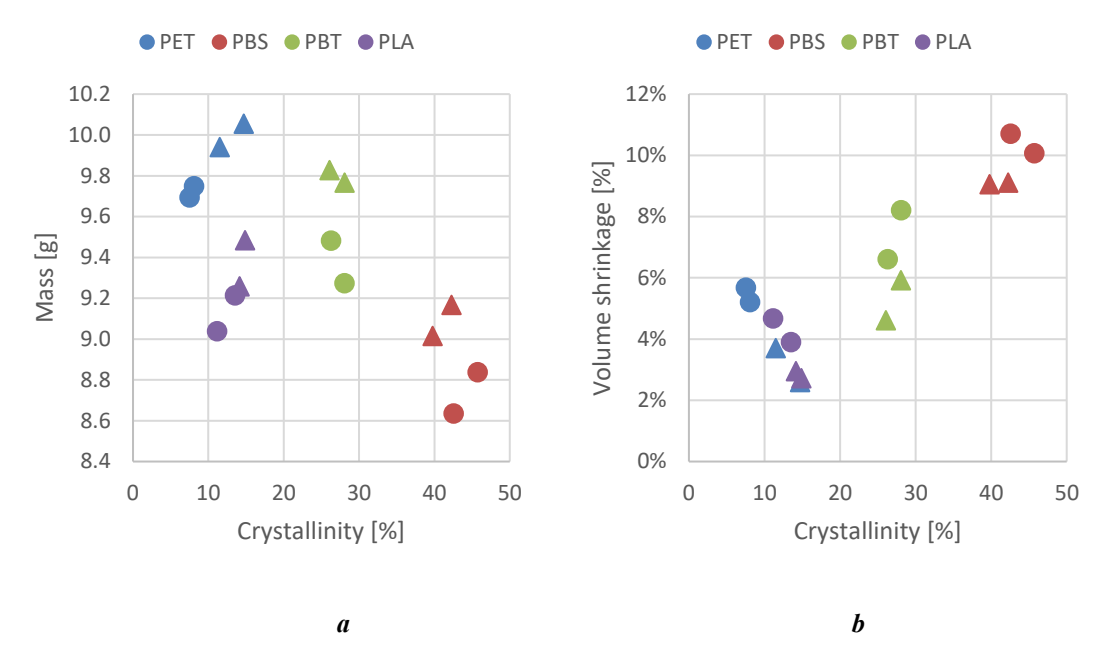


Fig. 52. Mass (a) and volumetric shrinkage (b) as a function of crystallinity ( $\bullet$ : without MMT,  $\blacktriangle$ : with MMT; the colours indicate the type of material)

Amorphous regions play the principal role in the shrinkage of polyesters that crystallize slowly. In addition to the direct effect of crystallization on the shrinkage of specimens through density changes, crystallization also indirectly restricts the movement of amorphous regions. During flow, the recoverable elastic strain can relax in the amorphous regions until it reaches the T<sub>g</sub> temperature [156]. As a result, there is a correlation between total volumetric shrinkage and crystallinity, especially for PET and PLA with smaller crystalline particle size distributions as shown in Figure (52/b).

## 4.5. Structure of polyester/MMT nanocomposites

After adding MMT into the polyester matrix, structural forms of the resulting nanocomposites were obtained as shown in Figure 53. To analyze the structure of the nanocomposites and to gain information on the dispersion of MMT inside the polyester matrix, the samples were examined using scanning electron microscopy (SEM) and X-rays.

When MMT was added to the polymer matrix, there were two possibilities. Either agglomerations were detected using scanning electron microscopy or intercalation, where X-rays were used to clarify their distribution.

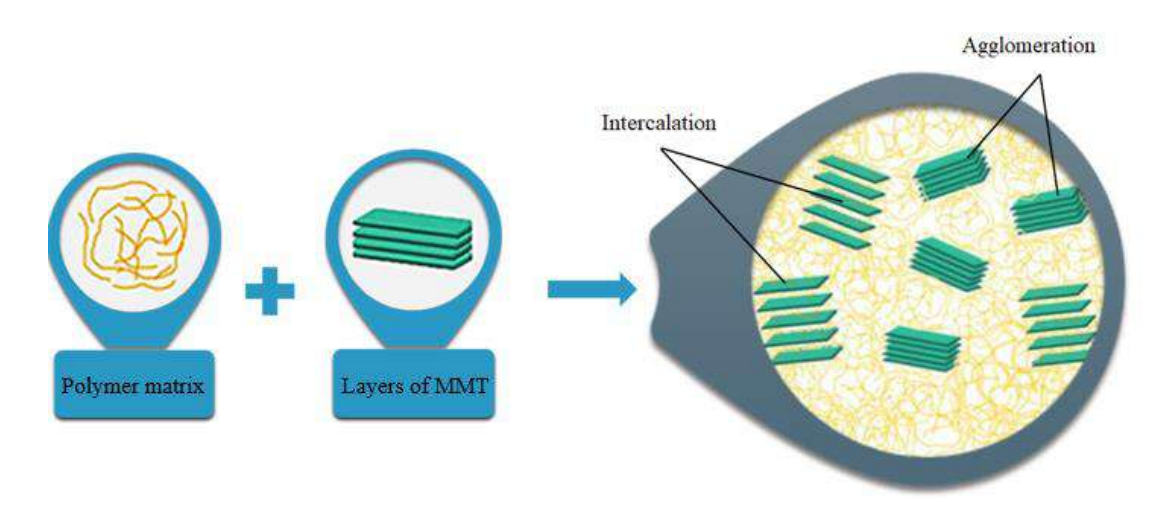


Fig. 53. Structural morphologies in polyester/MMT nanocomposites

### 4.5.1. Structure of nanocomposites analyzed by SEM

Figure 54 displays the distribution of MMT by using EDS to detect silicon element mapping. The smallest aggregates are observed in PBT (average size 5-10  $\mu$ m) and PET (10-20  $\mu$ m), while PLA (10-30  $\mu$ m) and PBS (10-50  $\mu$ m) have the largest aggregate size. Because of the high shear forces in the twin-screw extruder, reprocessing resulted in a finer distribution of MMT, as some of the larger aggregates in the 2x extruded materials were fragmented into smaller ones.

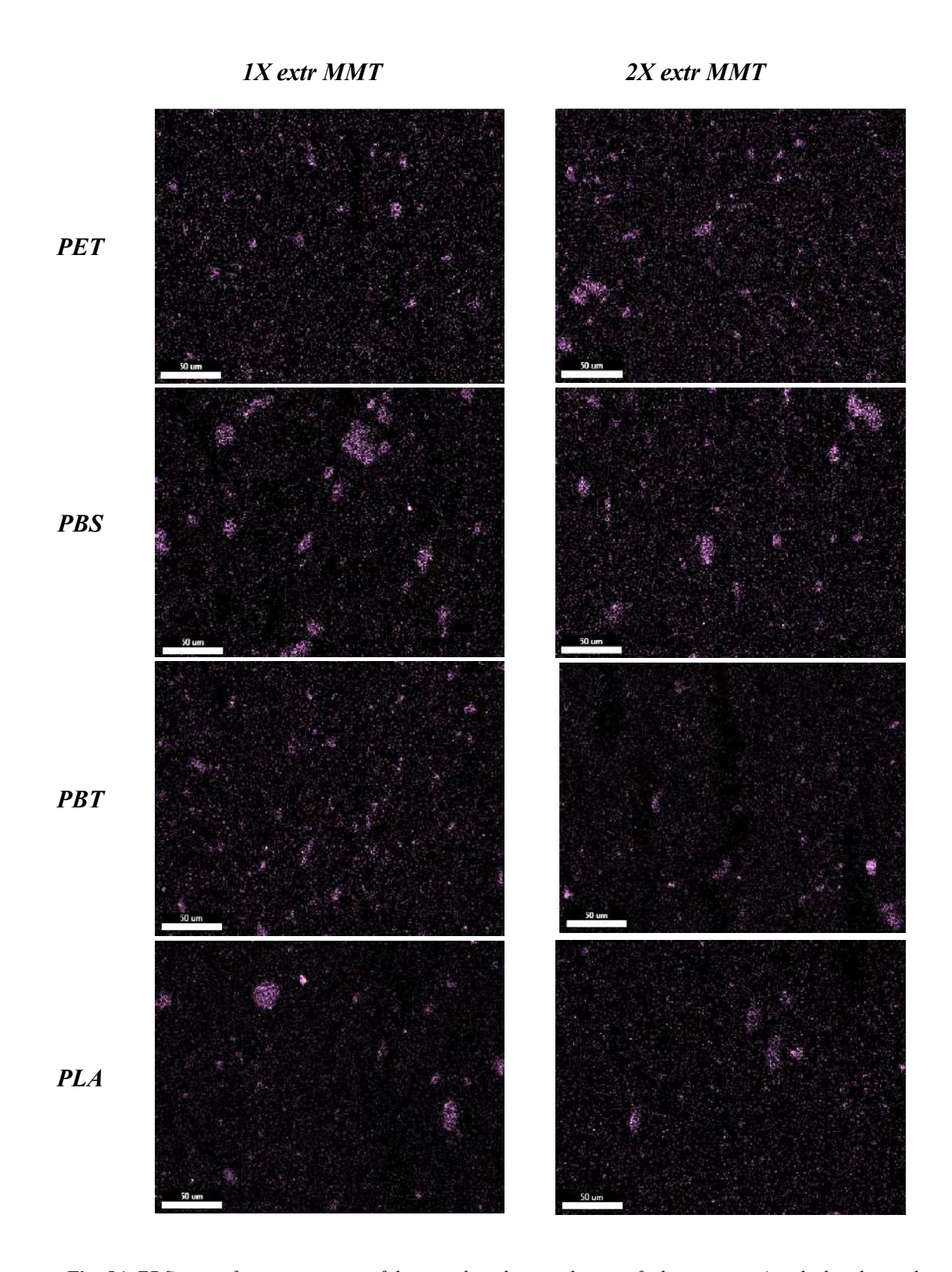


Fig. 54. EDS map of a cross section of the samples: the enrichment of silicon atoms (marked with purple dots) indicates the MMT aggregates

### 4.5.2. Structure of nanocomposites by WAXD

The influence of recycling on the wide-angle X-ray diffraction (WAXD) patterns of several polyester/MMT nanocomposites, including the sample containing only MMT, can be seen in Figure 55. The diffraction patterns of polyester/MMT nanocomposites indicated significant changes when MMT was added to polymers. The 2θ values for these nanocomposites ranged from 2.86° to 3.04°, while MMT powder had a greater angle of 4.5°. According to Bragg's law, the shift to lower angles in the nanocomposites indicates the intercalation of MMT into the polymer matrices [87], which increases the spacing between the MMT silicate layers. Upon recycling, the type of polyester used had an effect on the basal spacing of the MMT layers.

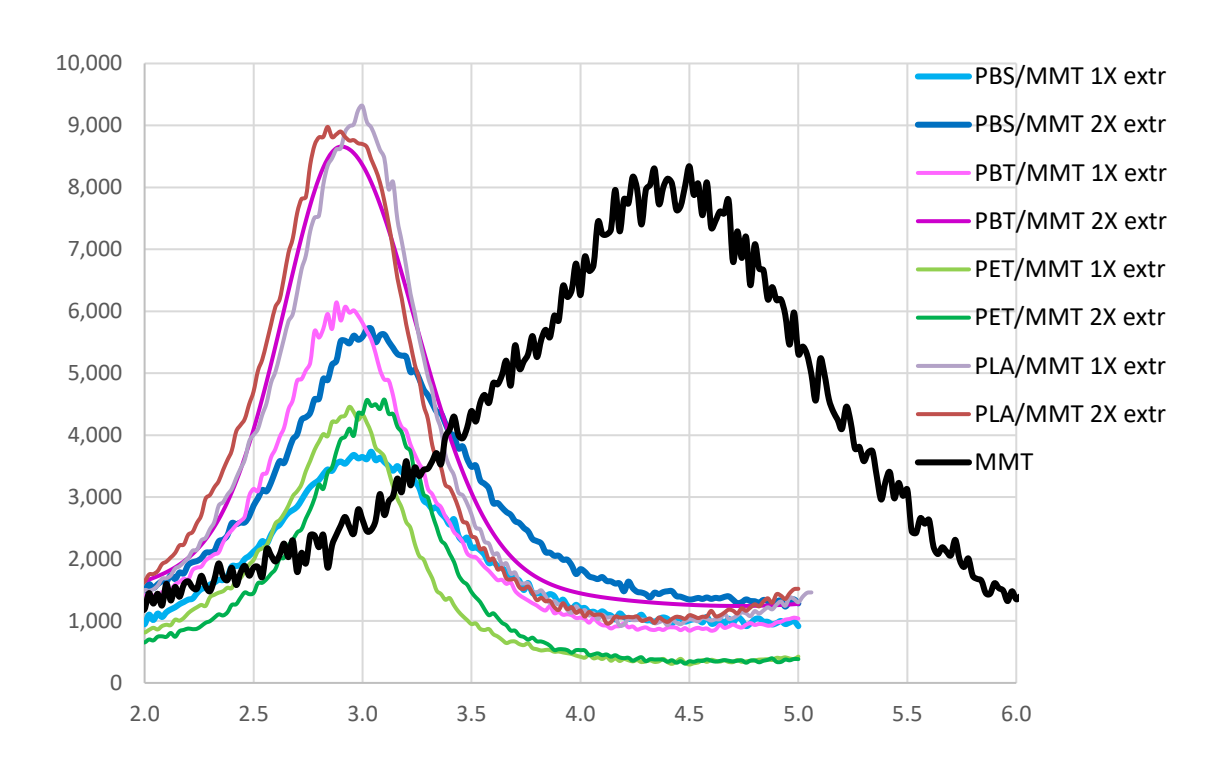


Fig. 55. WAXD patterns of MMT powder and various recycled polyester/MMT nanocomposites

The values of stack sizes (D) and the number of layers (N), which are determined by the different nanocomposite crystallite sizes and layer thickness, are shown in Table 12. PBS/MMT nanocomposites showed the least number of MMT layers while PET/MMT had the highest number of layers and largest stack sizes indicating more stacked MMT. Recycling resulted in varying degrees of dispersion of MMT in the polyester matrix used. Reprocessing reduced both layer thickness and stack size possibly due to mechanical and thermal stresses during extrusion,

while the number of MMT layers increased slightly in all cases except for PBS due to improved stacking or aggregation of MMT layers [87].

**Table 12.** Effect of recycling on layer thickness  $(d_{001})$ , stack size (D), full width at half maximum  $(\beta)$ , and the number of MMT layers (N) for different types of polyester/MMT nanocomposites

	d <sub>001</sub> [nm]	β[∘]	D [nm]	N
ММТ	1.98			
PBS/MMT 1X extr	3.02	0.85	9.35	3.1
PBS/MMT 2X extr	2.92	0.86	9.24	3.2
PBT/MMT 1X extr	3.03	0.73	10.88	3.6
PBT/MMT 2X extr	3.04	0.72	11.03	3.6
PET/MMT 1X extr	2.99	0.65	12.22	4.1
PET/MMT 2X extr	2.86	0.65	12.20	4.3
PLA/MMT 1X extr	2.97	0.71	11.19	3.8
PLA/MMT 2X extr	2.86	0.72	11.03	3.9

## 4.6. Mechanical properties of the nanocomposites

### 4.6.1. *Izod impact strength*

The notched Izod pendulum test was used to measure the impact resistance of the materials, and the flexural test was applied to determine the quasi-static mechanical properties. The results of the impact test showed that the notched impact strength for PBS was about 5-9 kJ/m², while it ranged between 2-4 kJ/m² for PLA, PBT, and PET. By reprocessing the different polyesters, a decrease in impact strength of 6-8% was observed for PET and PBS due to the degradation and the increasing crystalline fraction. However, reprocessing did not significantly affect the impact strength of PBT and PLA. The addition of MMT resulted in a significant decrease in the impact strength of PBS/MMT nanocomposites, which was attributed to the large MMT agglomerates causing significant degradation. An approximately 30% reduction in notched impact strength was found for PET and PBT, while PLA experienced only

a slight change. It should be noted that the PLA without reinforcement has a very low impact strength. Recycling in the presence of MMT led to a slight decrease in the notched impact strength of PET and PLA nanocomposites, while the opposite occurred for PBT and PBS (slight increase). In the PBS/MMT nanocomposites, the repeated processing led to a decrease in the size of MMT agglomerates and the improved distribution, thus compensating for the observed decrease in unreinforced materials, as shown in Figure 56.

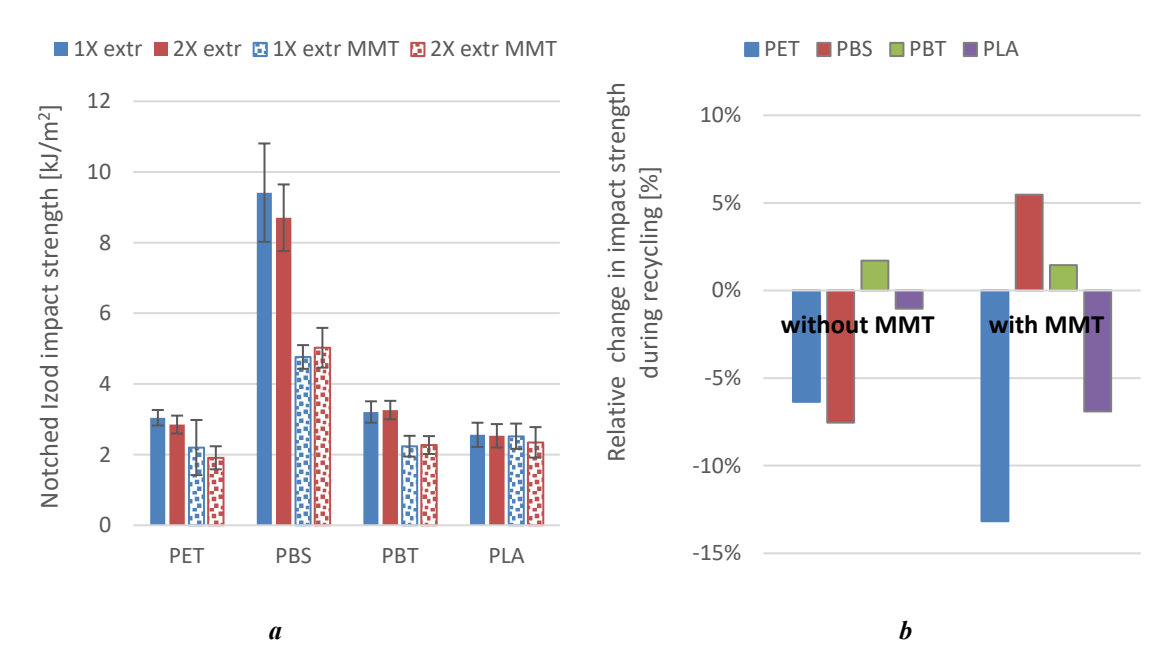


Fig. 56. a) Impact resistance of the polyesters and polyester/MMT-nanocomposites; b) Effect of MMT and recycling (1X, 2X) on impact strength.

SEM micrographs of the fracture surfaces were taken after the Izod impact test (Figure 57). It can be seen from these images that the surfaces of the 1x-processed unreinforced materials appear almost flat for PET and PLA with low impact strength, while the surface roughness of the PBS with higher impact strength is more obvious. Du et al. [157] confirmed that the notched impact strength is in connection with the fracture surface roughness in the case of partially crystalline polyesters as the material's toughness is generally related to energy dissipation events that occur near the crack. When the Izod impact test was carried out at room temperature, PBS was the only material that was subjected to a temperature significantly higher than T<sub>g</sub>, providing the possibility of thermally activated rearrangement during the impact loading process.

The reprocessing did not affect the characteristic of the fracture surfaces significantly, with the exception of PET, which showed a more brittle fracture. The presence of MMT reduced the plastic deformation that was observed on the fracture surfaces, with sharper patterns showing a more brittle fracture. Reprocessing the polyester/MMT composites also did not significantly change these structures.

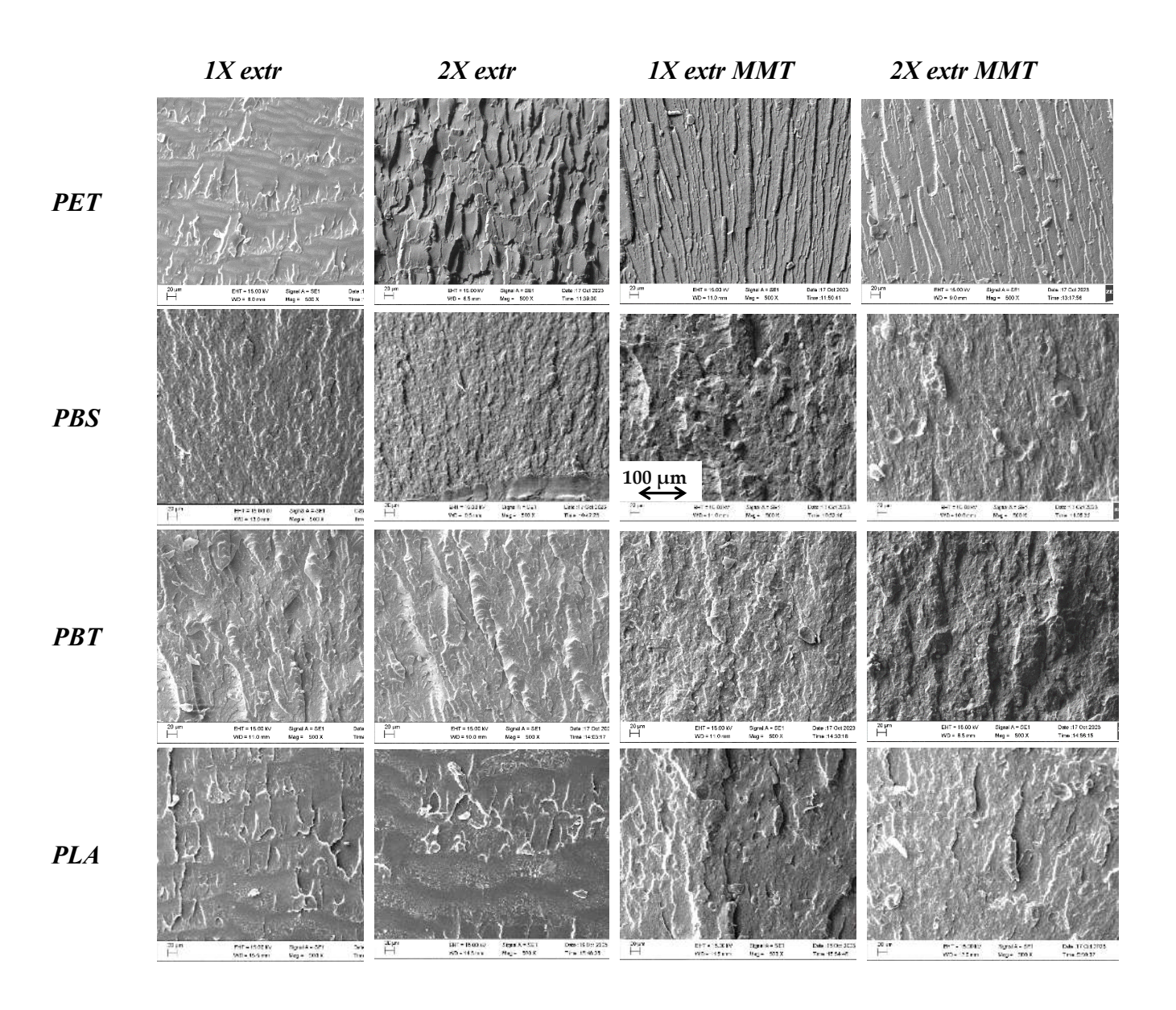


Fig. 57. SEM images of the cross sections of polyesters and polyester/MMT-nanocomposites (500x magnification)

### 4.6.2. Flexural strength

Figure 58 presents the flexural test curves obtained from 3-point bending test of the specimens. These curves illustrate the mechanical response of the samples under flexural stress and how MMT reinforcement and multiple extrusion cycles affect the flexural performance of the polyesters used. Thus, the differences in strength, ductility and failure behaviour between these materials are illustrated. The reinforced materials with MMT showed improved mechanical performance, while the recycled samples (2X extr and 2X extr MMT) exhibited some degradation in properties. PLA was found to have a brittle nature with a sharp peak, while PBT had the highest strength resistance, indicating greater stiffness. The experiment was repeated a number of times and the values were averaged. 3-point bending test curves for polyester specimens and their nanocomposites are given in the Appendix.

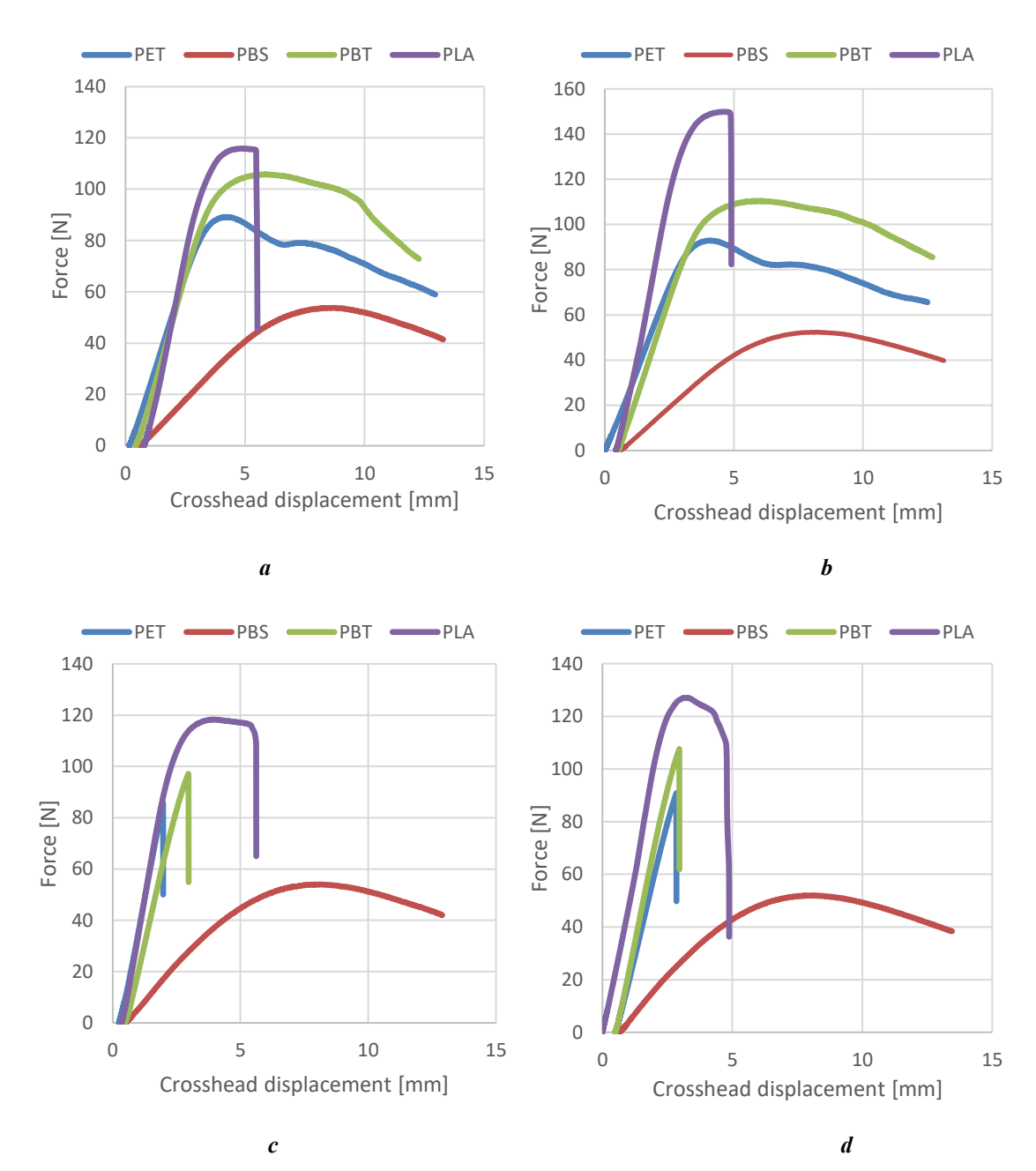


Fig. 58. Effect of MMT and recycling (1X, 2X) on flexural behaviour of the polyesters and polyester/MMT-nanocomposites;(a) 1X extr; b)2X extr; c)1X extr MMT; d)2X extr MMT)

The flexural strength and flexural modulus of polyesters and polyester/MMT nanocomposites can be seen in Figure 59. Regarding the flexural strength, the highest value was measured for PLA, reaching about 125 MPa, and around 110 MPa for PET and PBT, while only 60 MPa for PBS. The addition of MMT caused a large decrease in the flexural strength of PBT about 20%, and a smaller decrease for PET and PLA about 10% while it had no effect on the flexural strength of PBS. The reprocessing did not significantly affect the flexural strength of the polyesters and polyester/MMT nanocomposites.

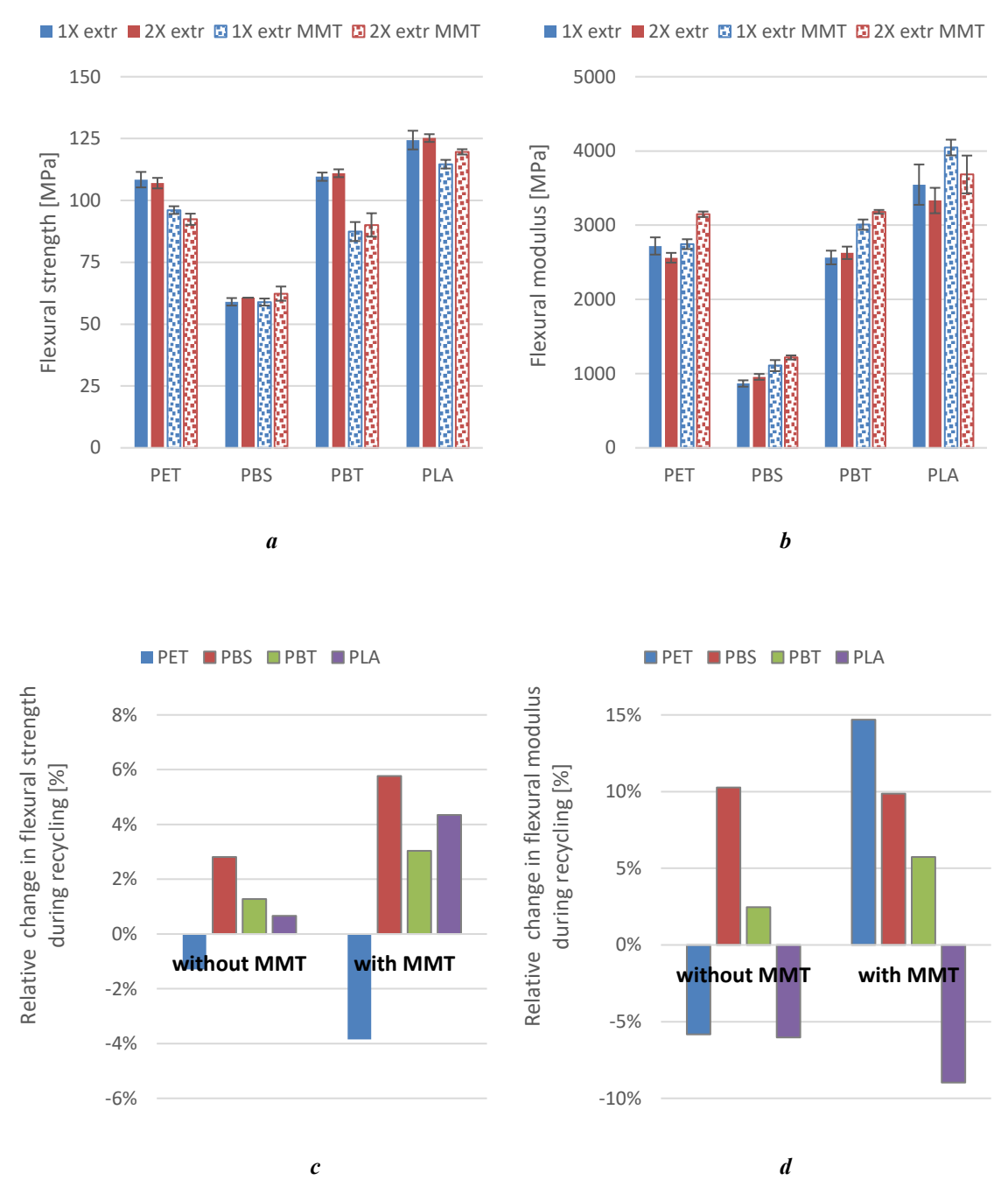
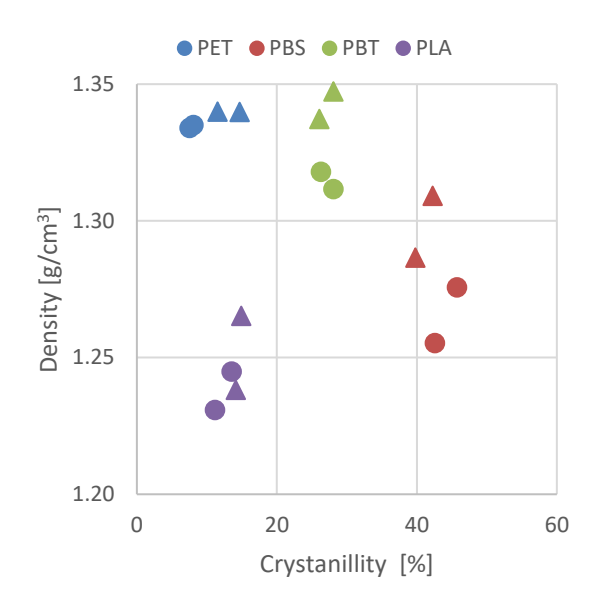


Fig. 59. a) Flexural strength; b) Flexural modulus; c) Change of flexural strength and d) flexural modulus of the polyesters and polyester/MMT-nanocomposites during recycling with and without MMT

The flexural modulus values differ slightly from the flexural strength values. The flexural modulus ranges between 2500-4000 MPa for PET, PBT, and PLA. The unreinforced PBS exhibited the highest flexibility, with a flexural modulus of 867 MPa, while the PLA/MMT nanocomposite displayed the highest stiffness with a flexural modulus of elasticity of around 4000 MPa. The unreinforced polyesters did not change significantly as a result of recycling. The addition of MMT led to an increase in stiffness in all specimens. The increase was about

28% for PBS, 17% for PBT, 14% for PLA, and only 1% for PET. The stiffness of the nanocomposites continued to increase during recycling, except for PLA, where a slight decrease occurred. This is shown in Figure (59/b).

Both density and crystallinity of the samples play a role in strength and stiffness changes during recycling of unreinforced materials [158]. The results indicated a weak correlation between the two quantities in the samples tested (Figure 60). The density can be affected by the holding pressure, whose duration can be affected by the gate freezing determined by the crystallization temperature and the injection pressure, which can vary due to changes in viscosity resulting from degradation [159]. In addition, the orientation of amorphous and crystalline particles and molecular entanglements within amorphous regions contribute significantly to crystallization [160].



*Fig. 60.* Density as a function of crystallinity (•: without MMT, ▲: with MMT; the colours indicate the type of material)

## 4.7. Dynamic mechanical properties of the injection moulded specimens

The glass transition temperature  $(T_g)$  of the injection moulded samples was measured in all cases using DMA as shown in Figure 61. It was found that recycling of both pure PET and PBS resulted in a slight decrease in  $T_g$  due to molecular degradation resulting from polymer chain scission. The incorporation of MMT into the PET matrix did not change the  $T_g$ , while in the case of PBS, this addition of MMT had an impact and resulted in a decrease in  $T_g$ . The combined effect of recycling and MMT addition increased the  $T_g$  of PBS. Regarding PBT and

PLA, the application of MMT or recycling had no significant impact on their glass transition temperature.

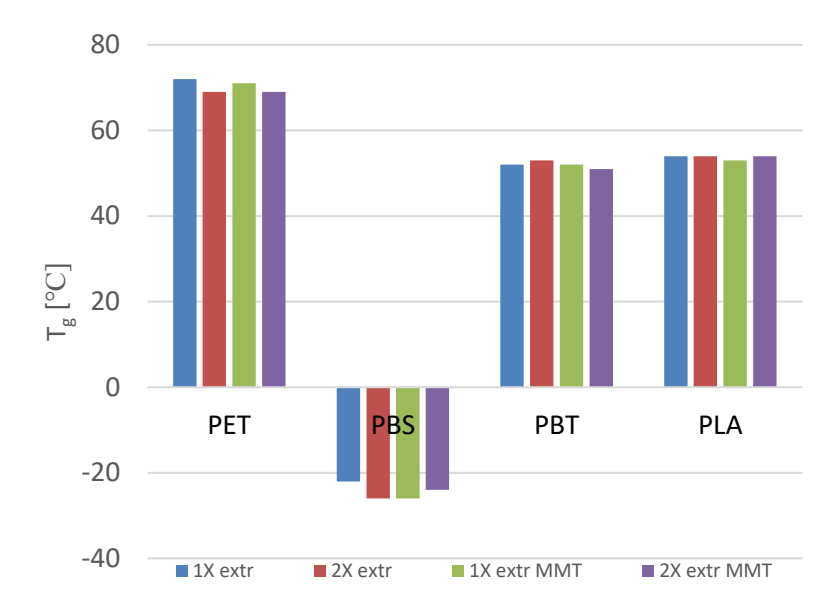
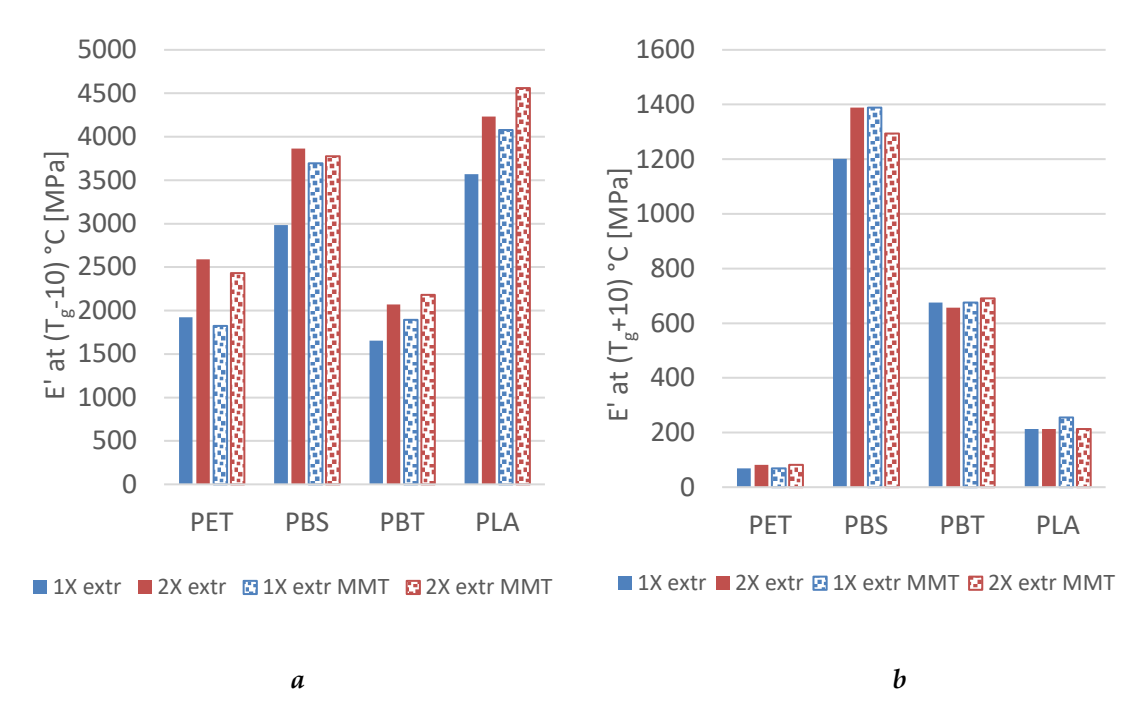


Fig. 61. The glass transition temperature  $(T_g)$  of polyesters and polyester/MMT nanocomposites

Since the values of T<sub>g</sub> of the materials were over a wide range, the storage moduli were also measured 10 °C below and above the Tg using DMA. Figure 62 shows the effect of recycling and MMT addition on the storage moduli (E') below and above Tg of the different polyester materials used and their nanocomposites. When measured below the glass transition temperature (T<sub>g</sub> - 10 °C), an increase in the storage moduli was observed for all pure and MMTenhanced materials upon recycling. At this temperature (below T<sub>g</sub>), the samples demonstrate a higher ratio of amorphous content compared to the crystalline content. This amorphous phase affects the mechanical properties of the resulting samples. So, during manufacturing, the degraded chains in the amorphous phase can lead to a more oriented structure and thus an increase in stiffness. The results revealed that the effect of MMT differed depending on the type of polyester. When comparing pure materials with their compounds at the same processing stages (i.e. 1X extr with 1X extr MMT and 2X extr with 2X extr MMT), it was found that the addition of MMT led to an increase in the storage moduli of both PBT and PLA in all cases. In comparison, its addition led to a decrease in the moduli of PET. As for PBS, both phenomena were observed, meaning an increase in the storage moduli when MMT was added, and a decrease was observable as a result of the combined effect of recycling and MMT addition when compared.



*Fig.* 62. Storage moduli 10  $^{\circ}$ Ca) below and b) above  $T_g$  of polyesters and polyester/MMT nanocomposites

For materials with very high amorphous ratio during manufacturing, such as PET and PLA, the storage moduli above T<sub>g</sub> were lower than the values obtained below the glass transition temperature, as shown in Figure (62/b). The decrease in storage moduli for these materials (PET and PLA) ranged around 95% while it decreased by 30-40% for PBS and PBT. The incorporation of MMT and recycling of PET, PBT and PLA had little effect on the storage moduli. While PBS had a greater change, there was no clear trend for this change. This is attributed to the different organized structures that appeared in each sample. Since only the crystalline fraction significantly affects the mechanical properties above the glass transition temperature, PBS and PBT, the materials with higher initial crystallinity, showed a lower decrease in the change of the storage moduli at the T<sub>g</sub> step.

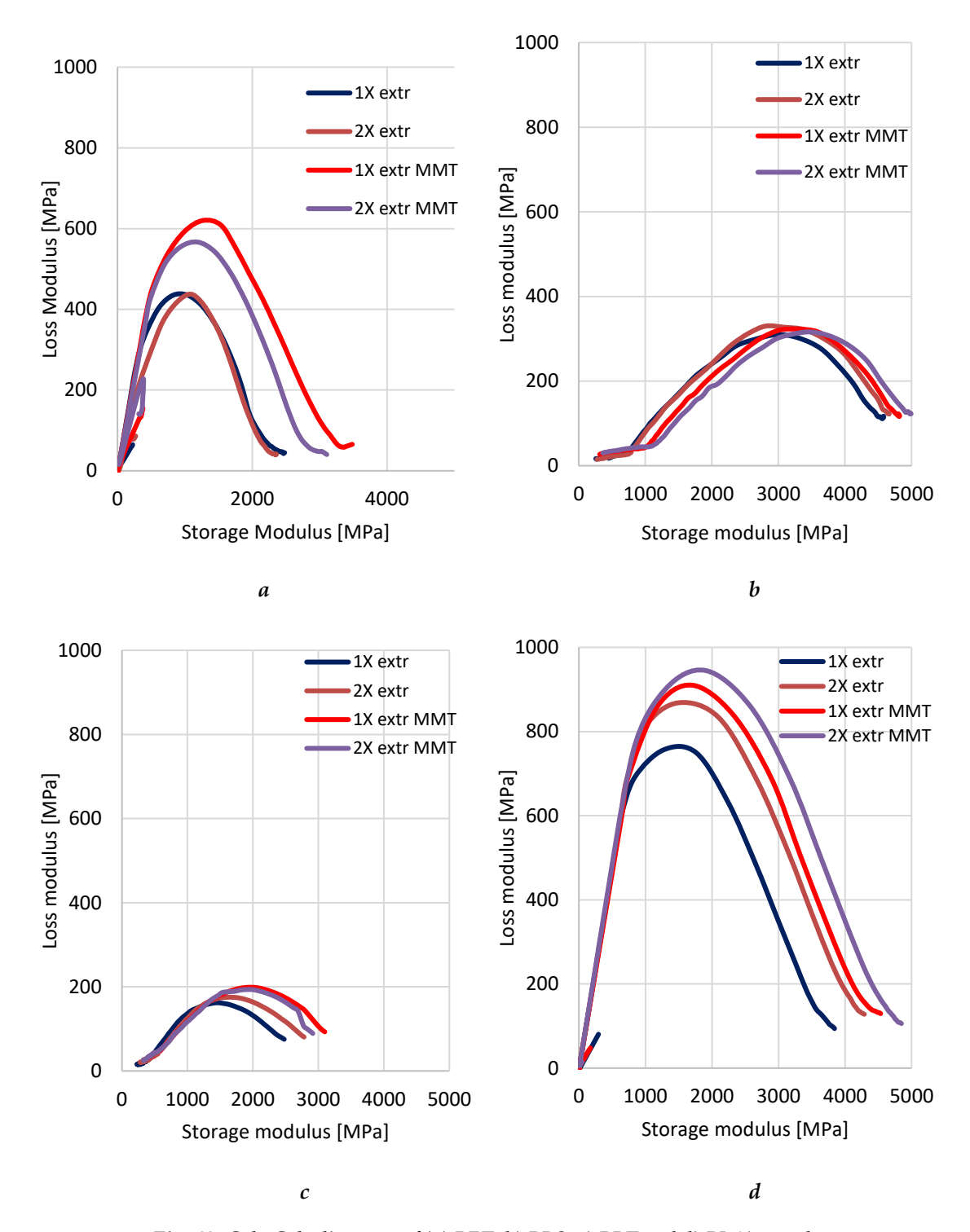


Fig. 63. Cole-Cole diagrams of (a) PET, b) PBS, c) PBT and d) PLA) samples

Figure 63 shows the Cole–Cole plots of PET, PBS, PBT, and PLA samples. From these plots, the dispersion of MMT and the resulting structure of the samples can be understood. The Cole-Cole plots were similar for all polyesters. The incorporation of MMT into polyester matrices leads to a shift in the Cole-Cole plot due to increased interaction between polymer chains and nanoclay particles. This shift indicates enhanced shear thinning behaviour and

improved network formation, especially in PET-based nanocomposites [73]. PBS and PLA exhibit different relaxation behaviour, which can be attributed to their semi-crystalline nature and biodegradability [82, 89]. The deviations were more pronounced in Cole–Cole plot of PLA. For PBT, the plots were slightly flattened and semi-circular compared to the other samples. Thus, the shape of the curves showed that the MMT nanofillers were dispersed, indicating that the structure of the composite was homogeneous. It was also observed that recycling did not significantly affect the structure.

### 5. SUMMARY

The demand for materials with superior mechanical, thermal and environmental properties is increasing to meet industrial needs. Therefore, this thesis investigates the effect of montmorillonite (MMT) incorporation and recycling on the properties of both petroleum-based and bio-based polyester nanocomposites. It focuses on improving the structural, thermal and mechanical characteristics of these nanocomposites and analyzing the effects of reprocessing on their performance. The attributes of four types of polyester/MMT nanocomposites were evaluated, and their behaviour was compared with that of unreinforced polyesters. Observations were drawn from conducting several mechanical, rheological, and morphological tests on samples subjected to multiple extrusion cycles and subsequent injection moulding at a uniform mould temperature of 60 °C, highlighting the complex interactions between degradation, processing conditions, and material properties during recycling.

The results showed that the inclusion of MMT significantly affects the behaviour of polyesters. Good dispersion was achieved at a concentration of 6 wt.% MMT, which proved to be critical in enhancing the physical network within the nanocomposites and increasing the elastic modulus in both the molten and solid state of polyesters. Degradation during reprocessing was found to directly affect shrinkage and mechanical properties, while having indirect effects via changes in viscosity and crystallization temperature. The behaviour of materials varies depending on the type of polyester. A significant change in the behaviour of nanocomposites versus non-reinforced polyesters was observed, especially in low-crystallinity polyesters such as PET and PLA. For these materials, the role of MMT as a nucleating agent significantly accelerated the crystallization process, affecting density, crystallinity and mechanical properties. This was especially evident during recycling. The dispersion of MMT within the polyester matrix played a crucial role in influencing the characteristics. While the incorporation of MMT initially hindered polymer chain mobility and thus decreased mechanical properties due to the presence of MMT agglomerates, recycling helped redistribute and disperse the nanoclay. This redistribution of MMT in some cases led to improved properties, compensating for molecular degradation. For example, the impact strength of PBT/MMT and PBS/MMT nanocomposites improved after recycling.

In addition, the study revealed that nanocomposites are more susceptible to degradation than pure polyesters. This degradation potential arises from the interactions between the polyester matrix and the modified clay. Ammonium linkage on the clay plates increases the acidic sites that accelerate the degradation, an effect that is amplified when MMT is well

distributed within the matrix. PET demonstrated a pronounced degradation that significantly affected its molecular weight, viscosity, and mechanical properties. In contrast, PLA and PBT exhibited increased viscosity in their MMT nanocomposites despite degradation.

DSC analyses also confirmed the role of thermodynamic driving forces related to interphase interactions, physical network structures, and molecular weight changes. The effect of reprocessing and MMT varied across different polyester matrices. For example, MMT enhanced the crystallinity of PLA at lower cooling rates. Furthermore, reprocessing increased the storage modulus for almost all materials. At T<sub>g</sub>, PET exhibited a higher storage modulus in the unreinforced case, while PLA, PBS, and PBT showed increased storage modulus with MMT reinforcement, especially in the recycled samples. The Cole-Cole plots indicated a homogeneous dispersion of the nanofillers that remained stable even after reprocessing, suggesting a strong composite structure.

Overall, the research concluded that recycling different types of polyesters and their nanocomposites is feasible and efficient. Biodegradable polyesters, in particular, demonstrated better recyclability compared to conventional petroleum-based polyesters. However, challenges remain, especially for polyester/MMT nanocomposites. While the addition of MMT improves mechanical properties and crystallinity, it also accelerates material degradation, affecting stiffness during recycling. The results highlighted significant changes in the attributes of the nanocomposites after recycling, which are more pronounced than for non-reinforced polyesters. Despite these challenges, the research supports recycling as a viable strategy for waste recovery, emphasizing the importance of balancing the benefits of reinforcement with long-term material stability for sustainable applications. These findings establish a path for the development of advanced, recyclable nanocomposites designed for specific engineering requirements.

### 5.1. Utilization of results

The research and development carried out within the framework of this doctoral thesis was driven by industrial requirements, in particular those of Jász-Plasztik Kft., one of the largest plastic processing companies in Hungary. With approximately 4000 employees and an annual plastic processing volume of 40,000–50,000 tons, the company has significant capabilities in packaging production, technical component manufacturing and recycling. Currently, Jász-Plasztik Kft. exclusively processes and recycles petroleum-based polyesters, such as PET and PBT. However, the increasing pressure from customers to introduce bio-based plastics into production has required research into sustainable alternatives.

In response to these industrial requirements, Dr. Ferenc Ronkay, Head of the Material Development Group at Jász-Plasztik Kft., proposed the current research topic. The aim was to facilitate the introduction, processability, and potential physical recycling of bio-based polyesters. The dissertation presents and quantifies the main results, demonstrating that the application of PLA/MMT nanocomposites can lead to tangible market benefits. A particularly significant practical result of this research is that PBS, primarily used for film production, was successfully processed by injection moulding. Notably, the properties of these injection-moulded products showed only minor changes upon recycling, indicating that PBS could be a suitable material for the large-scale production of injection-moulded items, such as food storage containers. This result is particularly relevant in industries where the in-process recycling of production waste is a crucial environmental and economic consideration. Furthermore, additional investigations, such as gas permeability testing, are needed to fully assess their viability in industrial applications.

The research findings provide a deeper understanding of the effect of MMT enhancement on the recyclability of both bio-based and petroleum-based polyesters. They can be summarized as follows:

- 1- The successful incorporation of MMT into polyester during recycling demonstrates a path to producing high-value materials from waste, aligning with global sustainability goals. For example, industries focused on circular economies could benefit significantly.
- 2- The thesis highlights that bio-based polyesters such as PBS and PLA, due to their low degradation, exhibit enhanced recycling potential compared to petroleum-based polyesters such as PET. It was also shown that the addition of MMT reduces the molecular chain scission, enhancing stability. Thus, strong bio-based nanocomposite materials can be designed for high-

demand industrial applications, where material integrity is critical over multiple processing cycles, such as automotive and packaging.

- 3- Analysis of shrinkage properties in injection moulded samples revealed that MMT reduces shrinkage variation. This is beneficial in precision industries where dimensional accuracy is paramount such as medical device manufacturing, electronics and automotive parts manufacturing.
- 4- Improvements in dynamic mechanical properties, including storage modulus, confirm the potential of these nanocomposites in structural applications, especially in environments requiring thermal and mechanical stability.
- 5- The results can be utilized in various applications, especially in materials engineering, sustainable manufacturing and industrial polymer processing, to achieve performance, environmental and economic goals. In addition, the research results can serve as a foundation for further studies to explore additional polymer matrices, broader recycling applications and innovative processing technologies.

So, this dissertation advances the understanding of bio-based polyester nanocomposites, demonstrating their feasibility for industrial adoption while addressing critical sustainability challenges in polymer processing and recycling.



Fig. 64. Examples of uses of recycled nanocomposites

### 5.2. Theses - New scientific results

I have prepared nanocomposites by combining 6 wt.% of nanoclay (MMT) with four types of polyesters, which are bio-based (PBS and PLA), and two petroleum-based polyesters (PET and PBT). I have investigated and compared the morphological, michanical and rheological changes resulting from recycling polyesters and their nanocomposites. Also, I studied the effect of MMT reinforcement on the recycling process and I have achieved the following results:

### 1st thesis: About recycling of bio- based polyesters [III, IV, V, VI]

In my research, I demonstrated that bio-based polyesters (PLA and PBS) can be mechanically reprocessed similarly to petroleum-based ones (PET and PBT). After two extrusion cycles, PET showed a 13% decrease in intrinsic viscosity, while PLA dropped by only 4%, and PBS by just 1.5%. The presence of MMT in the nanocomposites intensified degradation, particularly in PET and PLA, due to the acidic decomposition of the ammonium-based surface modifier. Shrinkage and mechanical properties were most affected in PLA, whereas PBS exhibited only minor changes. The increase in crystallinity during reprocessing (PLA: +95%, PBS: minimal) limited amorphous chain mobility and influenced elasticity. Tensile and impact strength showed moderate variation: a slight decrease was observed in PBS, while PLA remained virtually unchanged.

# $\underline{\text{2}^{nd} \text{ Thesis - About the effect of MMT on crystallinity during recycling of bio- and}}\\ \underline{\text{petroleum-based materials}} \ [\text{IV}, \text{V}, \text{VI}]$

Using non-isothermal crystallization experiments, I investigated how MMT influences crystallization during reprocessing in different polyesters. I introduced two parameters — undercooling ( $\Delta T_{c,1}$ ) and change in crystallinity ( $\Delta X_{m,1}$ ) — to better evaluate these effects. MMT reduced  $\Delta T_{c,1}$  in PET and PBT (e.g., PET: from 9.4 to 3.7 °C), but increased it in PLA and PBS, suggesting distinct crystallization behaviors. PLA showed the most significant increase in crystallinity upon reprocessing (+95%), while PBT and PBS exhibited slight

decreases. These differences confirm that the interaction between MMT and the polymer matrix strongly influences crystallization kinetics during recycling.

## 3<sup>rd</sup> Thesis- About the effect of MMT on mechanical properties during recycling (bio-and petroleum-based materials) [IV, V, VI]

Using Izod impact tests and three-point bending tests, I have demonstrated that 6 wt.% MMT nano-reinforcement affects the physical recycling of various polyesters differently:

The impact strength decreased when recycled in the presence of MMT in the case of PBS/MMT by about 42 %, while it was 33 % for PET/MMT, 30 % for PBT/MMT, and 8 % for PLA/MMT. I have noted that MMT did not have a significant effect on the flexural strength in all cases during recycling. Furthermore, I have observed from the values of the flexural modulus, that the incorporation of nanoclay increased the stiffness of the nanocomposites during recycling by 5-14 %, except for PLA/MMT, which decreased the flexural modulus by 8 %.

The reason for this is that based on SEM images and X-ray diffractograms, I have found that MMT is located in the polymer matrices in two different ways: intercalated and agglomerated structures. During the reprocessing, the intercalated structures (layer spacing, stack number) do not change significantly, but the size of the agglomerates became smaller due to the improved distribution and fragmentation into smaller ones as a result of the high shear forces in the twin-screw extruder. Thus, the dispersion state of MMT plays a crucial role in the mechanical property recovery of recycled nanocomposites. Furthermore, degradation also plays a major role in influencing the mechanical properties, especially in PET. PET showed clear degradation that affected its molecular weight and viscosity, resulting in a more brittle fracture. The interaction between PET and organically modified MMT increases the degradation rate because of the elevated number of acidic sites on the clay plates.

# 4th Thesis- About the correlation between the rheological behaviour and the reprocessing cycles in nanocomposites [V, VI]

By conducting rheological analysis on reprocessed polyester/MMT nanocomposites, I have observed that the viscosity behaviour differs between polyesters. PET exhibited shear thinning with a significant decrease in viscosity upon recycling. This was attributed to its greater susceptibility to chain scission as this behaviour is related to the low molecular weight of PET and the influence of MMT, which could not counteract the degradation. Whereas PBS, PLA and PBT demonstrated a smaller decrease in viscosity after multiple reprocessing cycles, indicating their molecular structures and interactions with MMT provide better stability against shear and thermal degradation due to stronger intermolecular interactions and the enhancing effect of MMT. This confirms that the polymer matrix structure and MMT dispersion influence the long-term processability of these materials.

### 5.3. Further work

This research was conducted as part of an expanded effort to enhance the recyclability and mechanical performance of polyester-based nanocomposites. While significant progress has been made, several challenges remain that require further investigation.

### Improving reprocessing conditions:

The effect of multiple reprocessing cycles on the characteristics of polyester/MMT nanocomposites needs to be further analyzed. Optimizing extrusion and injection moulding parameters can reduce degradation effects and thus enhance recyclability.

### Long-term durability studies:

The aging behaviour of recycled polyester/MMT nanocomposites under environmental stresses such as UV exposure, humidity, and cyclic loading needs to be evaluated to determine their suitability for real-world applications.

#### ❖ Interface adhesion enhancements:

The interactions between MMT and polyester matrices should be improved using surface treatments or compatibilizers to enhance dispersion and mechanical stability, especially after recycling.

### ❖ Investigation of alternative nanofillers:

Other nanofillers, such as graphene or cellulose nanocrystals, should be tested as potential reinforcements to compare their impact on polyester properties and recyclability.

### Sustainability and economic feasibility analysis:

Life cycle assessment and cost analysis should be conducted to evaluate the feasibility of scaling recycled polyester/MMT nanocomposites for industrial applications, and to ensure their economic and environmental benefits.

### 6. MY PUBLICATIONS

I. Zoubeida Taha Taha, Andrea Ádámné Major, A review on MWCNTs: The effect of its addition on the polymer matrix, *Gradus*, 10 (2023). pp 1-14 <a href="https://gradus.kefo.hu/archive/2023-1/2023">https://gradus.kefo.hu/archive/2023-1/2023</a> 1 ENG 012 Taha.pdf.

- II. Zoubeida Taha Taha, Andrea Ádámné Major, Investigating the effect of adding multiwalled carbon nanotubes on the morphological properties of polybutylene terephthalate, In: Kovács, T.A., Nyikes, Z., Berek, T., Daruka, N., Tóth, L. (eds) Critical Infrastructure Protection in the Light of the Armed Conflicts. HCC 2022. Advanced Sciences and Technologies for Security Applications. Q4 Springer, Cham. 2024, Paper, Chapter 41, pp 473-482 <a href="https://doi.org/10.1007/978-3-031-47990-8-41">https://doi.org/10.1007/978-3-031-47990-8-41</a>.
- III. Zoubeida Taha Taha, Andrea Ádámné Major, Ferenc Ronkay, Effect of Reprocessing on the Crystallization of Different Polyesters, Acta Technica Jaurinensis, Q3 17(2023) pp. 1-7, 2023, <a href="https://acta.sze.hu/index.php/acta/article/view/723/620">https://acta.sze.hu/index.php/acta/article/view/723/620</a>.
- IV. Zoubeida Taha Taha, Andrea Ádámné Major and Ferenc Ronkay, Effect of Reprocessing on the Viscosity and Mechanical Properties of PLA and PLA/MMT Nanocomposites, *Engineering proceedings*, Q3, 79(2024) <a href="https://www.mdpi.com/2673-4591/79/1/48">https://www.mdpi.com/2673-4591/79/1/48</a>.
- V. Zoubeida Taha Taha, Péter Gerse, Attila Bata, Béla Molnar, Emese Slezák, Ádámné Major Andrea, Ferenc Ronkay, Influence of recycling on different polyesters and their MMT nanocomposites: Effects on morphology, mechanical properties, and rheological behaviour, *Progress in Rubber Plastics and Recycling Technology*, Q3 IF: 1.6, 2025, https://doi.org/10.1177/14777606241313078.

VI. Zoubeida Taha Taha, Attila Bata, Béla Molnár, Ferenc Ronkay, Impact of Montmorillonite Reinforcement on the Physical Recyclability of Biobased and Petroleum-Based Polyesters, *Heliyon*, *Q1 IF: 3.6* 11(2025), e43022, <a href="https://doi.org/10.1016/j.heliyon.2025.e43022">https://doi.org/10.1016/j.heliyon.2025.e43022</a>.

### 7. REFERENCES

1. Tilley RJD (2004) Understanding Solids The Science of Materials. Wiley Sons ltd, London

- 2. Wang RM, Zheng SR, Zheng YP (2011) Polymer matrix composites and technology. Polym matrix Compos Technol. https://doi.org/10.1533/9780857092229
- 3. Harris B (1999) Engineering composite materials. Composites. https://doi.org/10.1016/0010-4361(87)90420-4
- 4. Chung DDL (2010) Composite Materials Science and Applications. https://doi.org/10.1007/978-1-84882-831-5
- 5. Fan Q, Duan H, Xing X (2024) A review of composite materials for enhancing support, flexibility and strength in exercise. Alexandria Eng J 94:90–103
- 6. Margarita V (2024) Modern Approaches To the Use of Composite Materials in Construction. Am J Eng Technol 6:57–65
- 7. William D. Callister J (2007) Materials Science and Engineering :An Introduction. J John Wiley Sons Inc. https://doi.org/10.1007/BF01184995
- 8. Khan F, Hossain N, Mim JJ, Rahman SM, Iqbal MJ, Billah M, Chowdhury MA (2024) Advances of composite materials in automobile applications A review. J Eng Res. https://doi.org/10.1016/j.jer.2024.02.017
- 9. S. Mohanty, S. K Nayak, B.S. Kaith SK (2015) Polymer Nanocomposites Based on Inorganic and Organic Nanomaterials. S Stud. https://doi.org/10.1002/9781119179108
- 10. Omanovi E, Badnjevi A, Kazlagi A, Hajlovac M (2020) Nanocomposites: ABrief Review. Health Technol (Berl) 10:51–59
- 11. Okpala CC (2013) Nanocomposites An Overview. 8:17–23
- 12. Al-mutairi N (2022) Nanocomposites Materials Definitions, Types and Some of Their Applications: a Review Nanocomposites Materials Definitions, Types and Some of Their Applications: a Review. Eur J Res Dev Sustain 3:2
- 13. Okpala CC (2014) The Benefits and Applications of Nanocomposites. Int J Adv Eng Technol 1–6
- 14. Scheirs J, Long TE (2003) Modern Polyesters: Chemistry and Technology of Polyesters and Copolyesters. John Wiley and Sons. USA
- 15. Zhang Q, Song M, Xu Y, Wang W, Wang Z, Zhang L (2021) Bio-based polyesters: Recent progress and future prospects. Prog Polym Sci 120:101430
- 16. Rabnawaz M, Wyman I, Auras R, Cheng S (2017) A roadmap towards green packaging: The current status and future outlook for polyesters in the packaging industry. Green Chem 19:4737–4753
- 17. Naser AZ, Deiab I, Darras BM (2021) Poly(lactic acid) (PLA) and polyhydroxyalkanoates (PHAs), green alternatives to petroleum-based plastics: a review. RSC Adv 11:17151–17196

18. Salleh KM, Zulkifli A, Mazlan NSN, Zakaria S (2023) Biobased Materials. In: Handb. Bioplastics Biocomposites Eng. Appl. Wiley, pp 23–48

- 19. Wang Y, Huang J, Liang X, Wei M, Liang F, Feng D, Xu C, Xian M, Zou H (2023) Production and waste treatment of polyesters: application of bioresources and biotechniques. Crit Rev Biotechnol 43:503–520
- 20. Franz R, Welle F (2022) Recycling of Post-Consumer Packaging Materials into New Food Packaging Applications—Critical Review of the European Approach and Future Perspectives. Sustain. https://doi.org/10.3390/su14020824
- 21. Shanmugam V, Das O, Neisiany RE, Babu K, Singh S, Hedenqvist MS, Berto F, Ramakrishna S (2020) Polymer Recycling in Additive Manufacturing: an Opportunity for the Circular Economy. Mater Circ Econ. https://doi.org/10.1007/s42824-020-00012-0
- 22. Vyavahare SA, Kharat BM, More AP (2024) Polybutylene terephthalate (PBT) blends and composites: A review. Vietnam J Chem 62:579–589
- 23. Alberto Lopes J, Tsochatzis ED (2023) Poly(ethylene terephthalate), Poly(butylene terephthalate), and Polystyrene Oligomers: Occurrence and Analysis in Food Contact Materials and Food. J Agric Food Chem 71:2244–2258
- 24. Rydz J, Sikorska W, Kyulavska M, Christova D (2015) Polyester-based (bio)degradable polymers as environmentally friendly materials for sustainable development. Int J Mol Sci 16:564–596
- 25. Sisson AL, Schroeter M, Lendlein A (2011) Polyesters.
- 26. Hillmyer MA, Tolman WB (2014) Aliphatic polyester block polymers: Renewable, degradable, and sustainable. Acc Chem Res 47:2390–2396
- 27. Mahmoud Zaghloul MY, Yousry Zaghloul MM, Yousry Zaghloul MM (2021) Developments in polyester composite materials An in-depth review on natural fibres and nano fillers. Compos Struct. https://doi.org/10.1016/j.compstruct.2021.114698
- 28. Massa DJ (2023) Polyester Materials and Properties. In: Polyest. Film. Wiley, pp 19–46
- 29. Scheirs J, Long TE (2003) Modern Polyesters: Chemistry and Technology of Polyesters and Copolyesters. John Wiley and Sons.
- 30. Yang PB, Davidson MG, Edler KJ, Brown S (2021) Synthesis, Properties, and Applications of Bio-Based Cyclic Aliphatic Polyesters. Biomacromolecules 22:3649–3667
- 31. Heidarzadeh N, Rafizadeh M, Taromi FA, Puiggalí J, Del Valle LJ, Franco L (2017) Preparation of random poly(butylene alkylate-co-terephthalate)s with different methylene group contents: crystallization and degradation kinetics. J Polym Res. https://doi.org/10.1007/s10965-017-1318-0
- 32. Chen M, Cai C, Bao J, Du Y, Gao H, Liu X (2022) Effect of aliphatic segment length and content on crystallization and biodegradation properties of aliphatic-aromatic co-polyesters. Polym Degrad Stab 203:110080

33. Tu Y-M, Wang X-M, Yang X, Fan H-Z, Gong F-L, Cai Z, Zhu J-B (2021) Biobased High-Performance Aromatic–Aliphatic Polyesters with Complete Recyclability. J Am Chem Soc 143:20591–20597

- 34. Larrañaga A, Lizundia E (2019) A review on the thermomechanical properties and biodegradation behaviour of polyesters. Eur Polym J 121:109296
- 35. Nisticò R (2020) Polyethylene terephthalate (PET) in the packaging industry. Polym Test. https://doi.org/10.1016/j.polymertesting.2020.106707
- 36. Westerhoff P, Prapaipong P, Shock E, Hillaireau A (2008) Antimony leaching from polyethylene terephthalate (PET) plastic used for bottled drinking water. Water Res 42:551–556
- 37. Li-Na J (2013) Study on preparation process and properties of polyethylene terephthalate (pet). Appl Mech Mater 312:406–410
- 38. Sulyman M, Haponiuk J, Formela K (2016) Utilization of Recycled Polyethylene Terephthalate (PET) in Engineering Materials: A Review. Int J Environ Sci Dev 7:100–108
- 39. Barthélémy E, Spyropoulos D, Milana MR, Pfaff K, Gontard N, Lampi E, Castle L (2014) Safety evaluation of mechanical recycling processes used to produce polyethylene terephthalate (PET) intended for food contact applications. Food Addit Contam Part A 31:490–497
- 40. Bayer FL (2002) Polyethylene terephthalate recycling for food-contact applications: Testing, safety and technologies: A global perspective. Food Addit Contam 19:111–134
- 41. Campo EA (2008) Selection of Polymeric Materials: How to Select Design Properties from Different Standards. Sel Polym Mater How to Sel Des Prop from Differ Stand 1–253
- 42. Ha CS (2006) Poly(butylene terephthlate) (PBT) based nanocomposites. Polym Nanocomposites 234–255
- 43. Thomas S, Visakh PM (2011) Engineering and Specialty Thermoplastics: Polyethers and Opportunities. Scrivener Publ LLC 1–14
- 44. Bîrca A, Gherasim O, Grumezescu V, Grumezescu AM (2019) Introduction in thermoplastic and thermosetting polymers. Mater Biomed Eng Thermoset Thermoplast Polym 1–28
- 45. Misra ARSS (1980) Morphological Studies on Polybutylene Ter eph t halate. Mater. Res. 342:
- 46. Möginger B, Lutz C, Polsak A, Müller U (1991) Morphological studies of deformed polybutylene terephthalate (PBT). Colloid Polym Sci 269:535–542
- 47. Margolis J Engineering Plastics Handbook. Canada
- 48. Deshmukh GS, Peshwe DR, Pathak SU, Ekhe JD (2011) A study on effect of mineral additions on the mechanical, thermal, and structural properties of poly(butylene terephthalate) (PBT) composites. J Polym Res 18:1081–1090

49. Deshmukh GS, Peshwe DR, Pathak SU, Ekhe JD (2011) Evaluation of mechanical and thermal properties of Poly (butylene terephthalate) (PBT) composites reinforced with wollastonite. Trans Indian Inst Met 64:127–132

- 50. Huang J, Wang J, Qiu Y, Wu D (2016) Mechanical properties of thermoplastic polyester elastomer controlled by blending with poly(butylene terephthalate). Polym Test 55:152–159
- 51. Okolie O, Kumar A, Edwards C, Lawton LA, Oke A, McDonald S, Thakur VK, Njuguna J (2023) Bio-Based Sustainable Polymers and Materials: From Processing to Biodegradation. J Compos Sci. https://doi.org/10.3390/jcs7060213
- 52. Moshood TD, Nawanir G, Mahmud F, Mohamad F, Ahmad MH, AbdulGhani A (2022) Sustainability of biodegradable plastics: New problem or solution to solve the global plastic pollution? Curr Res Green Sustain Chem. https://doi.org/10.1016/j.crgsc.2022.100273
- 53. Garlotta D (2019) A Literature Review of Poly (Lactic Acid) A Literature Review of Poly (Lactic Acid). J Polym Environ 9:63–84
- 54. Wu Y, Gao X, Wu J, Zhou T, Nguyen TT, Wang Y (2023) Biodegradable Polylactic Acid and Its Composites: Characteristics, Processing, and Sustainable Applications in Sports. Polymers (Basel). https://doi.org/10.3390/polym15143096
- 55. Farah S, Anderson DG, Langer R (2016) Physical and mechanical properties of PLA, and their functions in widespread applications A comprehensive review. Adv Drug Deliv Rev 107:367–392
- 56. Weinstein JE, Dekle JL, Leads RR, Hunter RA (2020) Degradation of bio-based and biodegradable plastics in a salt marsh habitat: Another potential source of microplastics in coastal waters. Mar Pollut Bull 160:111518
- 57. Weinstein JE, Dekle JL, Leads RR, Hunter RA (2020) Degradation of bio-based and biodegradable plastics in a salt marsh habitat: Another potential source of microplastics in coastal waters. Mar Pollut Bull 160:111518
- 58. Alateyah AI, Dhakal HN, Zhang ZY (2013) Processing, properties, and applications of polymer nanocomposites based on layer silicates: A review. Adv Polym Technol 32:1–49
- 59. Zewde B, Atoyebi O, Zvonkina IJ, Thomspon T, Hargrove A, Scott A, Raghavan D (2020) Biopolymer Nanocomposites and Their Applications. World Sci Ser Nanosci Nanotechnol 20:45–108
- 60. Alexandre M, Dubois P (2000) Polymer-layered silicate nanocomposites: Preparation, properties and uses of a new class of materials. Mater Sci Eng R Reports 28:1–63
- 61. Lim ST, Hyun YH, Choi HJ, Jhon MS (2002) Synthetic biodegradable aliphatic polyester/montmorillonite nanocomposites. Chem Mater 14:1839–1844
- 62. Al-Khanbashi A, El-Gamal M, Moet A (2005) Reduced shrinkage polyester-montmorillonite nanocomposite. J Appl Polym Sci 98:767–773
- 63. Bikiaris DN (2013) Nanocomposites of aliphatic polyesters: An overview of the

effect of different nanofillers on enzymatic hydrolysis and biodegradation of polyesters. Polym Degrad Stab 98:1908–1928

- 64. Ke YC, Yang Z Bin, Zhu CF (2002) Investigation of properties, nanostructure, and distribution in controlled polyester polymerization with layered silicate. J Appl Polym Sci 85:2677–2691
- 65. Heuzey MC, Ghanbari A, Carreau PJ (2022) Polyethylene terephthalate/organoclay nanocomposites: Improvement of morphology and viscoelastic properties by using a chain-extender. Appl Clay Sci 225:106551
- 66. Wang Y, Gao J, Ma Y, Agarwal US (2006) Study on mechanical properties, thermal stability and crystallization behavior of PET/MMT nanocomposites. Compos Part B Eng 37:399–407
- 67. Xiao W, Yu H, Han K, Yu M (2005) Study on PET fiber modified by nanomaterials: Improvement of dimensional thermal stability of PET fiber by forming PET/MMT nanocomposites. J Appl Polym Sci 96:2247–2252
- 68. Chen Z, Luo P, Fu Q (2009) Preparation and properties of organo-modifier free PET/MMT nanocomposites via monomer intercalation and in situ polymerization. Polym Adv Technol 20:916–925
- 69. Majdzadeh-Ardakani K, Zekriardehani S, Coleman MR, Jabarin SA (2017) A Novel Approach to Improve the Barrier Properties of PET/Clay Nanocomposites. Int J Polym Sci 2017:14–17
- 70. Kalkar AK, Deshpande VD, Vatsaraj BS (2014) Isoconversional kinetic analysis of DSC data on nonisothermal crystallization: Estimation of Hoffman-Lauritzen parameters and thermal transitions in PET/MMT nanocomposites. Polymer (Guildf) 55:6948–6959
- 71. Antoniadis G, Paraskevopoulos KM, Vassiliou AA, Papageorgiou GZ, Bikiaris D, Chrissafis K (2011) Nonisothermal melt-crystallization kinetics for in situ prepared poly(ethylene terephthalate)/monmorilonite (PET/OMMT). Thermochim Acta 521:161–169
- 72. Wu D, Zhou C, Hong Z, Mao D, Bian Z (2005) Study on rheological behaviour of poly(butylene terephthalate)/ montmorillonite nanocomposites. Eur Polym J 41:2199–2207
- 73. Wu D, Zhou C, Fan X, Mao D, Bian Z (2005) Morphology, crystalline structure and isothermal crystallization kinetics of polybutylene terephthalate/montmorillonite nanocomposites. Polym Polym Compos 13:61–71
- 74. Kalkar AK, Deshpande VD, Vatsaraj BS (2013) Poly(butylene terephthalate)/montmorillonite nanocomposites: Effect of montmorillonite on the morphology, crystalline structure,isothermal crystallization kinetics and mechanical properties. Thermochim Acta 568:74–94
- 75. Soudmand BH, Shelesh-Nezhad K (2020) Study on the gear performance of polymer-clay nanocomposites by applying step and constant loading schemes and image analysis. Wear 458–459:203412

76. Wu D, Zhou C, Fan X, Mao D, Bian Z (2006) Nonisothermal crystallization kinetics of poly(butylene terephthalate)/montmorillonite nanocomposites. J Appl Polym Sci 99:3257–3265

- 77. Hwang S, Khaydarov AA, Park J, Yoo E, Im S (2011) Effects of clay modification on crystallization behavior, physical, and morphological properties of poly(butylene terephthalate) nanocomposites. Macromol Res 19:699–710
- 78. Sharma R, Malik P, Jain P (2015) Rheological and Morphological Properties of Impact Modified PBT / PTT Blends Based Nanocomposites. II:1–5
- 79. Taktak S, Fakhfakh S, Rondot S, Tara A, Jbara O (2022) Behavior under electron irradiation of two clay-based polymer nanocomposites PPgMA/OMMT and PBS/OMMT. Mater Chem Phys 275:125230
- 80. Phua YJ, Chow WS, Mohd Ishak ZA (2011) The hydrolytic effect of moisture and hygrothermal aging on poly(butylene succinate)/organo-montmorillonite nanocomposites. Polym Degrad Stab 96:1194–1203
- 81. Someya Y, Nakazato T, Teramoto N, Shibata M (2008) Thermal and mechanical properties of poly (butylene succinate) nanocomposites with various organomodified montmorillonites. Acta Polym Sin 1123–1128
- 82. Ray SS, Okamoto K, Okamoto M (2006) Structure and properties of nanocomposites based on poly(butylene succinate) and organically modified montmorillonite. J Appl Polym Sci 102:777–785
- 83. Sinha Ray S, Okamoto K, Maiti P, Okamoto M (2002) New Poly(butylene succinate)/Layered Silicate Nanocomposites: Preparation and Mechanical Properties. J Nanosci Nanotechnol 2:171–176
- 84. Di Y, Iannace S, Di Maio E, Nicolais L (2005) Poly(lactic acid)/organoclay nanocomposites: Thermal, rheological properties and foam processing. J Polym Sci Part B Polym Phys 43:689–698
- 85. Fukushima K, Fina A, Geobaldo F, Venturello A, Camino G (2012) Properties of poly(lactic acid) nanocomposites based on montmorillonite, sepiolite and zirconium phosphonate. Express Polym Lett 6:914–926
- 86. Zhu B, Wang Y, Liu H, Ying J, Liu C, Shen C (2020) Effects of interface interaction and microphase dispersion on the mechanical properties of PCL/PLA/MMT nanocomposites visualized by nanomechanical mapping. Compos Sci Technol 190:108048
- 87. Ray SS, Yamada K, Okamoto M, Ueda K (2003) Biodegradable polylactide/montmorillonite nanocomposites. J Nanosci Nanotechnol 3:503–510
- 88. Feijoo JL, Cabedo L, Giménez E, Lagaron JM, Saura JJ (2005) Development of amorphous PLA-montmorillonite nanocomposites. J Mater Sci 40:1785–1788
- 89. Wu TM, Wu CY (2006) Biodegradable poly(lactic acid)/chitosan-modified montmorillonite nanocomposites: Preparation and characterization. Polym Degrad Stab 91:2198–2204
- 90. Calcagno CIW, Mariani CM, Teixeira SR, Mauler RS (2008) The role of the MMT

- on the morphology and mechanical properties of the PP/PET blends. Compos Sci Technol 68:2193–2200
- 91. Hwang SS, Liu SP, Hsu PP, Yeh JM, Chang KC, Lai YZ (2010) Effect of organoclay on the mechanical/thermal properties of microcellular injection molded PBT-clay nanocomposites. Int Commun Heat Mass Transf 37:1036–1043
- 92. Sharma R, Jain P, Dey Sadhu S (2019) Study of Morphological and Mechanical Properties of PBT/PTT Blends and Their Nanocomposites and Their Correlation. Arab J Sci Eng 44:1137–1150
- 93. Soudmand BH, Shelesh-Nezhad K, Hassanifard S (2020) Toughness evaluation of poly(butylene terephthalate) nanocomposites. Theor Appl Fract Mech 108:102662
- 94. Y.J. Phua, Chow WS, Ishak ZAM (2013) Organomodification of Montmorillonite and its Effects on the Properties of Poly(butylene succinate)Nanocomposites. Polym Eng Sci 1–11
- 95. Yue X, Cao P, Yang M, Li C, Wang Z (2022) Improving flame retardant and smoke suppression efficiency for PBS by adding a tannin surface and interfacial modified IFR/MMT synergist. Eur Polym J 181:111662
- 96. Wang Y, Zhang S, Wu X, Lu C, Cai Y, Ma L, Shi G, Yang L (2017) Effect of montmorillonite on the flame-resistant and mechanical properties of intumescent flame-retardant poly(butylene succinate) composites. J Therm Anal Calorim 128:1417–1427
- 97. Bata A, Gerse P, Slezák E, Ronkay F (2023) Time- and temperature-dependent mechanical and rheological behaviours of injection moulded biodegradable organoclay nanocomposites. Adv Ind Eng Polym Res. https://doi.org/10.1016/j.aiepr.2023.11.003
- 98. Othman SH, Ling HN, Talib RA, Naim MN, Risyon NP, Saifullah M (2019) PLA/MMT and PLA/halloysite bio-nanocomposite films: Mechanical, barrier, and transparency. J Nano Res 59:77–93
- 99. Wu X, Yuan J, Yu Y, Wang Y (2009) Preparation and characterization of polylactide/montmorillonite nanocomposites. J Wuhan Univ Technol Mater Sci Ed 24:562–565
- 100. Alrawi LI, Noriman NZ, Alomar MK, Alakrach AM, Dahham OS, Hamzah R, Betar BO, Jassam TM (2020) Tensile and morphology properties of PLA/MMT-TiO2 bionanocomposites. Defect Diffus Forum 398 DDF:131–135
- 101. Ramesh P, Prasad BD, Narayana KL (2020) Effect of MMT Clay on Mechanical, Thermal and Barrier Properties of Treated Aloevera Fiber/ PLA-Hybrid Biocomposites. Silicon 12:1751–1760
- 102. Lopes Alves J, de Tarso Vieira e Rosa P, de Redondo Realinho VC, de Sousa Pais Antunes M, Ignacio Velasco J, Morales AR (2021) Single and hybrid organoclay-filled PLA nanocomposites: Mechanical properties, viscoelastic behavior and fracture toughening mechanism. J Appl Polym Sci 138:1–12

103. Wang DY, Gohs U, Kang NJ, Leuteritz A, Boldt R, Wagenknecht U, Heinrich G (2012) Method for simultaneously improving the thermal stability and mechanical properties of poly(lactic acid): Effect of high-energy electrons on the morphological, mechanical, and thermal properties of pla/mmt nanocomposites. Langmuir 28:12601–12608

- 104. Ray SS, Okamoto K, Okamoto M (2003) Structure-property relationship in biodegradable poly(butylene succinate)/layered silicate nanocomposites. Macromolecules 36:2355–2367
- 105. Chin S Carbon Nanotube Reinforced Composites Nanostructured Materials in Electrochemistry Block Copolymers in Nanoscience Bulk Nanostructured Materials Nanomaterials for the Life Sciences Nanomaterials Nanotechnologies for the Life Sciences Nanoparticles and Cat.
- 106. Rajini N, Winnowlin Jappes JT, Rajakarunakaran S, Poornanand P (2012) Electrical properties of montmorillonite nanoclay reinforced unsaturated polyester nanocomposite. IEEE-International Conf Adv Eng Sci Manag ICAESM-2012 141–145
- 107. Wang Q, Hou Y, Ma S, Wang T, Zhang J, Qin S, Li T, Bai Z (2022) Study on insulating properties of polyethylene terephthalate/montmorillonite nanocomposites. AIP Adv. https://doi.org/10.1063/5.0077665
- 108. de Paiva LB, Morales AR, Valenzuela Díaz FR (2008) Organoclays: Properties, preparation and applications. Appl Clay Sci 42:8–24
- 109. Gurunathan T, Mohanty S, Nayak SK (2015) A review of the recent developments in biocomposites based on natural fibres and their application perspectives. Compos Part A Appl Sci Manuf 77:1–25
- 110. Ronkay F, Molnár B, Szalay F, Nagy D, Bodzay B, Sajó IE, Bocz K (2019) Development of flame-retarded nanocomposites from recycled PET bottles for the electronics industry. Polymers (Basel) 11:1–19
- 111. Tanaka T, Montanari GC, Mülhaupt R (2004) Polymer nanocomposites as dielectrics and electrical insulation- perspectives for processing technologies, material characterization and future applications. IEEE Trans Dielectr Electr Insul 11:763–784
- 112. Ezzeddine I, Ghorbel N, Ilsouk M, Arous M, Lahcini M, Bouharras FZ, Raihane M, Kallel A (2021) Dielectric and thermal characteristics of Beidellite nanoclay-reinforced poly(butylene succinate). Mater Chem Phys 258:123855
- 113. Melorose J, Perroy R, Careas S (2015) Dielectric Polymer Nanocomposites.
- 114. Sinha Ray S, Okamoto M (2003) Polymer/layered silicate nanocomposites: A review from preparation to processing. Prog Polym Sci 28:1539–1641
- 115. Utracki LA (2010) Clay-containing polymeric nanocomposites and their properties. IEEE Electr Insul Mag 26:8–17
- 116. Ray SS, Bousmina M (2005) Biodegradable polymers and their layered silicate nanocomposites: In greening the 21st century materials world. Prog Mater Sci

- 50:962-1079
- 117. Hopewell J, Dvorak R, Kosior E (2009) Plastics recycling: Challenges and opportunities. Philos Trans R Soc B Biol Sci 364:2115–2126
- 118. Shen L, Nieuwlaar E, Worrell E, Patel MK (2011) Life cycle energy and GHG emissions of PET recycling: Change-oriented effects. Int J Life Cycle Assess 16:522–536
- 119. Muringayil Joseph T, Azat S, Ahmadi Z, Moini Jazani O, Esmaeili A, Kianfar E, Haponiuk J, Thomas S (2024) Polyethylene terephthalate (PET) recycling: A review. Case Stud Chem Environ Eng 9:100673
- 120. Bianchi S, Bartoli F, Bruni C, Fernandez-Avila C, Rodriguez-Turienzo L, Mellado-Carretero J, Spinelli D, Coltelli MB (2023) Opportunities and Limitations in Recycling Fossil Polymers from Textiles. Macromol 3:120–148
- 121. Chowreddy RR, Nord-Varhaug K, Rapp F (2019) Recycled Poly(Ethylene Terephthalate)/Clay Nanocomposites: Rheology, Thermal and Mechanical Properties. J Polym Environ 27:37–49
- 122. Bizarria MTM, Giraldi ALF de M, Carvalho CM de, Velasco JI, Vila MA d'A', Mei LHI (2010) Morphology and thermomechanical properties of recycled PET–organoclay nanocomposites. J Appl Polym Sci 116:2658–2667
- 123. Lamberti FM, Román-Ramírez LA, Wood J (2020) Recycling of Bioplastics: Routes and Benefits. J Polym Environ 28:2551–2571
- 124. Verma D, Fortunati E (2019) Biobased and biodegradable plastics. Handb Ecomater. https://doi.org/10.1007/978-3-319-68255-6\_103
- 125. Addis S, Ejegu H, Dubale M, Mamuye W (2021) Development of Sustainable and Functional Fabrics from Recycled and Nanocomposite Polyester Fibers. Adv Mater Sci Eng. https://doi.org/10.1155/2021/7087152
- 126. Rigail-Cedeño A, Diaz-Barrios A, Gallardo-Bastidas J, Ullaguari-Loor S, Morales-Fuentes N (2019) Recycled HDPE/PET clay nanocomposites. Key Eng Mater 821 KEM:67–73
- 127. Merijs Meri R, Zicans J, Ivanova T, Berzina R, Japins G, Locs J (2012) Structure and properties of recycled aromatic thermoplastic polyester nanocomposites. Key Eng Mater 527:44–49
- 128. Merijs Meri R, Zicans J, Ivanova T, Berzina R, Japins G, Maksimov R, Heim HP (2012) Structure and properties of the nanocomposites developed on the basis of recycled polyesters. ECCM 2012 Compos Venice, Proc 15th Eur Conf Compos Mater 24–28
- 129. Mallakpour S, Behranvand V (2017) Using recycled polymers for the preparation of polymer nanocomposites: Properties and applications. Hybrid Polym Compos Mater Appl. https://doi.org/10.1016/B978-0-08-100785-3.00007-3
- 130. Rosnan RM, Arsad A (2013) Effect of MMT concentrations as reinforcement on the properties of recycled PET/HDPE nanocomposites. J Polym Eng 33:615–623
- 131. Giraldi ALF, Bizarria MTM, Silva AA, Mariano C, Velasco JI, D'Avila MA, Mei

LHI (2009) Effect of clay content and speed screw rotation on the crystallization and thermal behaviors of recycled PET/clay nanocomposites. J Nanosci Nanotechnol 9:3883–3890

- 132. Razak MZA, Arsad A, Rahmat AR, Hassan A (2012) Influence of MMT as reinforcement on rheological behavior, mechanical and morphological properties of recycled PET/ABS thermoplastic nanocomposites. J Polym Eng 32:177–183
- 133. Salah LS, Ouslimani N, Danlée Y, Beltrán FR, Huynen I, Ulagares de la Orden M (2023) Investigation of mechanical recycling effect on electromagnetic properties of polylactic acid (PLA) nanoclay nanocomposites: Towards a valorization of recycled PLA nanocomposites. Compos Part C Open Access. https://doi.org/10.1016/j.jcomc.2022.100339
- 134. Films XA, Naidu DS (2020) polymers E ff ect of Clay Nanofillers on the Mechanical and Water Vapor Permeability Properties of. Polymers (Basel) 2279
- 135. Nanocor I Datasheet of MMT.
- 136. Molnar B, Ronkay F (2019) Effect of solid-state polycondensation on crystalline structure and mechanical properties of recycled polyethylene-terephthalate. Polym Bull 76:2387–2398
- 137. Righetti MC, Di Lorenzo ML, Cinelli P, Gazzano M (2021) Temperature dependence of the rigid amorphous fraction of poly(butylene succinate). RSC Adv 11:25731–25737
- 138. Heidrich D, Gehde M (2022) The 3-Phase Structure of Polyesters (PBT, PET) after Isothermal and Non-Isothermal Crystallization. Polymers (Basel). https://doi.org/10.3390/polym14040793
- 139. Mysiukiewicz O, Barczewski M (2020) Crystallization of polylactide-based green composites filled with oil-rich waste fillers. J Polym Res. https://doi.org/10.1007/s10965-020-02337-5
- 140. Pielichowski K, Njuguna J, Majka TM (2023) Thermal degradation during the processing of polymers. In: Therm. Degrad. Polym. Mater. Elsevier, pp 327–338
- 141. Schyns ZOG, Patel AD, Shaver MP (2023) Understanding poly(ethylene terephthalate) degradation using gas-mediated simulated recycling. Resour Conserv Recycl. https://doi.org/10.1016/j.resconrec.2023.107170
- 142. Xu X, Ding Y, Qian Z, Wang F, Wen B, Zhou H, Zhang S, Yang M (2009) Degradation of poly(ethylene terephthalate)/clay nanocomposites during melt extrusion: Effect of clay catalysis and chain extension. Polym Degrad Stab 94:113–123
- 143. Guo W, Yang B, Xia R, Su L, Miao J, Qian J, Chen P, Yu X, Zhang Q, Deng S (2013) Three-Dimensional Simulation of the Shrinkage Behavior of Injection-Molded Poly Lactic Acid (PLA): Effects of Temperature, Shear Rate and Part Thickness. J Res Updat Polym Sci 2:168–173
- 144. Kracalik M, Laske S, Witschnigg A, Holzer C (2012) Effect of the mixture

composition on shear and extensional rheology of recycled PET and ABS nanocomposites. Macromol Symp 311:33–40

- 145. Herken T, Fecke N, Schöppner V (2015) Experimental analysis of the material degradation of PET on a co-rotating twin-screw extruder for varying vacuum pressures. AIP Conf Proc. https://doi.org/10.1063/1.4918382
- 146. He H, Liu B, Xue B, Zhang H (2022) Study on structure and properties of biodegradable PLA/PBAT/organic-modified MMT nanocomposites. J Thermoplast Compos Mater 35:503–520
- 147. Sabatini V, Farina H, Basilissi L, Di Silvestro G, Ortenzi MA (2015) The Use of Epoxy Silanes on Montmorillonite: An Effective Way to Improve Thermal and Rheological Properties of PLA/MMT Nanocomposites Obtained via "in Situ" Polymerization. J Nanomater. https://doi.org/10.1155/2015/418418
- 148. Dai P, Zhang W, Pan Y, Chen J, Wang Y, Yao D (2011) Processing of single polymer composites with undercooled polymer melt. Compos Part B Eng 42:1144–1150
- 149. Vilanova PC, Ribas SM, Guzman GM (1985) Isothermal crystallization of poly(ethylene-terephthalate) of low molecular weight by differential scanning calorimetry: 1. Crystallization kinetics. Polymer (Guildf) 26:423–428
- 150. Liao Y, Hu Y, Ikeda K, Okabe R, Wu R, Ozaki R, Xu Q (2024) Exploring the effect of cooling rate on non-isothermal crystallization of copolymer polypropylene by fast scanning calorimetry. China Foundry. https://doi.org/10.1007/s41230-024-3108-8
- 151. Najafi N, Heuzey MC, Carreau PJ (2013) Crystallization behavior and morphology of polylactide and PLA/clay nanocomposites in the presence of chain extenders. Polym Eng Sci. https://doi.org/10.1002/pen.23355
- 152. Aliotta L, Gazzano M, Lazzeri A, Righetti MC (2020) Constrained amorphous interphase in poly(l-lactic acid): Estimation of the Tensile elastic modulus. ACS Omega 5:20890–20902
- 153. Mileva D, Tranchida D, Gahleitner M (2018) Designing polymer crystallinity: An industrial perspective. Polym Cryst 1:1–16
- 154. Dangseeyun N, Srimoaon P, Supaphol P, Nithitanakul M (2004) Isothermal melt-crystallization and melting behavior for three linear aromatic polyesters. Thermochim Acta 409:63–77
- 155. Androsch R, Jariyavidyanont K, Janke A, Schick C (2023) Poly (butylene succinate): Low-temperature nucleation and crystallization, complex morphology and absence of lamellar thickening. Polymer (Guildf) 285:126311
- 156. Kwon K, Isayev AI, Kim KH (2006) Theoretical and experimental studies of anisotropic shrinkage in injection moldings of various polyesters. J Appl Polym Sci 102:3526–3544
- 157. Du P, Xue B, Song Y, Lu S, Yu J, Zheng Q (2010) Fracture surface characteristics and impact properties of poly(butylene terephthalate). Polym Bull 64:185–196

158. Cilleruelo L, Lafranche E, Krawczak P, Pardo P, Lucas P (2008) Injection moulding of long-glass-fibre-reinforced poly(ethylene terephthalate): Influence of processing conditions on flexural and impact strengths. Polym Polym Compos 16:577–588

- 159. Horváth S, Kovács JG (2024) Effect of Processing Parameters and Wall Thickness on the Strength of Injection Molded Products. 68:78–84
- 160. Hoare L, Hull D (1977) The effect of orientation on the mechanical properties of injection molded polystyrene. Polym Eng Sci 17:204–212

### 8. APPENDIX

MFI values (Figure 65) showed that recycling both unreinforced and MMT-reinforced polyesters led to increased MFI for PBS, PBT and PLA, indicating slight degradation. The incorporation of MMT slightly decreased the MFI in PBS, while in PLA and PBT, MMT-filled samples showed slightly higher MFI values than their pure counterparts, suggesting that the clay promoted mild chain scission. In contrast, PET exhibited a significant MFI increase with MMT addition and reprocessing, confirming pronounced degradation due to chain scission, which MMT was unable to prevent.

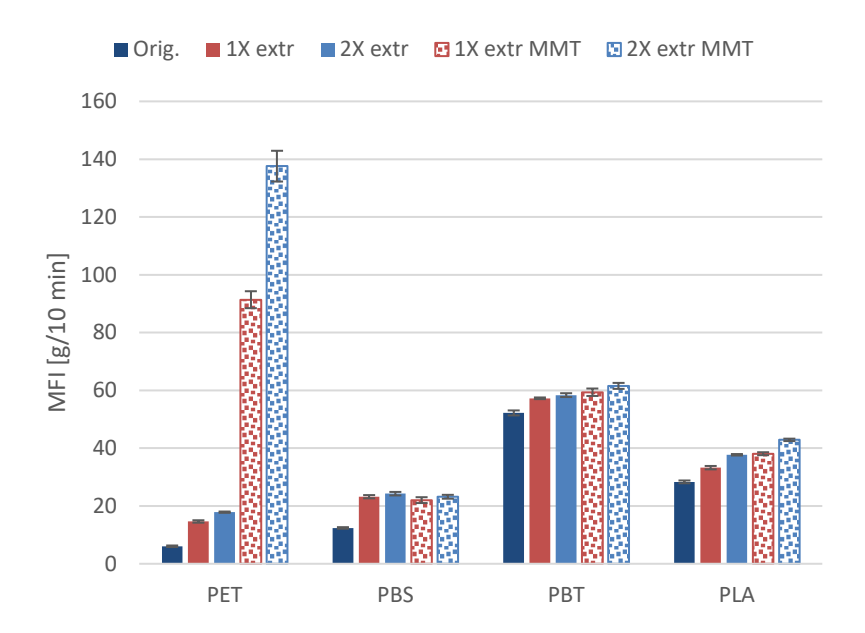


Fig. 65. Melt flow index of polyesters and polyester/MMT nanocomposites (Measurements were conducted under the following conditions: PET at 260 °C / 1.20 kg, PBT at 250 °C / 2.16 kg, PLA at 210 °C / 2.16 kg, and PBS at 190 °C / 2.16 kg)

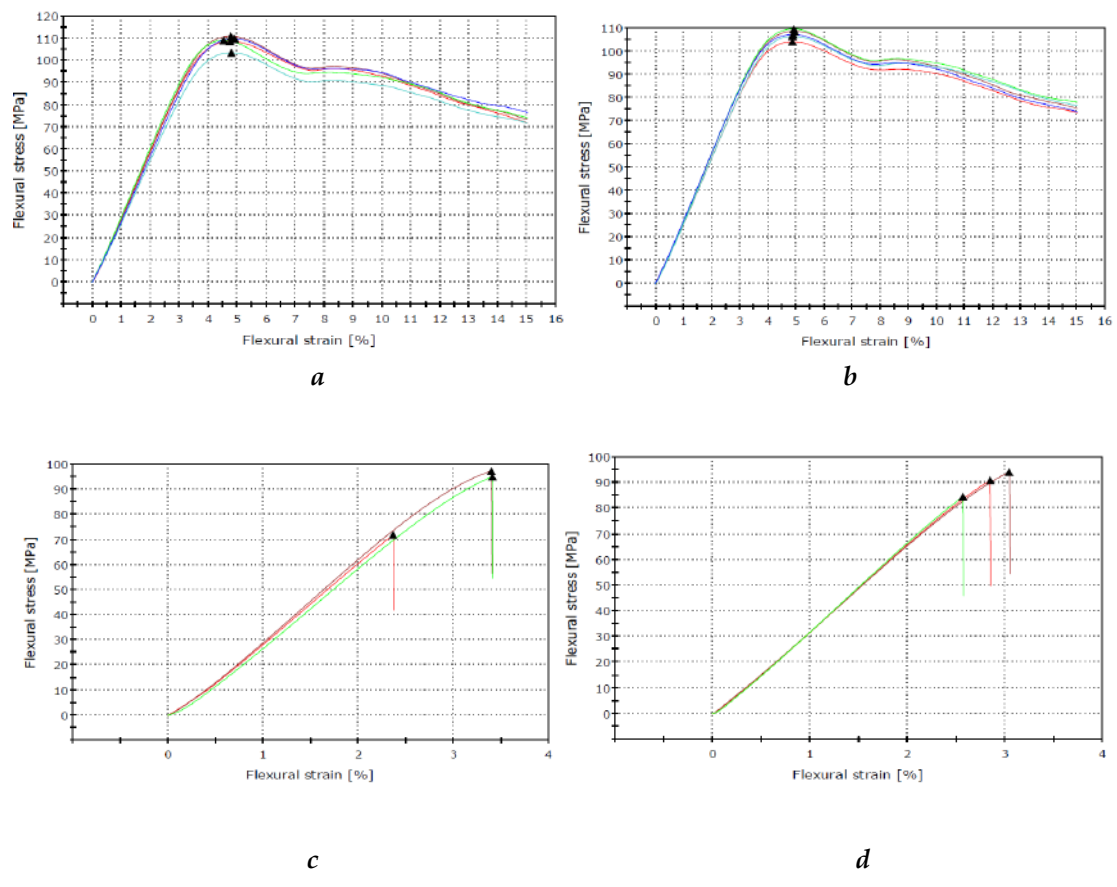


Fig. 66. 3-point bending test curves for PET and PET/MMT samples (a) 1X extr PET; b) 2X extr PET; c) 1X extr PET/MMT; d) 2X extr PET/MMT)

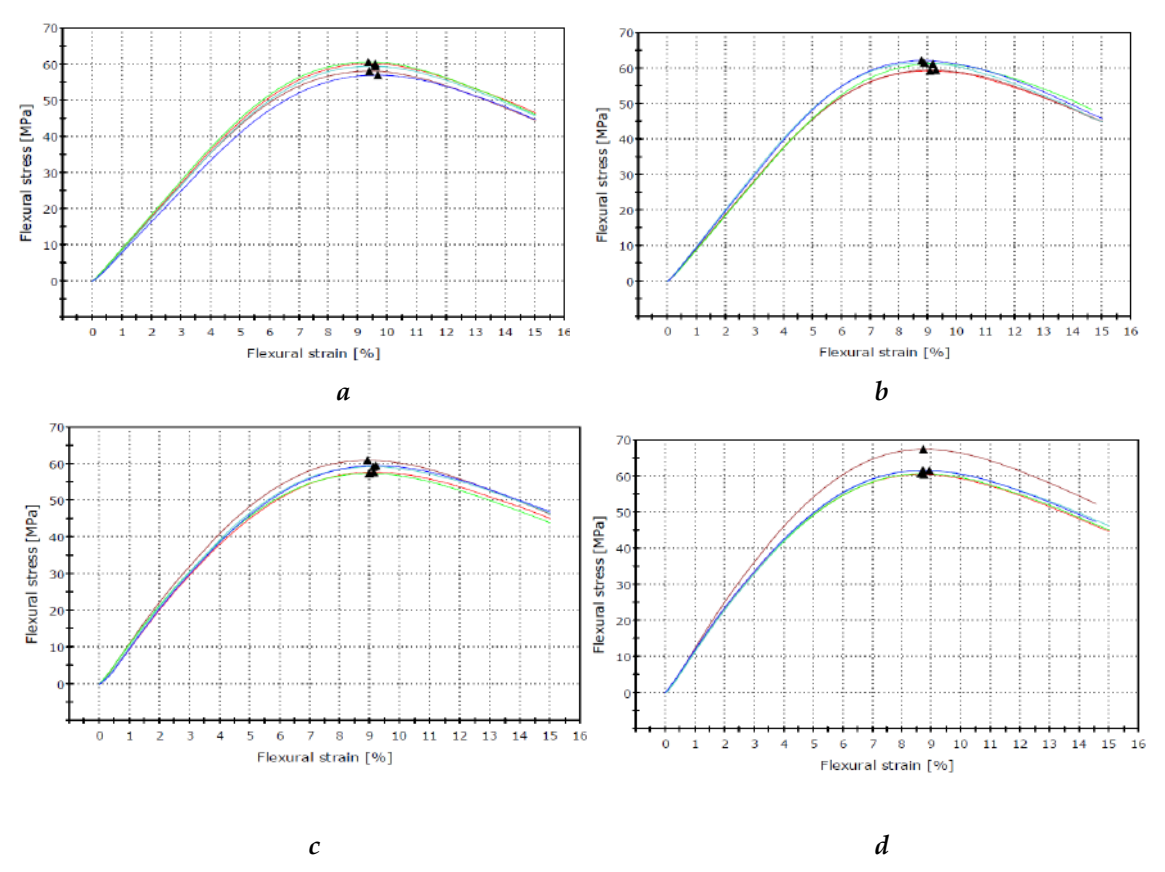


Fig. 67. 3-point bending test curves for PBS and PBS\_MMT Samples (a) 1X extr PBS; b)2X extr PBS; c)1X extr PBS/MMT; d) 2X extr PBS/MMT)

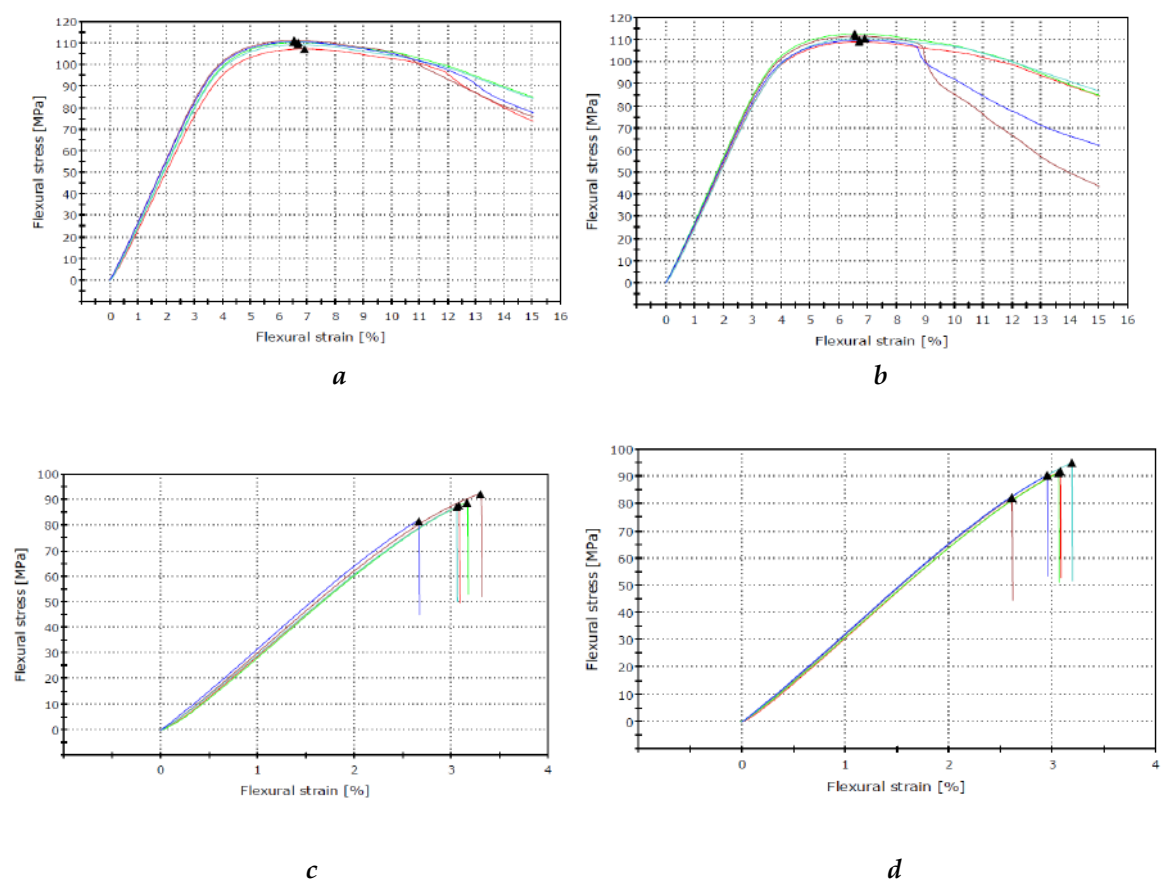


Fig. 68. 3-point bending test curves for PBT and PBT/MMT samples (a) 1X extr PBT; b) 2X extr PBT; c) 1X extr PBT/MMT; d) 2X extr PBT/MMT)

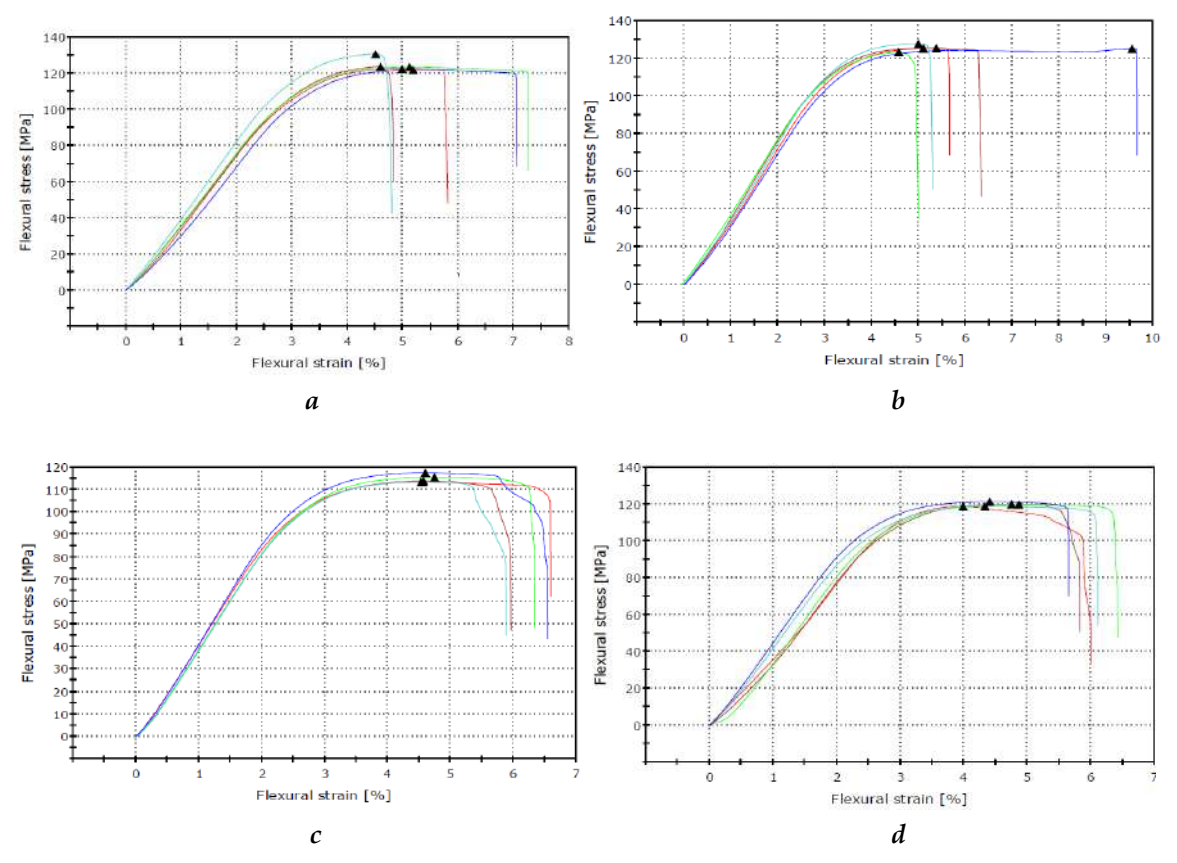


Fig. 69. 3-point bending test curves for PLA and PLA/MMT samples (a) 1X extr PLA; b) 2X extr PLA; c) 1X extr PLA/MMT; d) 2X extr PLA/MMT)